

University of Kentucky

UKnowledge

Theses and Dissertations--Molecular and Cellular Biochemistry

Molecular and Cellular Biochemistry

2022

The Role of Protein Tyrosine Phosphatase Receptor Type F in intestinal homeostasis and colorectal cancer

Ashley T. Skaggs

University of Kentucky, ashley.stevens17@uky.edu

Author ORCID Identifier:

 <https://orcid.org/0000-0001-6732-1640>

Digital Object Identifier: <https://doi.org/10.13023/etd.2022.267>

[Right click to open a feedback form in a new tab to let us know how this document benefits you.](#)

Recommended Citation

Skaggs, Ashley T., "The Role of Protein Tyrosine Phosphatase Receptor Type F in intestinal homeostasis and colorectal cancer" (2022). *Theses and Dissertations--Molecular and Cellular Biochemistry*. 58. https://uknowledge.uky.edu/biochem_etds/58

This Doctoral Dissertation is brought to you for free and open access by the Molecular and Cellular Biochemistry at UKnowledge. It has been accepted for inclusion in Theses and Dissertations--Molecular and Cellular Biochemistry by an authorized administrator of UKnowledge. For more information, please contact UKnowledge@lsv.uky.edu.

STUDENT AGREEMENT:

I represent that my thesis or dissertation and abstract are my original work. Proper attribution has been given to all outside sources. I understand that I am solely responsible for obtaining any needed copyright permissions. I have obtained needed written permission statement(s) from the owner(s) of each third-party copyrighted matter to be included in my work, allowing electronic distribution (if such use is not permitted by the fair use doctrine) which will be submitted to UKnowledge as Additional File.

I hereby grant to The University of Kentucky and its agents the irrevocable, non-exclusive, and royalty-free license to archive and make accessible my work in whole or in part in all forms of media, now or hereafter known. I agree that the document mentioned above may be made available immediately for worldwide access unless an embargo applies.

I retain all other ownership rights to the copyright of my work. I also retain the right to use in future works (such as articles or books) all or part of my work. I understand that I am free to register the copyright to my work.

REVIEW, APPROVAL AND ACCEPTANCE

The document mentioned above has been reviewed and accepted by the student's advisor, on behalf of the advisory committee, and by the Director of Graduate Studies (DGS), on behalf of the program; we verify that this is the final, approved version of the student's thesis including all changes required by the advisory committee. The undersigned agree to abide by the statements above.

Ashley T. Skaggs, Student

Dr. Tianyan Gao, Major Professor

Dr. Trevor Creamer, Director of Graduate Studies

The Role of Protein Tyrosine Phosphatase Receptor Type F in intestinal homeostasis and colorectal cancer

DISSERTATION

A dissertation submitted in partial fulfillment of the requirements for the degree of Doctor of Philosophy in the College of Medicine at the University of Kentucky

By

Ashley Taylor Skaggs

Lexington, Kentucky

Director: Dr. Tianyan Gao, Professor of Molecular and Cellular Biochemistry

Lexington, Kentucky

2022

Copyright © Ashley T. Skaggs 2022
<https://orcid.org/0000-0001-6732-1640>

ABSTRACT OF DISSERTATION

The Role of Protein Tyrosine Phosphatase Receptor Type F in intestinal homeostasis and colorectal cancer

Protein phosphorylation defines one of the most important regulatory mechanisms in cell signaling. PTPRF, protein tyrosine phosphatase receptor type F, belongs to the class I R2A subfamily of protein tyrosine phosphatases (PTP). The overall objective of this dissertation is to investigate the molecular mechanisms by which PTPRF regulates normal and cancer stem cells by controlling Wnt signaling.

Dysregulation of Wnt signaling promotes the initiation and progression of colorectal cancer (CRC). We first determined the functional importance of PTPRF in regulating Wnt signaling in CRC. Combining cell culture, 3D tumor organoid and xenograft models, results from our study establish PTPRF as a positive regulator of the Wnt pathway and an oncogenic PTP in CRC.

To understand how PTPRF protein expression is regulated, we identify that NEDD4L, an E3 ubiquitin ligase, controls PTPRF protein stability and membrane localization. NEDD4L ubiquitinates PTPRF at the plasma membrane to induce PTPRF internalization. Functionally, NEDD4L blocks the ability of PTPRF to activate Wnt signaling. This study identifies NEDD4L-dependent ubiquitination of PTPRF as a novel mechanism that fine-tunes the regulation of Wnt signaling.

To define the molecular mechanisms by which PTPRF promotes Wnt activation, we discover that PTPRF activates the Wnt pathway by controlling the phosphorylation of Cav1. PTPRF-mediated dephosphorylation of Cav1-Y14 leads to prolonged signalosome retention at the plasma membrane, enhanced pLRP6 and downstream Wnt activation. Using PTPRF KO mouse model, we show that PTPRF supports Wnt signaling *in vivo* to enhance intestinal stem cell function. This study identifies Cav1 as a novel substrate of PTPRF and a functional connection between PTPRF and Wnt signalosome.

Collectively, our studies demonstrate that PTPRF plays a key role in promoting Wnt signaling to support normal and cancer stem cell functions and provide a rationale for targeting PTPRF in Wnt-driven diseases.

KEYWORDS: Phosphatase, Wnt signaling, Colorectal Cancer, Intestinal Stem Cells

Ashley T. Skaggs

06/15/2022

The Role of Protein Tyrosine Phosphatase Receptor Type F in intestinal
homeostasis and colorectal cancer

By

Ashley T. Skaggs

Dr. Tianyan Gao

Director of Dissertation

Dr. Trevor Creamer

Director of Graduate Studies

06/15/2022

Date

DEDICATION

To my family for always believing in me.

ACKNOWLEDGMENTS

First, I would like to thank my amazing mentor Dr. Tianyan Gao. Without her support and mentorship, I could not have completed my PhD. You challenged me to think critically about the experiments and encouraged me to explore on my own. You were hands off but always there when I needed to talk things through in your office. You made my grad school experience so enjoyable! I am so honored to have been your grad student and worked under such a respectable and kind mentor for the past 5 years.

To my committee Dr. Matthew Gentry, Dr. Jessica Blackburn, and Dr. Ren Xu, you all made me a better scientist, but also supported me personally throughout this journey. I would also like to thank Dr. Chintan Kikani for taking the time to serve as my outside examiner. To the Gao lab, we were small but mighty! I must thank Dr. Xiaopeng Xiong for his technical expertise and confidence he instilled in me. XP you taught me everything I know, and I cannot thank you enough for your guidance. To Sumati, we quickly became best friends and more than just colleagues. We shared the highs and lows of grad school, and I am so thankful to have had a strong female role model in the lab and in life. To Dr. Stephanie Rock, thank you for being my best friend and technical ally in the lab. I am so thankful for your technical support providing protocols and reagents. But most importantly, I am thankful for your friendship outside the lab. Thank you to Dr. Tong Gan who was my first friend in the lab and initiated this project with me, and to Dylan Rivas for his technical help. In addition, I would like to thank the Markey Cancer Center for providing a collaborative and innovative space to conduct research. To the Molecular and Cellular Biochemistry Department, thank you for being so supportive of your students and being a wonderful department to work for.

Lastly and most importantly, I would like to thank my family and friends. Thank you to my husband Ethan who has been my rock during my PhD. Thank you for taking me to lab every morning, giving me a safe space to come home free of the stress of graduate school, and for making me laugh when I needed it most. You were my biggest supporter and always interested in how my “eyebrows” were doing (AKA western blot bands). To my golden retriever Charlie who was next to me as I wrote my entire dissertation, never leaving his spot guarding my office. You were always there for a hug or a walk when I needed a break from writing. To my parents Shaun and Angela, thank you for instilling the hard work ethic in me needed to complete grad school. You always told me I could do anything I put my mind to, and I now see what is possible with that hard work. Thank you to my sister Emily for always being there for me and being such a supportive sister. To my grandparents Charlie and Barbara Booze for always believing in me and telling me I was destined to change the world. Without your love and support I would not have thought I could accomplish this goal. Finally, thank you to the entire Stevens and Skaggs families!

To Lyndsay, my best friend. I could not have gotten through grad school without you! It’s hard to believe 5 years ago we didn’t know each other considering how close we have become and all that we have shared the past 5 years – volleyball, nights out, UK football games, even being my bridesmaid! We instantly became best friends as we were so alike – almost like long lost sisters. I am so thankful for your lifelong friendship and support through graduate school. I look forward to seeing where life takes us next!

TABLE OF CONTENTS

ACKNOWLEDGMENTS	iii
TABLE OF CONTENTS	v
LIST OF TABLES.....	viii
LIST OF FIGURES	ix
CHAPTER 1. INTRODUCTION	1
1.1 Protein Tyrosine Phosphatase Family	1
1.1.1 Mechanism of dephosphorylation by PTPs	2
1.1.2 Classification of PTPs.....	3
1.1.3 PTPRF.....	4
1.1.4 Known PTPRF substrates and interacting proteins	7
1.1.5 Biochemical regulation.....	8
1.1.6 The Role of PTPRF in Cancer	9
1.2 Wnt/ β -catenin signaling	9
1.2.1 Wnt Signalosome.....	11
1.2.2 Regulation via endocytosis	11
1.2.3 Caveolin-mediated endocytosis	12
1.3 Colorectal Cancer.....	13
1.4 Intestinal Stem Cells.....	14
1.4.1 Intestinal Physiology	14
1.4.2 Lineage differentiation of intestinal epithelial cells (IECs).....	15
1.4.3 Source of Wnt ligand in ISC niche	16
1.5 NEDD4L: An E3 ubiquitin ligase.....	18
1.5.1 Ubiquitination	18
1.5.2 NEDD4L.....	19
1.6 Overall Goals of Dissertation	20
CHAPTER 2. Materials and Methods.....	31
2.1 Methods to study Colorectal Cancer.....	31
2.1.1 Cell lines and Reagents.....	31
2.1.2 Cell Proliferation Assay.....	32
2.1.3 <i>In vitro</i> colony formation assay	33
2.1.4 Western blot analysis.....	33
2.1.5 Immunoprecipitation.....	34
2.1.6 Quantitative RT-PCR.....	34
2.1.7 Wnt reporter assay	35
2.1.8 Immunofluorescence staining.....	35
2.1.9 RNA sequencing (RNA-seq) analysis	35
2.1.10 <i>In vivo</i> xenograft tumor model.....	36
2.1.11 Statistical Analysis.....	37
2.2 Methods to study Ubiquitination	37
2.2.1 Plasmids.....	37

2.2.2	Cell culture and reagents	39
2.2.3	Immunofluorescence (IF) imaging	39
2.2.4	Ubiquitination assays and western blot analysis	40
2.2.5	Wnt reporter assays.....	40
2.2.6	Statistical analysis.....	41
2.3	<i>Methods to Study Intestinal Stem Cells</i>	41
2.3.1	Cells and reagents	41
2.3.2	Expression plasmids	42
2.3.3	Western blot.....	42
2.3.4	Immunofluorescence staining	43
2.3.5	Mice	44
2.3.6	Intestinal crypt isolation and colony formation assays.....	44
2.3.7	FACS analysis of Lgr5-EGFP ⁺ intestinal stem cells	45
2.3.8	RNA <i>in situ</i> hybridization (ISH).....	45
2.3.9	Statistical analysis.....	46
CHAPTER 3.	Inhibition of Protein Tyrosine Phosphatase Receptor Type F Suppresses Wnt Signaling in Colorectal Cancer	48
3.1	<i>Abstract</i>	48
3.2	<i>Introduction</i>	49
3.3	<i>Results</i>	51
3.3.1	Knockdown of PTPRF inhibits cell proliferation	51
3.3.2	PTPRF expression suppresses colony formation in tumor organoids	52
3.3.3	PTPRF suppression reduces Wnt signaling	53
3.3.4	PTPRF regulates Wnt signaling at the level upstream of the destruction complex.....	53
3.3.5	PTPRF interacts with LRP6.....	54
3.3.6	Downregulation of PTPRF decreases <i>in vivo</i> tumor growth	56
3.4	<i>Discussion</i>	57
CHAPTER 4.	NEDD4L promotes the ubiquitination and internalization of PTPRF to inhibit Wnt Signaling 84	
4.1	<i>Abstract</i>	84
4.2	<i>Introduction</i>	85
4.3	<i>Results</i>	86
4.3.1	The expression of PTPRF is regulated by NEDD4L.....	86
4.3.2	NEDD4L controls PTPRF ubiquitination	87
4.3.3	NEDD4L-mediated ubiquitination of PTPRF relies on its phosphatase activity	89
4.3.4	NEDD4L-mediated ubiquitination promotes endocytosis of PTPRF via the caveolin pathway 90	
4.3.5	NEDD4L removes PTPRF from the plasma membrane to inhibit Wnt signaling	91
4.4	<i>Discussion</i>	93
CHAPTER 5.	PTPRF regulates Wnt signaling and intestinal stem cell renewal via dephosphorylation of caveolin-1 109	
5.1	<i>Abstract</i>	109
5.2	<i>Introduction</i>	110

5.3	<i>Results</i>	113
5.3.1	PTPRF activates Wnt signaling in a phosphatase dependent manner	113
5.3.2	PTPRF interacts with LRP6.....	114
5.3.3	PTPRF dephosphorylates Y14 of Cav1 to enhance Wnt signaling	115
5.3.4	Deletion of PTPRF inhibits cell proliferation in mouse intestine.....	117
5.3.5	Deletion of PTPRF decreases the stemness and Wnt signaling in intestinal epithelial cells 118	
5.4	<i>Discussion</i>	120
CHAPTER 6. Discussion and Future Directions		137
6.1	<i>Overall Summary</i>	137
6.1.1	Additional Mechanisms Underlying PTPRF-mediated Regulation of Wnt Signaling	138
6.1.2	A Potential Role of PTPRF in Notch Signaling	141
6.1.3	Limitations	141
6.1.4	Translational Implications	143
6.2	<i>Future Directions</i>	144
REFERENCES		149
VITA.....		161

LIST OF TABLES

Table 2.1 Oligonucleotides utilized in qRT-PCR analysis.	47
Table 3.1 The Gene Set Enrichment Analysis (GSEA) of PTPRF expression in colon cancer patients.....	80
Table 3.2 Top pathways identified by GSEA based on the RNA-seq analysis of control and sh-PTPRF cells.....	82
Table 3.3 The tissue distribution of altered PTPRF gene expression in human cancers..	83

LIST OF FIGURES

Figure 1.1 Protein Phosphatases and PTP superfamily	21
Figure 1.2 RPTP classification	22
Figure 1.3 Wnt/ β -catenin signaling pathway	23
Figure 1.4 Endocytosis pathways that regulate Wnt signaling	24
Figure 1.5 Caveolin1 Structure and domains.....	25
Figure 1.6 Incidence rate of Colorectal cancer in US and KY	26
Figure 1.7 Colorectal Cancer Progression	27
Figure 1.8 Intestinal Physiology and Signaling pathways	28
Figure 1.9 Intestinal epithelial cell lineage differentiation pathway	29
Figure 1.10 NEDD4L structure and domain map	30
Figure 3.1 Knockdown of PTPRF inhibits cell proliferation in colon cancer cells	62
Figure 3.2 Knockdown of PTPRF decreases tumor organoid formation.....	64
Figure 3.3 Knockdown of PTPRF decreases tumor spheroid formation in suspension culture.	65
Figure 3.4 The expression of PTPRF positively regulates Wnt signaling.....	66
Figure 3.5 Knockdown of PTPRF inhibits cell proliferation and Wnt signaling in SW480 cells.	68
Figure 3.6 PTPRF regulates Wnt signaling at a step upstream of the β -catenin destruction complex.....	70
Figure 3.7 The status of GSK3 phosphorylation in PTPRF knockdown.....	71
Figure 3.8 PTPRF interacts with LRP6.	72
Figure 3.9 Colocalization of PTPRF and LRP6 in colon cancer cells.....	74
Figure 3.10 PTPRF-mediated activation of Wnt signaling requires clathrin-dependent endocytosis.....	75
Figure 3.11 Knockdown of PTPRF inhibits xenograft tumor growth and Wnt signaling.....	77
Figure 4.1 The expression of PTPRF is regulated by NEDD4L.....	96
Figure 4.2 NEDD4L controls PTPRF ubiquitination	98
Figure 4.3 NEDD4L-mediated ubiquitination of PTPRF uses the K29 and K63 linkage.	100
Figure 4.4 The phosphatase activity of PTPRF promotes its ubiquitination and degradation.....	101
Figure 4.5 NEDD4L-mediated ubiquitination removes PTPRF from the plasma membrane.....	103
Figure 4.6 The ubiquitination of PTPRF triggers caveolin-mediated internalization. ...	104
Figure 4.7 The expression of NEDD4L promotes trafficking of PTPRF to MVBs.	106
Figure 4.8 NEDD4L-mediated degradation of PTPRF decreases Wnt signaling.	108
Figure 5.1 PTPRF activates Wnt signaling in a phosphatase dependent manner.	123
Figure 5.2 Localization of PTPRF and LRP6 basally and upon Wnt stimulation.....	125
Figure 5.3 PTPRF dephosphorylates Y14 of Cav1.....	127

Figure 5.4 The dephosphorylation of Cav1-Y14F increases Wnt signaling and membrane localization.....	129
Figure 5.5 Knockout of PTPRF decreases the proliferation and colony formation of intestinal epithelial cells.....	131
Figure 5.6 Knockout of PTPRF decreases the stemness of intestinal stem cells.....	133
Figure 5.7 Knockout of PTPRF decreases Wnt signaling in vivo.	135
Figure 5.8 The molecular mechanism underlying PTPRF-mediated regulation of the Wnt pathway.	136
Figure 6.1 Summary Diagram of PTPRF function in Wnt signaling	147
Figure 6.2 Decrease in Notch signaling in PTPRF KO mice	148

CHAPTER 1. INTRODUCTION

1.1 Protein Tyrosine Phosphatase Family

The regulation of protein activity through the addition of a phosphate group to a Serine, Threonine, or Tyrosine residue on a protein substrate through reversible phosphorylation is a simple, yet elegant, process that serves as the main regulator of signaling pathways important for cell growth, differentiation, metabolism, and cell cycle regulation [1] (Figure 1.1A). As one of the most common post-translational modifications, protein phosphorylation is carried out by the combined action of kinases and phosphatases. Although adding phosphate groups to various cellular proteins by kinases often leads to the activation of important signaling pathways, the removal of the phosphate moiety by protein phosphatases to balance the action of kinases is proven to be equally critical. Since the discovery of tyrosine phosphorylation in 1979 by Dr. Tony Hunter [1, 2], intensive investigations have been focused on identifying proteins that can be phosphorylated on tyrosine residues and characterizing the function and regulation of tyrosine kinases. Protein tyrosine phosphatases (PTP), a family of enzymes that remove the phosphate group from tyrosine residues, are largely understudied. Increasing evidence suggests that protein tyrosine phosphatases are essential in maintaining the balance of reversible phosphorylation and cell signaling. The current knowledges of PTPs are briefly reviewed in the following sections.

1.1.1 Mechanism of dephosphorylation by PTPs

The catalytic mechanism for classical protein tyrosine phosphatases is highly conserved throughout the PTP family, with only slight changes in protein structure of the catalytic domain to accommodate various sized substrates [3]. The minimal requirements for catalysis of phosphate removal are the catalytic core C(X)5R motif in the Phosphate binding loop (P-loop), containing the catalytic cysteine and the arginine required for coordination of the phosphate group intermediates, the Tryptophan-Proline-Aspartate (WRD) loop, and the Glutamine (Q)-loop. These 3 minimal requirements for catalysis allow the quick removal of phosphate from tyrosine residue on a protein substrate. Briefly, the mechanism occurs in 2 steps: 1) The pY-substrate binds to the phosphatase in its catalytic domain where the phosphate is coordinated by arginine in the C(X)5R motif. The phosphate of the substrate is attacked by the cysteine (from C(X)5R in P-loop) in a nucleophilic manner. This causes a conformational change in the WRD loop to position it around the pY substrate and allows the aspartate from WRD loop to then protonate the dephosphorylated substrate, which then exits; and 2) The cysteine-phosphate intermediate is hydrolyzed. This is achieved by the Asp in WRD loop removing a proton from the water molecule to become neutral, leaving OH to bind to phosphate group, hydrolyzing the cysteine-phosphate bond. The water molecule is coordinated by glutamine in Q-loop. Finally, the free phosphate group is released, leaving the enzyme ready for the next pY-substrate [3, 4]. Mutations of Cys in the P-loop or Asp in the WRD loop abolish the catalytic activity of classical PTPs. Interestingly, the catalytically inactive PTPs often have higher affinities for their substrates and can be considered substrate-trapping mutants [5, 6]

1.1.2 Classification of PTPs

There are 107 PTP genes, comparing to total 90 tyrosine kinases, found in the human genome [1, 7]. PTPs can be divided into 4 classes based on their evolutionary divergence of phosphatase domains and catalytic mechanisms. Class I, the largest group with 99 members, are cysteine-based catalytic PTPs. Class II contains only one member which is cysteine-based as well but evolutionarily distinct from the other classes. Class III contains 3 members that are not only specific to phospho-tyrosine but also dephosphorylate threonine residues using a cysteine-based mechanism. Finally, class IV has 4 members that use a distinct aspartate-based catalytic mechanism [7] (Figure 1.1B).

Class I can be further classified into 2 groups: classical or dual specificity phosphatases (DSP). Classical PTPs have 38 members and are specific for tyrosine dephosphorylation only. They can be further divided into receptor (21 members) and non-receptor type PTPs (17 members). The DSP class contains 61 phosphatases that are subdivided into 8 groups based on their catalytic specificity and conservation of PTP domains.

Based on the composition of their extracellular domains, the receptor PTP (RPTP) family can be divided into 8 sub-classes, including R1/R6, R2A, R2B, R3, R4, R5, R7, R8 [8, 9] shown in Figure 1.2. Generally, they contain variable extracellular cell-adhesion molecule (CAM) domains, a transmembrane domain, and two intracellular phosphatase domains [10]. This thesis particularly focuses on a receptor type PTP, PTPRF.

1.1.3 PTPRF

Protein tyrosine phosphatase receptor type F (PTPRF) is a single-pass transmembrane phosphatase that is important for cell adhesion, neuronal development, and Wnt signaling. Originally termed Leukocyte Antigen Receptor (LAR) for its IgG-like extracellular domains [11]. It was the founding member of class IIA (R2A) identified in 1988 by Streuli, et. al. [11, 12]. Two other receptor PTPs, including PTPRD and PTPRS, also belong to the R2A sub-family (this sub-family of RPTPs also named LAR-family RPTPs). PTPRF is has been investigated mostly for its role in neuronal development [13]. PTPRF is cleaved post-translationally at the transmembrane region giving rise to the final protein consisting of an extracellular (E) domain and an intracellular phosphatase (P) domain that are non-covalently associated at the membrane [14]. The extracellular domain of PTPRF contains 9 fibronectin type III (FN3) and 3 Immunoglobulin-like (Ig-like) domains. For all three members of R2A RPTPs, the D1 phosphatase domain is active, and the D2 domain is deficient in phosphatase activity (also named pseudophosphatase domain). This is due to only two amino acid changes in D2 compared to D1 at Leu-1644 and Glu-1779 [15]. The corresponding residue for Leu-1664 in D1 domain is a tyrosine; and this Tyr to Leu change blocks the access of potential substrates to the catalytic site. Glu-1779 is in the WRD loop, taking the place of aspartate (D). This substitution increases steric hindrance for the WRD loop conformational change around the catalytic pocket, and that it forms hydrogen-bonds to adjacent loops increasing the strength needed to move WR(D/E) loop [15]. This was confirmed experimentally by mutagenesis of these two sites to restore D1 sequences (Leu-1644-Tyr and Glu-1779-Asp) and showed rescue of phosphatase activity *in vitro* [15].

Earlier studies of PTPRF have mainly used *Drosophila* models to investigate its pivotal role in axon outgrowth during development [16-18]. PTPRF (Dlar in *Drosophila*) was first identified as being involved in neuronal development for its expression in the nervous system [19, 20]. These studies examined the interaction of the extracellular domain of PTPRF to proteoglycans, such as chondroitin sulfate proteoglycans (CSPGs) and heparan sulfate proteoglycans (HSPGs), and how this interaction enhances neuron outgrowth. Specifically, it has been shown that PTPRF binds to syndecan, a transmembrane proteoglycan expressing high levels of HSPGs, to enhance the activity of PTPRF in promoting neuron outgrowth [21]. The interaction between syndecan and PTPRF is mediated through their respective extracellular domains. Additionally, loss-of-function mutations of PTPRF disrupt normal axon guidance of neurons in mice and *drosophila* [12, 19]. In addition to regulating axon migration, double knockout (KO) of PTPRF and its close relative PTPRS in mouse models disrupts cranio-facial bone formation [22], highlighting PTPRF's importance during the embryonic development. Mechanistically, Stewart, et al. demonstrated that cranio-facial defects observed in double knockout mice are due to a decrease in Wnt and an increase in BMP signaling. Another study using PTPRF and PTPRS double KO mice showed bladder malformation, another developmental defect *in vivo* [23]. Finally, PTPRF was shown to be important for mammary gland development in both mouse and human [24, 25]. Together, these studies demonstrated that PTPRF is critical for proper embryonic development.

Following the identification of PTPRF as an important regulator of neuronal development in *Drosophila*, additional studies have been focused on determining the mechanisms of action that control axon guidance. One such study was the identification

the role of PTPRF in regulating of focal adhesions [26]. Interestingly, loss of PTPRF expression decreases the formation of focal adhesions and attenuates cell adhesion to fibronectin in mouse embryonic fibroblasts. Focal adhesions are cell-matrix interactions important for linking actin filaments to the extracellular matrix. Moreover, this study suggested that PTPRF modulates focal adhesions through controlling c-Abl and Akt dependent regulation of CDK1. However, it is unclear if PTPRF directly dephosphorylates c-Abl. At cell adhesions, sites of cell-cell interactions, a family of evolutionarily conserved PTPRF interacting proteins was identified and termed LIP1 (LAR interacting protein 1), later named Liprin family proteins. Liprin- α proteins (including liprin- α 1, - α 2 and - α 3) have been shown to interact with PTPRF at its distal pseudophosphatase domain D2 [27]. The expression of liprin- α 1, also called PPFIA1 (PTPRF interacting protein α 1), induces clustering of PTPRF receptors at the membrane [28]. This was shown to decrease PTPRF phosphatase activity through enhancing the intermolecular interaction of D1 phosphatase domains between two PTPRF proteins. Mechanistically, the interaction of Liprin- α with PTPRF-D2 domain induces clustering of PTPRF, which leads to inhibition of phosphatase activity through blocking the access of substrate as a result of D1/D1 interaction.

Multiple studies have shown PTPRF interacts with β -catenin at adherens junctions and PTPRF is responsible for dephosphorylation of β -catenin to inhibit cell migration [29-31]. Similarly, PTPRF was shown to be involved in planar-cell polarity signaling in *Drosophila* through coordination with Fat2, a cadherin protein [32]. Moreover, PTPRF has been implicated in the negative regulation of various tyrosine kinase receptor signaling pathways, including EGFR, MET, and RET [23, 33-35]. Together, these studies show

PTPRFs involvement in regulating cellular migration signaling through both cell-cell and cell-matrix interactions, processes that are important in neuronal outgrowth.

1.1.4 Known PTPRF substrates and interacting proteins

Most of the above studies have been focused on investigating the functional importance of the extracellular domains of PTPRF in cell adhesion and neuronal development. As a result, there are few studies on the phosphatase role of PTPRF leaving a gap in substrate identification for PTPRF. Historically, after its first identification in 1988, a number of studies on determining the function of PTPRF in the 1990s have failed to identify specific substrates mainly due to the lack of tools and technologies. To date, there are only 3 published substrates of PTPRF.

The first identified substrate of PTPRF is the insulin receptor reported in 1992 [36-39]. Using antisense RNA to silence PTPRF, the authors found that insulin-stimulated autophosphorylation of insulin receptor was increased as detected by an anti-phosphotyrosine antibody. Additionally, a study from 1996 showed that siRNA-mediated knockdown of PTPRF led to an increase in tyrosine phosphorylation of EGFR upon EGF treatment [36]. While these studies established PTPRF's role in regulating receptor tyrosine kinase (RTK) signaling, the specific tyrosine site on the insulin receptor or EGFR has yet to be revealed, and these substrates have not been revisited since the initial studies.

The only recent study to identify a substrate for PTPRF was from 2013 using a siRNA screen for RPTPs against changes in RTK phosphorylation [5]. Using an active site mutant PTPRF-C/S as the substrate-trapping mutant, they confirmed PTPRF

dephosphorylates Tyr930 of EphA2, an RTK implicated in the MAPK signaling pathway. Thus, PTPRF may negatively regulate MEK/ERK signaling by dephosphorylating multiple RTKs. This lack of knowledge on specific substrates (or tyrosine residues) regulated by PTPRF highlights the need for additional studies focusing on determining the mechanisms by which PTPRF modulates various signaling pathways.

1.1.5 Biochemical regulation

PTPRF and other LAR-family RPTPs are post-translationally cleaved at the transmembrane region into its mature form consisting of an E-subunit, the 150-kDa extracellular domain, and the P-subunit, the 85-kDa intracellular phosphatase D1 and D2 domains [14, 40]. The cleavage site is a penta-arginine stretch at the C-terminus of the transmembrane region that is recognized by endoproteases where it is cleaved intracellularly [41]. The two subunits then associate at the membrane non-covalently to form the active RPTPs. Generally, RPTPs are thought to be regulated by a dimerization mechanism that involves the D1 active domain acting as a wedge in the D1 catalytic pocket of another RPTP [9, 42]. The exact mechanism for PTPRF phosphatase inhibition was unclear, as structural analysis proved a different mechanism than that of the dimeric D1 wedge model used by RPTP α (PTPRA) [15, 42]. Interestingly, previous studies suggest that the shedding of extracellular domain serves as a mechanism to inactivate PTPRF-mediated signaling by preventing the binding of PTPRF to ECM proteins [41, 43]

1.1.6 The Role of PTPRF in Cancer

PTPRF's involvement in cancer has proven to be dependent on cell type and signaling pathway affected. It has been shown as a tumor suppressor in colorectal cancer [44], in breast cancer via miR-24 [45], gastric adenocarcinoma [35], neuroendocrine tumors [46], liver, and prostate cancers. Generally, PTPRF acts as a tumor suppressor by ERK pathway inactivation. Additionally, it has been shown to be oncogenic in thyroid carcinomas which is associated with increased expression of the intracellular phosphatase subunit of PTPRF [47], in breast cancer with increased metastatic potential [48, 49], in Her2/Neu-transformed breast epithelial cell line [50], and in colorectal cancer [51]. Collectively, studies of PTPRF in various cancer types have shown that it can function as both a tumor suppressor and oncogenic [44-46, 48, 52, 53]. Thus, more studies are needed to determine the substrates of PTPRF in order to better understand the function and mechanism of action of PTPRF in cancer.

1.2 **Wnt/ β -catenin signaling**

The Wnt/ β -catenin signaling pathway is a highly conserved ligand-receptor binding pathway important for embryonic development and tissue homeostasis. A large family of Wnt ligands are expressed by various organisms from *Drosophila* to human. The Wnt ligand is a cysteine-rich secreted 40-kDa protein that is palmitoylated [54]. The lipid modification of the Wnt ligand was shown to be important for its binding to Frizzled receptor and activating downstream signaling [55]. The enzyme Porcupine (PORCN), an O-acyltransferase located on the ER, is responsible for the lipid modification and secretion of the Wnt ligand [54]. Once secreted from the cell, the Wnt ligand binds to cell surface

receptors in a paracrine fashion. The Wnt pathway has two main mechanisms of activation: canonical (β -catenin mediated) or non-canonical (Ca^{2+} or planar cell polarity signaling).

The main intracellular effector of the canonical Wnt pathway is β -catenin (shown in Figure 1.3). When Wnt ligand is not present, β -catenin is targeted for proteasomal degradation by the destruction complex composed of Axin, adenomatous polyposis coli (APC), GSK3 β , and CK1 α . This complex phosphorylates β -catenin which is a signal for β -TrCP mediated ubiquitination and proteasomal degradation to keep intracellular levels low. This process is initiated by CK1 α -mediated phosphorylation of β -catenin at Ser45, which primes for the subsequent phosphorylation at Thr41, Ser37, and Ser33 by GSK3 β [56].

When Wnt ligand is present, it binds Frizzled (Fzd) receptors, a family of 7-pass transmembrane receptors, and LRP5/6, a single-pass transmembrane co-receptor. The formation of heterodimeric Fzd-LRP receptor complex induces a conformational change leading to phosphorylation of LRP6 at Ser1490. This phosphorylated LRP6 (pLRP6) now serves as the binding site for Axin, a negative Wnt regulator. Binding of Axin to pLRP6 recruits additional effector proteins such as Dishevelled (DVL) to the destruction complex, inhibiting its ability to phosphorylate β -catenin so it is not degraded. This allows cytosolic levels of β -catenin to accumulate where it translocates to the nucleus to bind TCF/LEF transcription factors to activate Wnt target gene transcription (such as *Myc*, *CCND1*, *Lgr5*, and *Axin2*) [54, 56].

1.2.1 Wnt Signalosome

When Wnt ligand binds to its receptors Fzd and LRP6, it induces clustering of receptors into multiprotein complexes to form the Wnt signalosome [56, 57]. This allows better recruitment of effector proteins and a platform for protein-protein interactions. Traditionally, the signalosome was thought to be a mechanism of protein sequestration, physically separating GSK3 β from β -catenin to inhibit its degradation [58]. Now, it is accepted that in addition to sequestration of the destruction complex, the signalosome serves as a platform for ligand-receptor clustering and the recruitment of co-receptors/co-regulators that enhance Wnt signaling transduction. The clustering of receptors helps lead to increased downstream signaling, while subsequently removing a population of receptors from the membrane to prevent prolonged signaling.

The signalosome can be seen as discrete puncta located at the plasma membrane or right below it via fluorescence staining. Recent studies have highlighted how co-receptors may enhance the formation of Wnt signalosome by bringing additional membrane proteins together. EGFR was shown to enhance Wnt9a/FZD9b signaling [59]; and TMEM59 was found to enhance clustering of Fzd/LRP6 receptors and internalize with the Wnt signalosome [60]. These co-regulators provide additional levels of regulation that finetune the amplitude and duration of Wnt signaling.

1.2.2 Regulation via endocytosis

Once the signalosome is assembled, it is accepted that it internalizes to early endosome vesicles. The mode of internalization, however, is still debated. Classical

endocytosis pathways include the clathrin-endocytosis pathway and the caveolin-endocytosis pathway (clathrin-independent). Both endocytic routes have been implicated in the Wnt pathway and it is now accepted that the cell type and context determine which pathway is preferred. For example, it is known that clathrin-endocytosis is used for basal recycling of LRP6 from the membrane. This ligand-independent internalization of LRP6 uses the clathrin-endocytic route [61]. APC was shown to inhibit clathrin-endocytosis of LRP6 to prevent aberrant pathway activation basally [62]. Another group established that under normal Wnt activation in HEK293 and HeLa cells, the caveolin endocytic pathway is preferentially used for LRP6 endocytosis and is required for Wnt activation/ β -catenin stabilization, suggesting that caveolin-endocytosis plays a positive role in activating Wnt signaling (Figure 1.4) [63-65]. This requirement for caveolin in Wnt activation is not fully understood. It has been suggested that caveolin-mediated endocytosis of Wnt signalosome into early endosomes leads to a physical separation of GSK3 β from the destruction complex and β -catenin stabilization. However, additional studies are needed to further evaluate how caveolin-mediated endocytosis of Wnt signalosome is controlled at the plasma membrane.

1.2.3 Caveolin-mediated endocytosis

Caveolae are flask-shaped invaginations in the plasma membrane that serve as pits for lipid raft mediated endocytosis and signal transduction [66]. They were first identified in 1950 for their smooth structure, lacking the traditional fuzzy coat seen on clathrin-coated pits [66]. The size of caveolae is around 70 nm and formed by the association of two

effector proteins: Caveolin1 (CAV1) and accessory Cavin proteins. CAV1 is a hairpin like integral membrane protein that associates with other CAV1 proteins to form higher structure oligomer complexes called the caveolin coat. CAV1 contains a unstructured N terminal cytoplasmic tail followed by a scaffolding domain where the dimerization/oligomerization occurs, a membrane insertion/hairpin domain and a C-terminal tail that is palmitoylated for binding with lipid membrane (Figure 1.5) [67]. The formation of a caveolae occurs when approximately 140 CAV1 molecules cluster together with accessory Cavin proteins to assemble the caveolae pit [68]. This process is mediated by the composition of the plasma membrane as to where they will form. Once assembled, the caveolae bud off from the plasma membrane via dynamin fission to internalize. Caveolin-mediated endocytosis has been shown to facilitate the internalization of albumin, Insulin receptor, EGFR, and TGF β [66].

Tyrosine phosphorylation of CAV1 has been shown to occur at Y14 located at the N-terminal cytoplasmic tail. The balance between phosphorylated and dephosphorylated CAV1-Y14 has been implicated in changing the dynamics of cellular tension and stress as well as signaling downstream of caveolin-mediated endocytosis. Studies have shown that CAV1 phosphorylation at Y14 leads to increased internalization and disassembly of caveolin pits [69-72]. SRC kinase is known to induce CAV1 Y14 phosphorylation; however, no tyrosine phosphatase has been identified.

1.3 Colorectal Cancer

Colorectal cancer (CRC) is the 3rd leading cause of cancer related deaths in both men and women in the US every year [73]. Examining the incidence rates for all US states,

Kentucky ranks the highest in CRC incidence with rate of 48.4, significantly higher than the US average of 36.5 (Figure 1.6A). Some counties in eastern Kentucky region reach incidence rates of 57-86 (Figure 1.6B), making the study of CRC important.

CRC is characterized by the formation of adenoma polyps in the colon that progress to carcinomas. The main driver of CRC is mutations in the Wnt/ β -catenin pathway, mainly lost-function mutations in APC and gain-function mutations in β -catenin. This leads to ligand-independent activation of the Wnt/ β -catenin pathway downstream of the β -catenin destruction complex. Uncontrolled amplification of the Wnt pathway often initiates the oncogenic transformation of normal intestinal epithelial cells. Acquiring additional mutations in oncogenes and tumor suppressor genes, such as RAS, TP53, SMAD, PIK3CA and PTEN, promotes the stepwise progression of advance adenoma into invasive carcinoma [74]. (Figure 1.7)

1.4 Intestinal Stem Cells

1.4.1 Intestinal Physiology

Intestinal epithelial cells are the most highly replicative cell population in the human body, turning over every 3-5 days [75]. The intestine is divided into small and large intestine (colon) connecting the stomach to the rectum. The intestine is composed of 2 major structures: crypts at the base and villi that extend out into lumen to absorb nutrients. At the crypt base resides the intestinal stem cells (ISC), a highly replicative and self-renewing stem cell population that can give rise to all epithelial cell types in the intestine. The ISCs proliferate and differentiate from the crypt base up the villus axis to replace cells at the villus tip. This cycle occurs continuously throughout lifetime, making the ISC

proliferation vitally important to maintain intestinal homeostasis and health of all other cell types.

1.4.2 Lineage differentiation of intestinal epithelial cells (IECs)

ISCs can give rise to all intestinal epithelial cell types. There are 2 main branches: secretory and absorptive lineages. Secretory cell types include antimicrobial Paneth cells, gut hormone producing enteroendocrine cells, and mucin secreting goblet cells. The absorptive lineage includes enterocytes which absorb nutrients. In the lineage specification process, ISCs divide and differentiate into progenitor cells residing in the transit amplifying (TA) zone just above the crypt base. As progenitor cells (also called TA cells) migrate up, they further differentiate into cells of both secretory and absorptive lineages and replace older cells at the villus tip, which undergo apoptosis. The only cell type migrating downwards are the Paneth cells, which remain at the crypt base adjacent to the Lgr5⁺ stem cells [74]. A balance of all cell types highlights the importance of regulation of the Wnt signaling pathway in intestinal cell homeostasis. (Figure 1.8)

The main driver for which cell fate is chosen is the activity balance of the Wnt, Notch and BMP pathways [76, 77]. High Wnt activity allows for renewal of ISCs and the lineage specification of secretory cells, whereas when Wnt is low absorptive cells are produced. The Wnt/ β -catenin signaling is most active at the base of the crypts, supporting the ISC self-renewal. This is evident by the markers of ISCs being Wnt target genes, such as Lgr5 and Ascl2. As IECs migrate up the villus axis, the level of Wnt/ β -catenin signaling decreases whereas BMP signaling increases. The gradient expression of Wnt and BMP

ligands in an opposite direction along the crypt-villus axis dictate the final fate of IECs. (Figure 1.9).

1.4.3 Source of Wnt ligand in ISC niche

Considering Wnt signaling is the main driver for ISC renewal, the amount of Wnt ligand needed is large. Since the Wnt signaling gradient is most active at the crypt base, it was critical to understand what cell type the main secretor of Wnt ligand in the crypt is. Originally, the hypothesis was that Paneth cells located between the Lgr5⁺ stem cells were the source for Wnt ligands in the crypt. However, in 1997 mouse studies using ablation of Paneth cells did not alter crypt formation suggesting they were not the source of Wnt ligands [78]. This was later disproved in 2011 by Hans Clevers who proved Paneth cells indeed secrete Wnt ligands, and when added in co-culture with organoids increased the Lgr5⁺ stem cell population [79].

However, Clevers study was challenged when 2 independent groups in 2012 showed that removal of Paneth cells in mouse intestinal models showed no differences in intestinal crypt growth and homeostasis [80, 81]. Also, when the Wnt3a ligand is silenced in intestinal epithelial cells there are no changes in crypt homeostasis [82]. The Wnt secretion enzyme PORCN and Wingless were targeted for silencing in intestinal epithelial cells using the villin-Cre mouse or in subepithelial cells using Myh11-Cre [83, 84] and showed no changes effects on ISC growth. These findings collectively suggest that Paneth cells, epithelial cells, or subepithelial cells, are not the critical source of Wnt ligands for the niche.

Next, Greicius, et. al [85] looked at stromal cells surrounding the crypt, termed pericryptal myofibroblasts. They demonstrated that these cells secrete Wnts and are positive for the expression of platelet derived growth factor receptor alpha (PDGFR α +). Knockout of PORCN in the PDGFR α + cells *in vivo* rendered the cells incapable of secreting Wnts. As a result, the intestinal crypt formation was severely affected. Additionally, co-culture of PDGFR α + cells increased the growth of intestinal organoids showing a role for supporting ISCs. This study provided strong evidence suggesting that niche signals come from the stoma and not the specialized crypt cells themselves. Interestingly, a subsequent paper from the same group demonstrated that the Wnt-producing myofibroblast cells surrounding the crypt are naturally more resistant to xenobiotics, such as PORCN inhibitors and doxorubicin. This intrinsic resistance allows the intestinal stem cell niche to sustain normal intestinal homeostasis against the potential harmful effect of environmental factors [86]. Moreover, subsequent studies showed that knockout of PORCN specifically in the stromal myofibroblast cells using PDGFR-driven Cre disrupts intestinal crypt formation in newborn mice intestines [87]. Together, these studies supported a critical role of stromal myofibroblast cells in supporting the ISC niche.

Finally, studies from Klaus Kaestner's lab showed that Foxl1+ telocytes are the main niche cells that secrete Wnts and are required for ISC maintenance [88, 89]. Foxl1 is a transcription factor found to be expressed in a sub-population of subepithelial cells. Using a Foxl1-DTA inducible deletion mouse model, Foxl1+ telocytes were deleted after the induction of diphtheria toxin. Just a few days after, intestinal cell proliferation had stopped [88]. Shoshkes-Carmel, et. al. further demonstrated that the telocyte cells are responsible for Wnt production as deleting PORCN gene in Foxl1+ cells inhibited intestinal growth

[89]. To reconcile the difference in the source of Wnt ligands, Kaestner noted that PDGFR α + cells and telocytes are likely the same stromal cell population. All telocytes express PDGFR α , but that Foxl1+ cells are a special subtype of telocytes [90]. These studies highlight the importance for Wnt signaling in the intestinal crypt to better understand the source of Wnt ligands.

1.5 NEDD4L: An E3 ubiquitin ligase

1.5.1 Ubiquitination

Protein ubiquitination is the addition of ubiquitin molecule onto a protein substrate, in which the lysine residue of the substrate is linked to the C-terminal glycine residue of ubiquitin molecule [91]. The ubiquitin (Ub) molecule itself is a 76-amino acid protein that is highly conserved in all eukaryotic organisms [92]. Ubiquitin has 7 lysine residues that can be used for linking additional ubiquitin molecules to generate ubiquitin chains. These lysine residues on ubiquitin include Lys-6, Lys-11, Lys-27, Lys-29, Lys-3, Lys-48, Lys-63 [93]. The ubiquitination can be mono-ubiquitination (single Ub molecule), multi-ubiquitination (single Ub at multiple Lys sites) or poly-ubiquitination (chains of multiple Ub molecules) [94]. The type of lysine linkages used for poly-Ub chain determines the fate of the protein [94]. The most common pathway for ubiquitinated proteins is the Ub-proteasome pathway where Lys-48 linked poly-Ub chains are targeted to the proteasome for protein degradation [92]. Recent studies have revealed the importance of other poly-Ub chain linkages and their different cellular outcomes beyond protein degradation. For example, Lys-63 poly-Ub chains are a signal for protein trafficking, endocytosis, and

vesicular sorting [94], whereas Lys-29 chains have been implicated in the Wnt signaling pathway for proteasomal degradation and signaling inhibition [95].

1.5.2 NEDD4L

The ubiquitin ligase system utilizes a 3-step enzymatic reaction to transfer the Ub molecule to protein substrates and the enzymes involved are: E1 (Ub activating enzyme), E2 (Ub conjugating enzyme), and E3 (Ub ligase responsible for transferring ubiquitin molecules onto protein substrates). E3 ubiquitin ligases can be classified as RING or HECT type E3 ligase domains. RING-type E3 ligases, Ub is directly transferred from E2 onto the protein substrate, whereas HECT-type E3 ligases accept the Ub onto the E3 itself then onto the protein substrate [91]. Most E3 ligases fall under the RING type (~95%), with only 28 HECT-type E3 ligases identified in human genome [91, 94].

One of the intensively studied and largest HECT-type groups is the NEDD4 family E3 ligases. It consists of 9 members: NEDD4, NEDD4L, ITCH, SMURF1, SMURF2, WWP1, WWP2, NEDL1, NEDL2 [91]. Among them, NEDD4L (Neural Precursor Cell Expressed Developmentally Downregulated 4-like) is known to ubiquitinate membrane proteins [96]. NEDD4L contains one C2 and 4 WW domains in the N-terminus, which are important for calcium phospholipid binding and substrate interaction, respectively, followed by a C-terminal HECT E3-ligase domain (Figure 1.10) [91]. Epithelial Na⁺ channels (ENaC) has been identified as a substrate of NEDD4L in 1996 [97]. Subsequent studies have shown that NEDD4L-mediated ubiquitination leads to internalization and degradation of ENaC, controlling the levels of ENaC at membrane to maintain sodium balance. In addition, NEDD4L has been shown to regulate TGF β signaling by promoting

the ubiquitination and degradation of SMAD2/3 [96]. Interestingly, NEDD4L was found to primarily use Lys-63 linked Ub to modify its protein substrates [98].

1.6 Overall Goals of Dissertation

The main goals for this dissertation are to better characterize PTPRF's as a phosphatase. There is a lack of knowledge of PTPRF substrates, its properties in cancer development, and how it is regulated itself. The need for understanding PTPRF's regulation will enhance our understanding of its normal functions and provide evidence how it is involved in signaling pathways. Briefly, the goals of each chapter are outlined.

In Chapter 3 we will establish PTPRF's role in colorectal cancer using *in vitro* cancer cell culture models, cell proliferation assays, and tumor xenograft models. Additionally, its positive activation on the Wnt pathway upstream of the destruction complex will be established for the first time.

In Chapter 4 we explored the regulation of PTPRF via ubiquitination via E3 ligase NEDD4L. This ubiquitination of PTPRF occurs at the membrane and causes internalization of PTPRF, which inhibits the positive Wnt activation. This chapter further confirmed PTPRF as a positive Wnt activator and clarified its activation at the receptor level.

In Chapter 5, a novel substrate for PTPRF is discovered as Caveolin1, and how its dephosphorylation is the mechanism how PTPRF activates the Wnt pathway. Using *in vitro* cell based assays and *in vivo* intestinal stem cell model, we show that PTPRF regulates the Wnt pathway via signalosome retention.

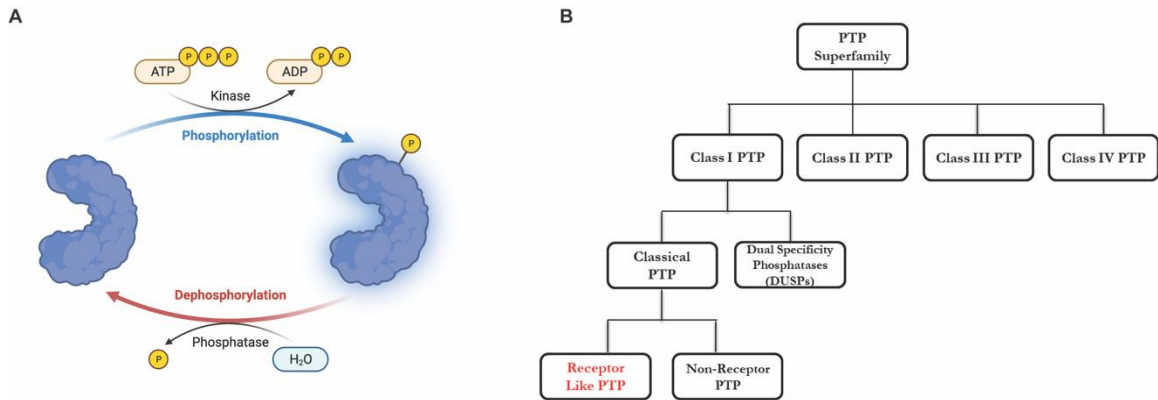


Figure 1.1 Protein Phosphatases and PTP superfamily

(A) Protein phosphatases act in coordination with protein kinases to control balance of reversible phosphorylation of protein substrates. This balance is key to regulating cellular signaling and protein activity. (B) Protein tyrosine phosphatase superfamily is divided into 4 classes based on sequence. Class 1 is divided into Classical (Tyr specific), or Dual Specificity (Tyr and Ser/Thr residues). Classical is further divided into Receptor or non-receptor type. Created with BioRender.com.

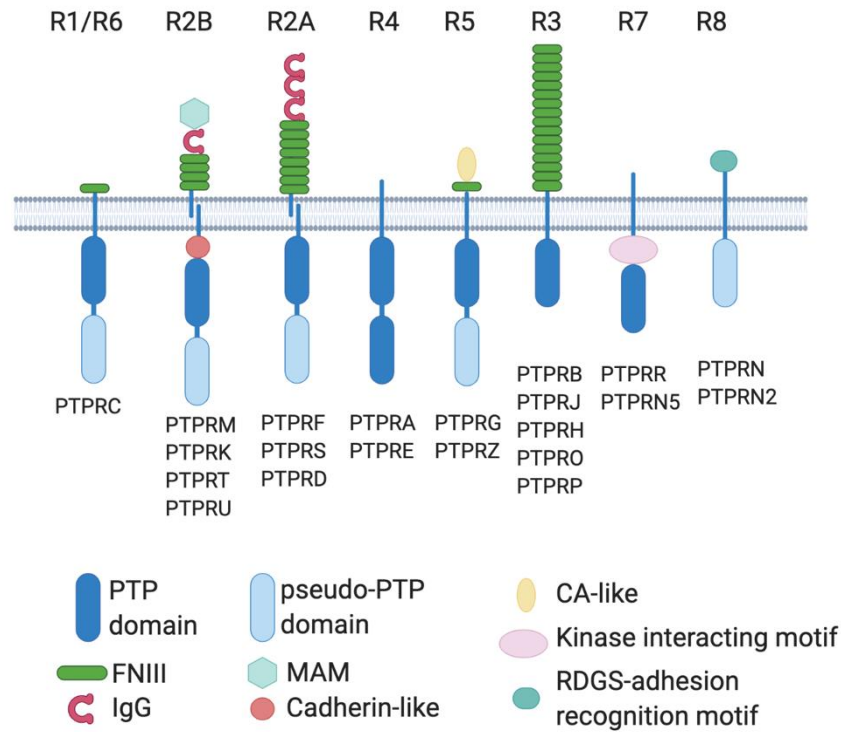


Figure 1.2 RPTP classification

Classification of the 21 receptor PTP's based on extracellular domain composition.

Generally, they contain variable extracellular cell-adhesion molecule domains, a single transmembrane domain, and two intracellular phosphatase domains. Created with BioRender.com.

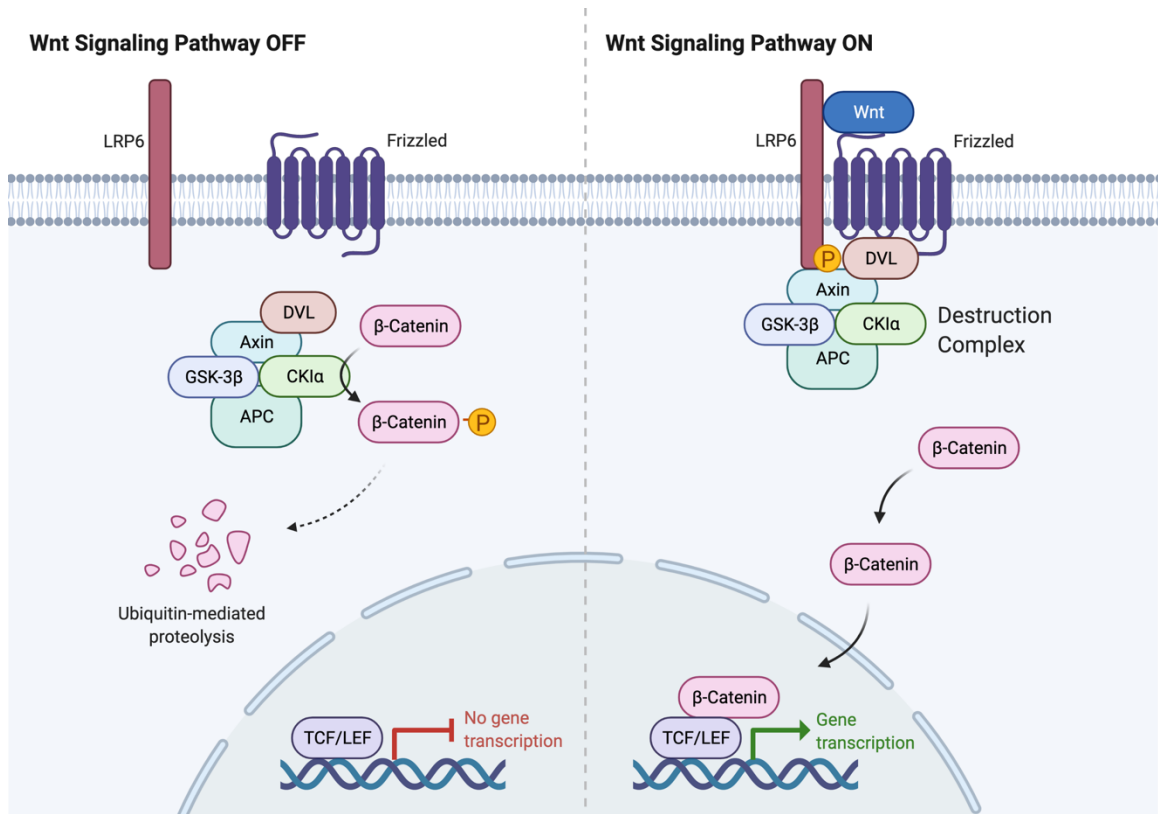


Figure 1.3 Wnt/ β -catenin signaling pathway

(Left) When Wnt ligand is absent, the destruction complex composed of APC, Axin, GSK3, and CK1 phosphorylates β -catenin for proteasomal degradation which blocks Wnt gene transcription. (Right) in the presence of extracellular Wnt ligand binding to receptors LRP6 and Frizzled, LRP6 is phosphorylated which binds and inhibits the destruction complex to allow β -catenin to translocate to the nucleus to activate Wnt target gene transcription. Adapted from “Wnt Signaling Pathway Activation and Inhibition”, by BioRender.com (2020). Retrieved from <https://app.biorender.com/biorender-templates>

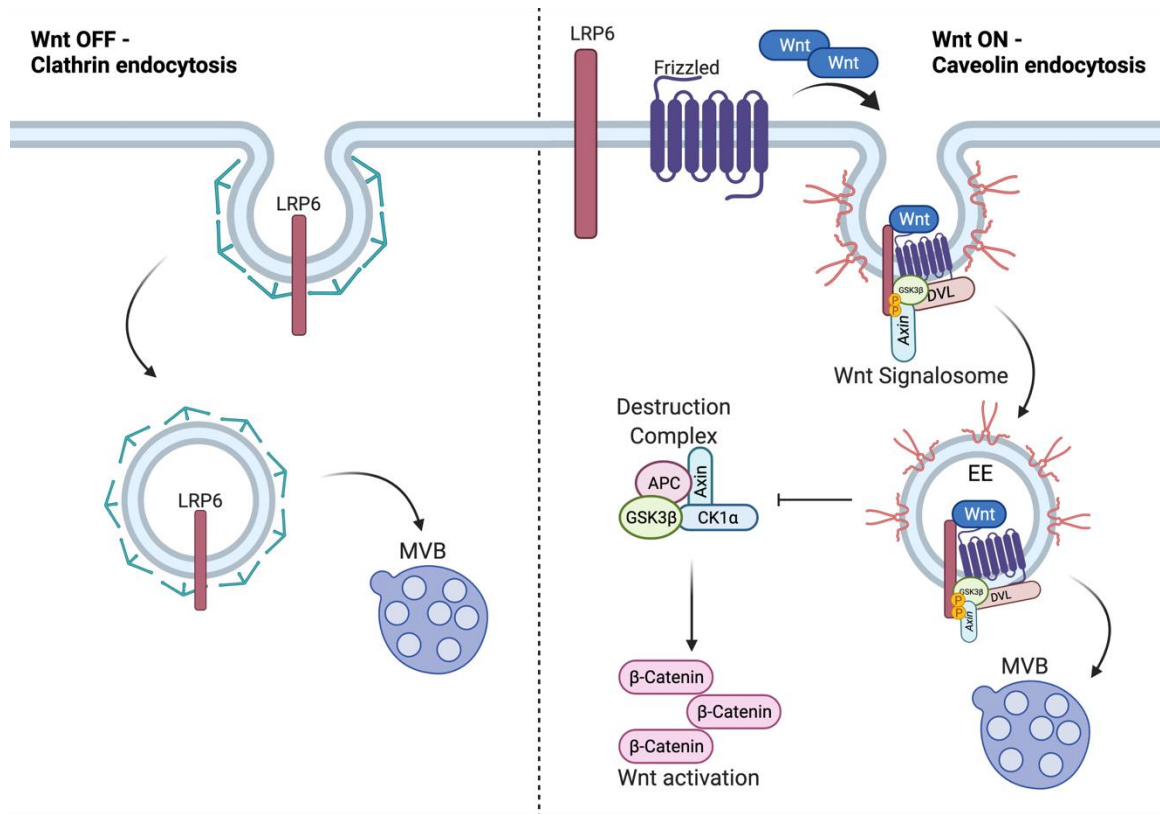


Figure 1.4 Endocytosis pathways that regulate Wnt signaling

(Left) When Wnt pathway is not activated, LRP6 receptors are removed from the membrane via clathrin endocytosis pathway. (Right) Active Wnt signaling leads to formation of the Wnt signalosome where receptors cluster and serve as a platform for signaling activation. The internalization of the signalosome via caveolin endocytic pathway inhibits the destruction complex which further helps activate Wnt pathway.

Adapted from [56]. Created with BioRender.com

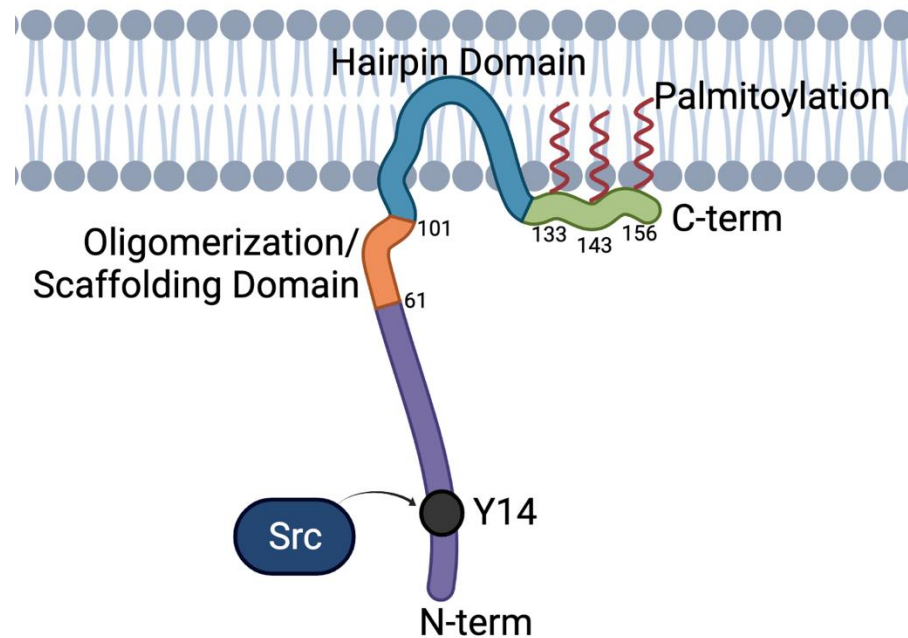


Figure 1.5 Caveolin1 Structure and domains.

Caveolin 1 is a hairpin-like integral membrane protein. It contains a N terminal tail that contains Y14 site that is phosphorylated by Src kinase, a dimerization domain where two Cav1 proteins bind together, a hairpin domain that inserts into the plasma membrane, and a C-terminal tail that is palmitoylated and binds to the membrane. Multiple Cav1 proteins associate together to form higher order complexes to form the caveolin coat. Adapted from Wong 2020 [99]. Created with BioRender.com

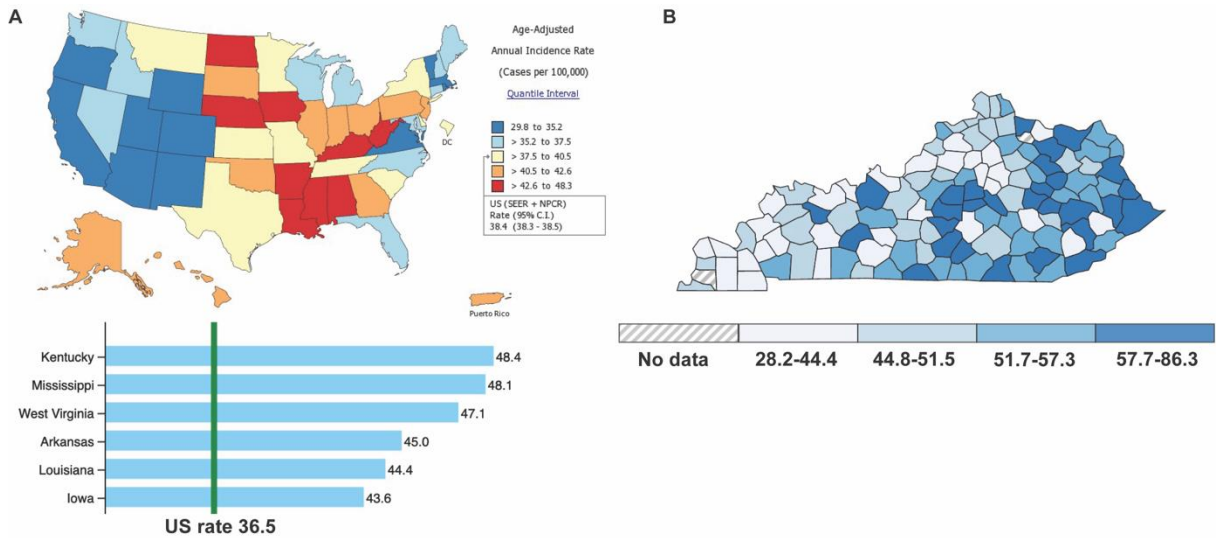


Figure 1.6 Incidence rate of Colorectal cancer in US and KY

(A) Map of United States colorectal cancer incidence rates. Kentucky ranks highest with rate of 48.4. (B) Kentucky county map of colorectal cancer incidence rate shows highest rates in eastern KY reaching 57-86 incidence rate. Figures Source: U.S. Cancer Statistics Working Group. U.S. Cancer Statistics Data Visualizations Tool, based on 2020 submission data (1999-2018): U.S. Department of Health and Human Services, Centers for Disease Control and Prevention and National Cancer Institute; <https://www.cdc.gov/cancer/dataviz>

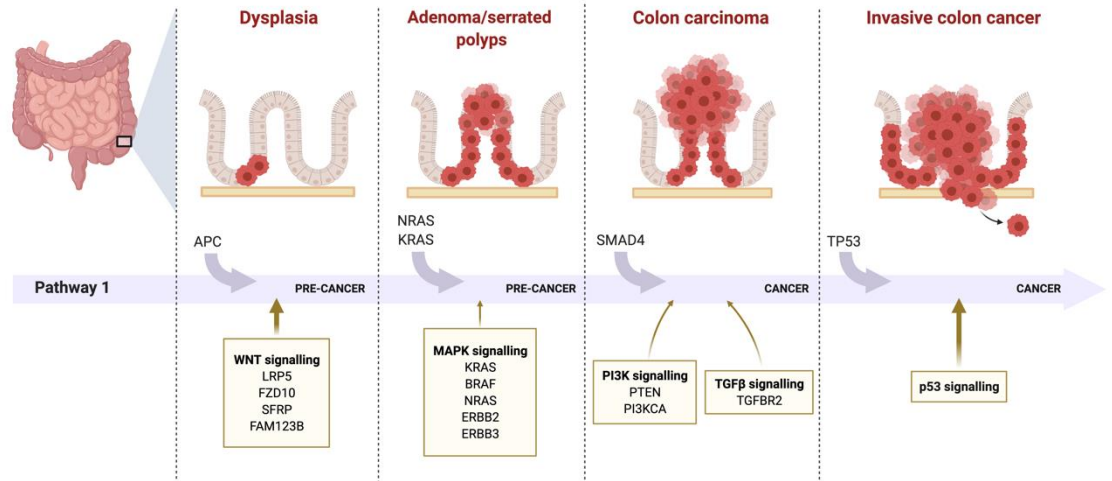


Figure 1.7 Colorectal Cancer Progression

Colorectal cancer is characterized by the formation of adenoma polyps in the colon that progress to carcinomas. The main driver of this process is mutations in the Wnt signaling pathway, mainly lost-function mutations in APC and gain-function mutations in β -catenin that initiate oncogenic transformation of normal intestinal epithelial cells into cancerous adenomas. Throughout the adenoma to carcinoma sequence, additional mutations in RAS, TP53, SMAD, PIK3CA and PTEN pathways are acquired to help advance to invasive colon cancer. Adapted from “Colon Cancer Progression”, by BioRender.com (2020). Retrieved from <https://app.biorender.com/biorender-templates>

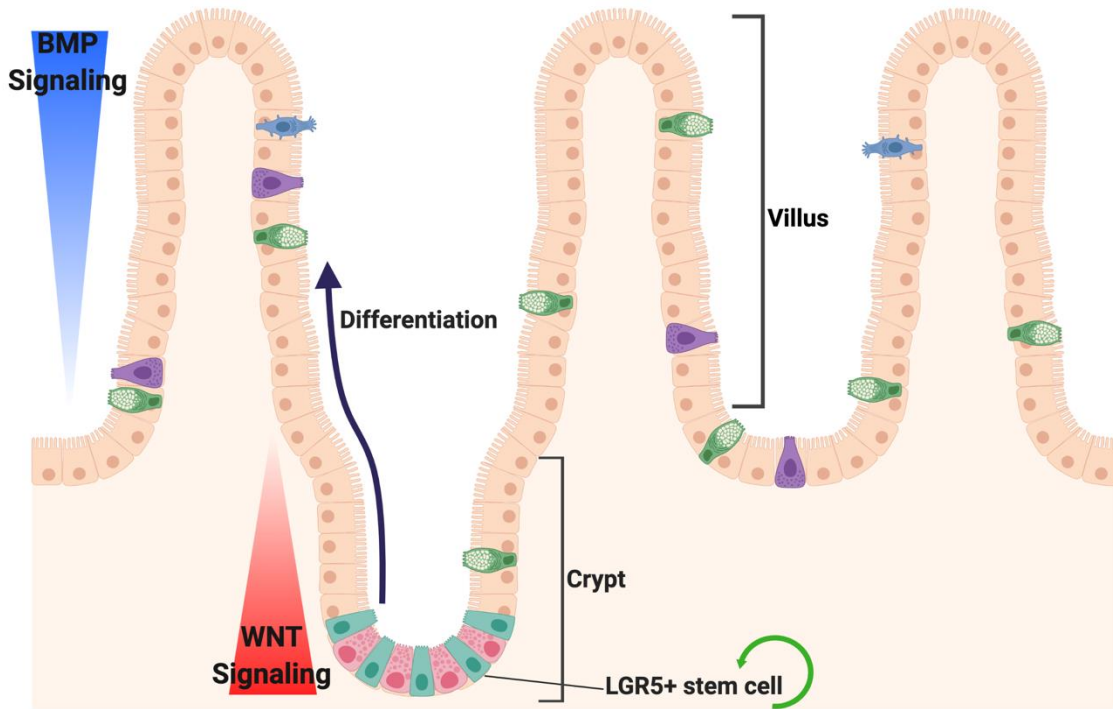


Figure 1.8 Intestinal Physiology and Signaling pathways

The intestine is divided into 2 structures: crypts located at the base and villi that extend out into the lumen. The crypt base contains the intestinal stem cells (ISC) that self-renew and give rise to all epithelial cell types that differentiate up the villus to replace cells every 3-5 days. Wnt signaling is most active at the crypt base and is critical for self-renewal of the ISCs, whereas at the villus BMP signaling is active to guide cell differentiation. Adapted from [100]. Created with BioRender.com.

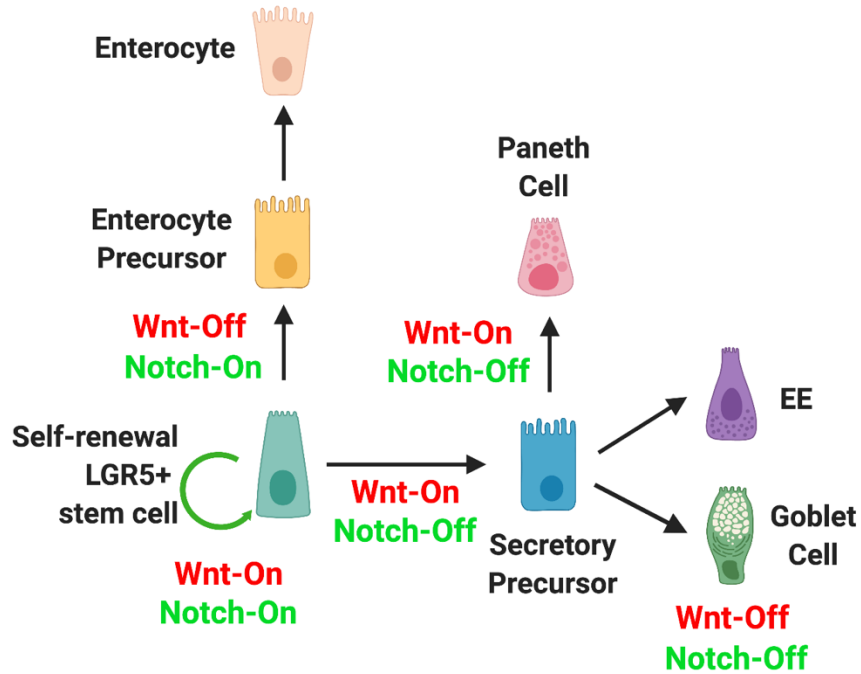


Figure 1.9 Intestinal epithelial cell lineage differentiation pathway

The differentiation of ISC into either absorptive or secretory lineage depends on the balance of the Wnt and Notch pathways. High Wnt and Notch signaling help the ISC self-renew. When Wnt is low and Notch is high, cells follow the absorptive lineage. When Wnt is high and Notch is low, cells follow the secretory pathway. Paneth cells differentiate down the crypt, so they require Wnt on and Notch off, however EE and Goblet cells are achieved with both pathways off as the cells move up the villus. Created with BioRender.com

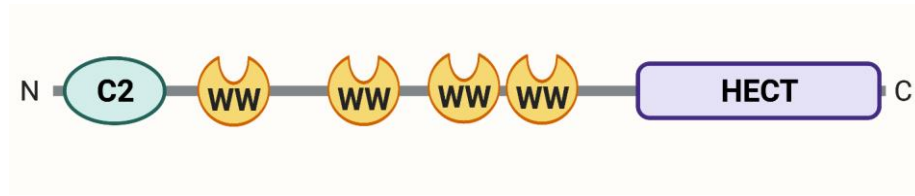


Figure 1.10 NEDD4L structure and domain map

NEDD4L is an E3 ubiquitin ligase. It contains N-terminal C2 calcium phospholipid binding domain, 4-WW domains for substrate interaction, and C-terminal HECT E3-ligase domain.

Figure created with BioRender.com

CHAPTER 2. MATERIALS AND METHODS

2.1 Methods to study Colorectal Cancer

2.1.1 Cell lines and Reagents

Primary colon cancer PT130 cells were established from patient-derived xenografts (PDX) as described previously [101, 102]. Mutational analysis showed that PT130 cells carry mutations in BRAF, TP53 and FBXW7 (but no mutations in APC and CTNNB1). Human colon cancer HCT116 cells, Wnt3A producing L cells and control L cells were purchased from ATCC. Human colon cancer cell lines were authenticated using short tandem repeat (STR) DNA profiling and tested negative for mycoplasma using PCR in March 2016 (Genetica, OH, USA). Cells were cultured in DMEM (PT130 and L cells) or McCoy's 5A medium (HCT116) supplemented with 10% fetal bovine serum (FBS, Sigma-Aldrich) and 1% penicillin-streptomycin. Stable PTPRF knockdown cells were generated using lentivirus-mediated RNAi and puromycin selection as described previously [103-105]. The shRNA targeting sequences for human PTPRF are as the following: 5'-CTTTACCCTTACTGGCCTCAA-3' (A3) and 5'-GCGATCACAGAGGAACTACAT-3' (A4); and for mouse Ptprf: 5'-CCACCAGTGTACTCTGACAT-3'. CHIR99021 and Pitstop-2 were obtained from Sigma-Aldrich.

The pCS-hLRP6-GFP construct was generously provided by Dr. Christof Niehrs (Institute of Molecular Biology, Germany) [106]. The pCMV6-XL5-hPTPRF (SC128009) and pCMV6-mPTPRF-Myc/Flag (MR222818) expression constructs were purchased from Origene. To construct RFP-tagged PTPRF, a monomeric RFP was fused in-frame to the C-terminus of full-length PTPRF and cloned into pcDNA3 vector.

2.1.2 Cell Proliferation Assay

Control and PTPRF knockdown colon cancer cells were seeded into 12-well plates (25,000 cells /well) and cultured in regular growth medium for 3-5 days. At the end of the experiments, cells were fixed and stained with 0.5% crystal violet in 20% methanol. The stained cells were dissolved in 1% SDS and absorbance at 570 nm was determined as described previously [102, 103]. For 3D cell growth, control and PTPRF knockdown cells were seeded into 12-well plates (30,000 cells/well) in 50% Matrigel and cultured in regular growth medium for 7 days. The relative cell growth was determined using the CellTiter-Glo 3D viability assay (Promega).

Tumor organoids derived from Apc/Kras double mutant mice was generated and described previously [101, 102]. To generate stable control and Ptprf knockdown organoids, tumor organoids were dissociated into small cell clusters using TrypLE (Thermo) and incubated with sh-Control or sh-Ptprf lentivirus in suspension. Cells were subsequently embedded in Matrigel in 3D growth medium (Advanced DMEM/F12 supplemented with 1×Glutamax, 1×N-2, 1×B-27, 1 mM N-Acetyl-L-cysteine and 1% penicillin/streptomycin), and puromycin was used to select for stable knockdown cells. To detect proliferating cells in tumor organoids, control and Ptprf knockdown Apc/Kras mouse tumor organoids were seeded into Matrigel and allowed to grow for 3 days until small organoids formed. The organoids grown in 3D were incubated with 5-ethynyl-2'-deoxyuridine (EdU) for 1 h prior to fixation. The EdU positive cells were stained using Click-iT EdU Alexa Fluor 488 Imaging Kit (Thermo). The organoids were washed with PBS and resuspended in DAPI-mounting media. Images were taken using a Nikon A1⁺ confocal microscope.

2.1.3 In vitro colony formation assay

For colony formation assays, control and Ptpf knockdown Apc/Kras tumor organoids were dissociated and single cell suspensions were subseeded into 3D Matrigel. The number of tumor organoids formed after 6 days were counted and analyzed. For gene expression analysis, tumor organoids were cultured in 3D Matrigel for 3-4 days and collected for RT-PCR.

For colony formation using HCT116 cells, 1,000 single cell suspensions of control and PTPRF knockdown cells were seeded in non-adherent 24-well plates in StemPro hESC SFM medium supplied with 1% GlutaMAX, 2% StemPro hESC supplement, 1.8% BSA, 8 ng/mL FGF-basic and 0.1 mM 2-mercaptoethanol (Thermo). After six days in culture, numbers of spheroids were counted under a light microscope.

2.1.4 Western blot analysis

Colon cancer cells or tumor tissues were collected and detergent-solubilized cell lysates were obtained as described previously [101, 102, 105]. Equal amounts of total protein lysates were resolved by SDS-PAGE and subjected to Western blot analysis. The following antibodies, including phospho-LRP6 (p-LRP6, Ser1490 site, #2568), total LRP6 (#2560), active- β -catenin (#8814), total β -catenin (#8480), phospho-GSK3 α/β (Ser21/9, #9331) and total GSK3 α/β (#5676) antibodies were purchased from Cell Signaling; the LAR monoclonal antibody (against the E-domain of PTPRF, sc-135969) was from Santa Cruz; PTPRF (against the P-domain of PTPRF, MABN604), γ -tubulin (T6557) and β -actin (A1978) antibodies were from Sigma-Aldrich.

2.1.5 Immunoprecipitation

CRC cell lines were transfected with PTPRF (or PTPRF-RFP) and LRP6-GFP expression plasmids using Lipofectamine 3000 (Thermo). Cells were then treated with Wnt3A conditioned media for indicated time and lysed in PPHB lysis buffer (50mM Na₂HPO₄, 1mM sodium pyrophosphate, 20mM NaF, 2mM EDTA, 2mM EGTA, 1% Triton X-100, pH 7.4, 1mM DTT, 200 μM benzamidine, 40 μg/mL leupeptin, 200 μM PMSF) as described previously [104, 105, 107]. The detergent-solubilized cell lysates were incubated with the anti-GFP nanobody affinity gel (Biolegend) overnight and subsequently washed 3 times with lysis buffer. The beads bound proteins were subjected to SDS-PAGE and Western blot analysis.

2.1.6 Quantitative RT-PCR

To measure relative gene expression by RT-PCR, total RNA was isolated from human cancer cells, mouse tumor organoids, or xenograft tumor tissues using the RNeasy Mini kit (Qiagen). Equal amounts of RNA were used as templates for the synthesis of cDNA using the High Capacity cDNA Reverse Transcription kit (Thermo). The resulting cDNA templates were placed into a 96 well plate with SYBR Green Master Mix (Qiagen) and primers listed in Supplemental Table S1. The RT-PCR assays were performed using StepOnePlus RT-PCR system (Thermo). All values were normalized to the level of β-actin.

2.1.7 Wnt reporter assay

Stable HEK293 Wnt reporter cells co-expressing p8xTOPFlash firefly and control Renilla luciferase plasmids were generated as described previously [108] and provided by Dr. Wei Chen (Duke University). The cells were infected with control or sh-PTPRF lentivirus and subsequently treated with Wnt3A-conditioned media for 4, 6, and 24 h as indicated. Alternatively, the cells were transfected with PTPRF expression plasmids and treated with Wnt3A-conditioned media for 8 h. The TOP-Flash activity was measured using the Dual-Luciferase Reporter Assay System (Promega). The relative Wnt activation was expressed as fold changes over untreated control cells and normalized to control cells.

2.1.8 Immunofluorescence staining

PT130 cells transfected with LRP6-GFP and PTPRF-RFP alone or in combination were seeded onto glass coverslips. The cells were fixed in 4% paraformaldehyde for 15 minutes and mounted in DAPI-mounting media. Images were taken using a Nikon A1+ confocal microscope. Pearson's colocalization coefficient was determined using Nikon NIS-elements software.

2.1.9 RNA sequencing (RNA-seq) analysis

To generate RNA expression profiles of control and PTPRF knockdown (sh-PTPRF-A3) PT130 cells, total RNA was isolated using RNeasy mini kit (Qiagen) and treated with DNase (Thermo). Sequencing libraries were generated and sequencing

performed by BGI Genomics. For the differential expression analysis, HTSeq was used to count gene expression level and DESeq2 was used to identify differentially expressed genes (fold change > 2) between the sh-PTPRF and control group. The mRNA expression data were subjected to the Gene Set Enrichment Analysis (GSEA) as described below to identify significantly enriched pathways.

2.1.10 *In vivo* xenograft tumor model

All animal procedures were done using protocols approved by the University of Kentucky Animal Care and Use Committee. Six to eight week-old NOD.Cg-Prkdcscid Il2rgtm1Wjl/SzJ (NSG, The Jackson Laboratory) mice were used. Control and sh-PTPRF-A3 HCT116 cells grown in regular growth medium were trypsinized. Total 1×10^6 cells were re-suspended in 5% Matrigel/DMEM at a final volume of 100 μ l and inoculated subcutaneously. Total six and ten mice were included in the control and sh-PTPRF group, respectively. The tumor size was measured with a digital caliper starting at 1 week after injection, and the measurements were repeated at week 2 and increased in frequency to 3 times per week thereafter. The tumor volume was defined as (longest diameter) \times (shortest diameter)²/2. At the end of 5 weeks, tumors were harvested and subjected to mRNA and protein analysis.

2.1.11 Statistical Analysis

In experiments to assess relative cell growth, EdU labeling, mRNA expression, colony formation and Wnt reporter activities, results were summarized using bar graphs and pairwise comparisons between different conditions were carried out using two-sample t-tests. A linear mixed model was employed to compare slope of tumor volume growth curves over time between groups. For the quantitative protein and mRNA expression analysis in xenograft tumors, represent average of 4 tumors in the control and 6 tumors in the sh-PTPRF group. All other experiments were repeated three times and results shown represent the average of three experiments.

For the Gene Set Enrichment Analysis (GSEA), the RNA-seq dataset from the TCGA Colon Adenocarcinoma (COAD) study were used and correlations between expressions of PTPRF and other genes were quantified by Spearman's correlation coefficient. The genes were then ordered from highest to lowest based on the correlation coefficient. For RNA-seq data obtained from control and sh-PTPRF cells, the fold change of each gene and p-value were used to create the ranked file list. The ranked list was inputted into the GSEA Desktop Application [109] to identify pathways that are associated with PTPRF expression in colon cancer or differentially enriched in PTPRF knockdown cells.

2.2 Methods to study Ubiquitination

2.2.1 Plasmids

The expression plasmids for mouse WT PTPRF with C-terminal Myc/Flag tag and human WT PTPRF with no tag were purchased from Origene [pCMV6-PTPRF-Myc/Flag

(MR222818) and pCMV6-XL5-PTPRF (SC128009), respectively]. The pSpCas9(BB)-2A-Puro (PX459) plasmid was obtained from Addgene (plasmid #62988). The following PTPRF mutants, including C1539S (catalytically inactive C/S mutant), Δ D1 (internal D1 domain deletion) and Δ D2 (deletion of the D2 domain), were generated using QuikChange mutagenesis. The coding sequence of WT, C/S, Δ D1 and Δ D2 mutant PTPRF were subcloned into pcDNA3-mRFP vector to create C-terminal RFP tagged PTPRF expression plasmids. To create PTPRF knockout (KO) cells using CRISPR/Cas9, guide RNAs (gRNAs) targeting exon 9 and exon 15 of human PTPRF were cloned into PX459 vector. The targeting sequences of gRNA are as the following: 5'-ACAAGCACAACACCGACGCG-3' (exon 9) and 5'-ACGACATCAAGGTCCGCGCA-3' (exon 15). The HA-tagged and His-tagged wild-type and catalytically inactive mutant of NEDD4L expression plasmids were obtained from Addgene (pCI-HA-NEDD4L, #27000; pCI-HA-NEDD4L/DD, #27001; pcDNA4-His-hNEDD4-2, #83433; pcDNA4-His-hNEDD4-2/CS, #86041). The pCI-HA-NEDD4L/DD plasmid contains C942A [110] whereas pcDNA4-His-hNEDD4-2/CS contains C942S mutation in the HECT domain [111]. Both mutants were termed NEDD4L/DD to distinguish them from the PTPRF-C/S mutant. Stable NEDD4L knockdown 293T cells were generated using lentivirus-based RNAi as previously described [51, 112]. The shRNA targeting sequences for human NEDD4L are as the following: 5'-GTTGCTGGTCTGGCCGTATTT-3' (B10) and 5'-GCCGATGAGAATAGAGAACTT-3' (B11). The CFP-Hrs and YFP-ubiquitin expression plasmids were kindly provided by Dr. Emily Galperin (University of Kentucky). The WT HA-tagged ubiquitin (HA-Ub) and a set of mutant ubiquitin

expression plasmids, including HA-Ub-K29, HA-Ub-K48 and HA-Ub-K63, were generously provided by Dr. Matthew Gentry (University of Kentucky).

2.2.2 Cell culture and reagents

293T cells (ATCC) cells were maintained in Dulbecco's modified Eagle medium (DMEM) supplemented with 10% fetal bovine serum (FBS) and 1% penicillin-streptomycin. PTPRF KO cells were generated by transfecting 293T cells with PX459-PTPRF-gRNA plasmids and selected with puromycin. Single clones of PTPRF KO cells were confirmed by sequencing of targeted genomic regions. Nystatin and Pitstop2 were purchased from Sigma-Aldrich. Polyethylenimine (PEI) was obtained from Polysciences. Wnt conditioned media were produced from L Wnt-3A cells (ATCC) cultured in DMEM + 10% FBS + 1% penicillin-streptomycin.

2.2.3 Immunofluorescence (IF) imaging

293T cells were seeded onto poly-lysine coated coverslips and subsequently transfected with a combination of plasmids as indicated using PEI-mediated methods [113, 114]. The localization of exogenously expressed proteins were revealed by fluorescence tags or antibody staining according to previously described method [115]. Briefly, cells were fixed in paraformaldehyde, permeabilized with 0.1% Triton-X100 and incubated with blocking buffer (PBS containing 1% BSA and 2% normal goat serum). The NEDD4L antibody (Cell Signaling, #4013) and Alexa 488-conjugated goat anti-rabbit secondary antibody were used to detect the expression of NEDD4L. Cell nuclei were stained with

DAPI-containing mounting medium. Images were acquired using Nikon Ti2 confocal microscope and Pearson coefficient was determined using Nikon NIS-elements software. To quantitatively describe the localization pattern of PTPRF, randomly chosen imaging fields were scored for the percentage of cells with PTPRF puncta. The results were averaged and statistically analyzed.

2.2.4 Ubiquitination assays and western blot analysis

293T cells were collected and detergent-solubilized cell lysates were obtained as described previously [101, 102, 105]. Equal amounts of total protein lysates were resolved by SDS-PAGE and subjected to western blot analysis. For detection of PTPRF ubiquitination, cells were co-transfected with HA-Ub. Detergent-solubilized cell lysates were immunoprecipitated with the anti-FLAG M2 affinity gel (Sigma-Aldrich) and the ubiquitination was detected using the HA antibody. The following antibodies were used for western blot analysis, and NEDD4L antibodies were purchased from Cell Signaling; the LAR monoclonal antibody (against the E-domain of PTPRF, sc-135969) was from Santa Cruz; PTPRF (against the P-domain of PTPRF, MABN604), anti-HA high affinity rat monoclonal antibody (3F10) and β -actin (A1978) antibodies were from Sigma-Aldrich.

2.2.5 Wnt reporter assays

PTPRF KO cells were co-transfected with p8xTOPFlash Firefly and control Renilla luciferase plasmids using PEI-mediated transfection. The transfected cells were treated with Wnt3A-conditioned media for 8 h. The TOP-Flash activity was measured using the

Dual-Luciferase Reporter Assay System (Promega). The relative Wnt activation was expressed as fold changes over control cells.

2.2.6 Statistical analysis

Quantitative results from at least three independent experiments are presented as means with SD as indicated in figure legends. Statistical analyses were performed using the GraphPad software. Student's t-test and one-way ANOVA were used for pairwise and multiple comparisons, respectively.

2.3 Methods to Study Intestinal Stem Cells

2.3.1 Cells and reagents

293T cells (ATCC) cells were maintained in Dulbecco's modified Eagle medium (DMEM) supplemented with 10% fetal bovine serum (FBS) and 1% penicillin-streptomycin. PTPRF KO cells were generated by transfecting 293T cells with PX459-PTPRF-gRNA plasmids and selected with puromycin. Single clones of PTPRF KO cells were confirmed by sequencing of targeted genomic regions. Polyethylenimine (PEI) was obtained from Polysciences. Wnt conditioned media were produced from L Wnt-3A cells (ATCC) cultured in DMEM + 10% FBS + 1% penicillin-streptomycin. The following organoid culture supplements were obtained from Thermo, including N-2 Supplement (100X) (#17502-048), B-27 Supplement (50X) (#17504-044) and GlutaMAX (100X) (#35050061). EGF (#AF-100-15B), Noggin (#250-38B) and R-spondin-1 (#120-38B)

were purchased from Peprotech; and N-Acetyl-L-cysteine (#A9165) was from Sigma-Aldrich.

2.3.2 Expression plasmids

The expression plasmids for mouse WT PTPRF with C-terminal Myc/Flag tag was purchased from Origene [pCMV6-PTPRF-Myc/Flag (MR222818)]. The pSpCas9(BB)-2A-Puro (PX459) plasmid was obtained from Addgene (plasmid #62988). The catalytically inactive PTPRF (C1539S, termed C/S mutant) was generated using QuikChange mutagenesis. The coding sequence of WT PTPRF were subcloned into pcDNA3-mRFP vector to create C-terminal RFP tagged PTPRF expression plasmid. To create PTPRF knockout (KO) cells using CRISPR/Cas9, guide RNAs (gRNAs) targeting exon 9 and exon 15 of human PTPRF were cloned into PX459 vector. The targeting sequences of gRNA are as the following: 5'-ACAAGCACAACACCGACGCG-3' (exon 9) and 5'-ACGACATCAAGGTCCGCGCA-3' (exon 15). The C-terminal GFP-tagged LRP6 plasmid (pCS2-LRP6-GFP) was generously provided by Dr. Christof Niehrs (DKFZ, Heidelberg, Germany) [116] The coding sequence of LRP6-GFP was subcloned into pcDNA4 vector.

2.3.3 Western blot

Cells or mouse tissues were collected and lysed in lysis buffer to obtain detergent-solubilized cell lysates as described previously [101, 102, 105]. Equal amounts of total protein lysates were resolved by SDS-PAGE and subjected to western blot analysis. The

following antibodies were used for western blot analysis; phospho-LRP6 (p-LRP6, Ser1490 site, #2568), total LRP6 (#2560), total Cav1 (#3267) and Myc (#13987) antibodies were purchased from Cell Signaling; the phospho-Cav1 (Tyr14) was from Invitrogen (#PA5-37506); the LAR monoclonal antibody (against the E-domain of PTPRF, sc-135969) was from Santa Cruz; PTPRF (against the P-domain of PTPRF, MABN604) and β -actin (A1978) antibodies were from Sigma-Aldrich.

2.3.4 Immunofluorescence staining

293T cells were seeded onto poly-lysine coated coverslips and subsequently transfected with a combination of plasmids as indicated using PEI-mediated methods [113, 114]. The localization of exogenously expressed proteins were revealed by fluorescence tags or antibody staining according to previously described method [115]. Briefly, cells were fixed in paraformaldehyde, permeabilized with 0.1% Triton-X100 and incubated with blocking buffer (PBS containing 1% BSA and 2% normal goat serum). The LRP6 antibody (R&D, #MAB1505) and Alexa 488-conjugated goat anti-rabbit secondary antibody were used to detect the expression of LRP6. To prepare frozen mouse tissue sections, proximal intestines were opened longitudinally, formalin fixed for 2 h and then switched to 30% sucrose solution. Cryostat sectioning of frozen tissues were carried out by the Biospecimen Procurement and Translational Pathology Shared Resource Facility. To stain for proliferating cells and Paneth cells, the Ki67-Cy5 antibody (Invitrogen #50-5698-82) and LYZ1 (DAKO #A0099) antibody were used, respectively. Briefly, the frozen sections were thawed and washed in PBS with 1% DMSO and 0.1% Triton X-100. Sections were permeabilized and blocked with 1% BSA in PBST with 0.2% Triton X-100 for 1 h.

Fluorescent-conjugated primary antibody was incubated in PBS with 1% BSA in PBST with 0.1% Triton X-100 overnight at 4°C, then washed as described above followed by mounting. The nuclei were stained with DAPI-containing mounting medium. Images were acquired using Nikon Ti2 confocal microscope.

2.3.5 Mice

The generation of whole body PTPRF KO mice was previously described [24]. Mice were obtained from Dr. Maxime Bouchard (McGill University) with the permission of Dr. Wiljan Hendriks (Radboudumc). Two cohorts of mice were included in the studies: PTPRF^{+/+} (WT) and PTPRF^{-/-} (KO). Lgr5-EGFP-IRES-CreERT2 (Lgr5-EGFP) mice were obtained from Jackson Laboratory (B6.129P2- Lgr5^{tm1}(cre/ERT2)Cle/J, stock number 008875). To visualize Lgr5⁺ intestinal stem cells, Lgr5-EGFP mice were crossed to WT and PTPRF KO mice. Paired 8-10-week-old mice were used for experiments. All procedures were approved by the Institutional Animal Care and Use Committee of the University of Kentucky. Mice were maintained on a 14 h light/10 h dark cycle and provided with food and water ad libitum.

2.3.6 Intestinal crypt isolation and colony formation assays

Crypts were isolated as described previously [117]. Briefly, the small intestine was removed, opened longitudinally, washed with PBS, and cut into 3–5mm fragments. Fragments were incubated in cold PBS containing 10 mM EDTA for 60 min on ice, followed by vortexing and filtration through a 70 µM cell strainer. Isolated crypts were

collected for RNA and protein extraction or organoid colony formation. For organoid culture, crypts were embedded in growth factor reduced Matrigel (Corning) and cultured in ENR media [Advanced DMEM/F12 medium supplemented with penicillin/streptomycin, 1X Glutamax, 1X N-2, 1X B-27, and 1mM N-Acetyl-L-cysteine, EGF (40 ng/ml), Noggin (100 ng/ml) and R-spondin (1 µg/ml)]. For colony formation assays, freshly isolated crypts were manually counted and plated in triplicate in a 48-well plate. The colony (organoid) formation efficiency was quantified 3 days after initiation of cultures and normalized to the number of crypts plated per well at day 0.

2.3.7 FACS analysis of Lgr5-EGFP⁺ intestinal stem cells

Crypts were prepared for flow cytometry analysis as described previously [117]. Briefly, freshly isolated intestinal crypts were incubated in TrypLE Express (Invitrogen) for 15 minutes at 37°C and then passed through a 23G needle to achieve a single-cell suspension. Cells were washed in PBS, resuspended in PBS containing 1 mM EDTA, 25 mM HEPES, 1% FBS and DNase I (1 µg/mL), and filtered through a 40-µm cell strainer. Cells were labeled with epithelial cell adhesion molecule (EPCAM)-APC (BioLegend), and sorted with a BD FACS Symphony machine. Lgr5-EGFP⁺/EPCAM⁺ cells were quantified using FlowJo software.

2.3.8 RNA *in situ* hybridization (ISH)

RNAscope ISH assays were used to detect Lgr5 mRNA expression in mouse intestinal tissues. Briefly, single molecule ISH was performed using Advanced Cell

Diagnostics automated RNAscope 2.5 Leica Systems (Mm-Lgr5 probe, #312178) by the Markey Cancer Center Biospecimen Procurement and Translational Pathology Shared Resource Facility. Stained sections were imaged using an Aperio ScanScope XT slide scanner at 20X and Lgr5 expression was quantified using HALO software (Indica Labs).

2.3.9 Statistical analysis

Quantitative results from at least three independent experiments are presented as means with SD as indicated in figure legends. Statistical analyses were performed using the GraphPad software. Student's t-test and one-way ANOVA were used for pairwise and multiple comparisons, respectively.

Table 2.1 Oligonucleotides utilized in qRT-PCR analysis.

	Name	Forward (5'-3')	Reverse (5'-3')
Human genes	<i>ACTB</i>	CATGTACGTTGCTATCCAGGC	CTCCTTAATGTCACGCACGAT
	<i>AXIN2</i>	TACTACTCCTTATTGGGCGATCA	TTGGCTACTCGTAAAGTTTTGGT
	<i>CCND1</i>	TGGAGCCCGTGAAAAAGAGC	TCTCCTTCATCTTAGAGGCCAC
	<i>LGR5</i>	TCAGTCAGCTGCTCCCGAAT	CGTTTCCCGCAAGACGTAAC
	<i>MKI67</i>	AGAAGAAGTGGTGCTTCGGAA	AGTTTGCGTGGCCTGTACTAA
	<i>TCF7</i>	TTGATGCTAGGTTCTGGTGTACC	CCTTGGACTCTGCTTGTGTC
	<i>PTPRF</i>	ACCATGCTATGTGCCGCAG	CCTTGGTCGGATTCCCTCACT
Mouse genes	<i>Actb</i>	GGCTGTATTCCCCTCCATCG	CCAGTTGGTAACAATGCCATGT
	<i>Ccnd1</i>	TGACTGCCGAGAAGTTGTGC	CTCATCCGCCTCTGGCATT
	<i>Lgr5</i>	TGCCCATCACACTGTCACTGT	CACCCTGAGCAGCATCCTG
	<i>Ptprf</i>	TCCAGCCATTACGAGTGCAG	CCCATGTTCGATAGTCGGGAAC
	<i>Ki67</i>	ATCATTGACCGCTCCTTTAGGT	GCTCGCCTTGATGGTTCCT
	<i>Ascl2</i>	AAGCACACCTTGACTGGTACG	AAGTGGACGTTTGCACCTTCA
	<i>Sox9</i>	GTACCCGCATCTGCACAAC	TCCACGAAGGGTCTCTTCTC
	<i>Olfm4</i>	CAGCCACTTTCCAATTTCACTG	GCTGGACATACTCCTTCACCTTA
	<i>Bmi1</i>	ATCCCCACTTAATGTGTGTCCT	CTTGCTGGTCTCCAAGTAACG
	<i>Tcf7</i>	AGCTTTCTCCACTCTACGAACA	AATCCAGAGAGATCGGGGGTC
	<i>Myc</i>	TGAGCCCCTAGTGCTGCAT	AGCCCGACTCCGACCTCTT

CHAPTER 3. INHIBITION OF PROTEIN TYROSINE PHOSPHATASE RECEPTOR TYPE F SUPPRESSES WNT SIGNALING IN COLORECTAL CANCER

Gan T*, **Stevens AT***, Xiong X, Wen YA, Farmer TN, Li AT, Stevens PD, Golshani S, Weiss HL, Evers BM, Gao T. Inhibition of protein tyrosine phosphatase receptor type F suppresses Wnt signaling in colorectal cancer. *Oncogene*. 2020 Oct;39(44):6789-6801. PMID: PMC7606795. (*contributed equally)

3.1 Abstract

Wnt signaling dysregulation promotes tumorigenesis in colorectal cancer (CRC). We investigated the role of PTPRF, a receptor-type tyrosine phosphatase, in regulating Wnt signaling in CRC. Knockdown of PTPRF decreased cell proliferation in patient-derived primary colon cancer cells and established CRC cell lines. In addition, the rate of proliferation as well as colony formation ability were significantly decreased in tumor organoids grown in 3D, whereas the number of differentiated tumor organoids were markedly increased. Consistently, knockdown of PTPRF resulted in a decrease in the expression of genes associated cancer stem cells downstream of Wnt/ β -catenin signaling. Treating PTPRF knockdown cells with GSK3 inhibitor rescued the expression of Wnt target genes suggesting that PTPRF functions upstream of the β -catenin destruction complex. PTPRF was found to interact with LRP6 and silencing PTPRF largely decreased the activation of LRP6. Interestingly, this PTPRF-mediated activation of Wnt signaling was blocked in cells treated with clathrin endocytosis inhibitor. Furthermore, knockdown of PTPRF inhibited xenograft tumor growth *in vivo* and decreased the expression of Wnt target genes. Taken together, our studies identify a novel role of PTPRF as an oncogenic protein phosphatase in supporting the activation of Wnt signaling in CRC.

3.2 Introduction

Colorectal cancer (CRC) is the second leading cause of cancer deaths with the fourth highest cancer incidence in the US [118]. The incidence and mortality rates have decreased for the past several decades in adults ≥ 50 years old but have increased in those < 50 years old where tumors are more aggressive and conventional treatment are less effective [119, 120]. This increase in incidence has been concerning making the development of novel therapeutic targets a priority.

A common pathway for CRC development through the adenoma-carcinoma sequence is the dysregulation of the Wnt signaling pathway. Wnt is named after its simultaneous discovery in *Drosophila* segment polarity gene Wingless and murine proto-oncogene Int-1 [121]. The Wnt signaling pathway is a highly conserved pathway known to regulate cell migration, polarity, differentiation, proliferation, embryonic development and stem cell renewal [122-124]. Commonly, dysregulation in cancer occurs through the canonical or β -catenin dependent pathway [121]. This pathway consists of Wnt ligand binding to a transmembrane complex including the Frizzled family of Wnt receptors and co-receptor LRP5/6, and subsequent activation through the formation and endocytosis of the Wnt signalosome [125]. Wnt activation leads to inhibition of the β -catenin destruction complex, which includes Axin1, adenomatous polyposis coli (APC), the Ser/Thr kinases GSK-3 and CK1, protein phosphatase 2A (PP2A), and the E3-ubiquitin ligase β -TrCP, causing accumulation of cytoplasmic β -catenin to allow for the transcriptional activation of Wnt target genes (ie AXIN2, TCF7, CCND1 and MYC) [121, 122, 126, 127]. The Wnt signaling pathway is immeasurably complex with a multitude of components being discovered that can become potential targets for therapy.

Protein tyrosine phosphatases (PTP) act in conjunction with protein tyrosine kinases to modulate a large number of signaling pathways that are important in cancer. Whereas protein kinases have been extensively evaluated as translational targets in cancer treatment [128], significant knowledge gaps exist on the role of protein phosphatases in regulating oncogenic signaling [129]. The PTP superfamily consists of 107 members that are subdivided into four classes. The class I-III PTPs are cysteine-based phosphatases that use a similar catalytic mechanism despite having different substrate specificities; while the class IV PTPs are aspartate-based phosphatases [7]. Protein tyrosine phosphatase receptor type F (PTPRF) belongs to the classical subfamily of class I PTPs with PTPRD and PTPRS as close relatives [7]. Developmental biology studies using *Drosophila* models have demonstrated that loss-of-function mutations of PTPRF (initially named LAR for Leukocyte Common Antigen Related) disrupt normal axon guidance of neurons [130] and inhibits planar cell polarity signaling in epithelial cells [131]. Studies of PTPRF in cancer have yielded conflicting results showing that PTPRF functions as either an oncogene or a tumor suppressor in different cancer types [46, 132-136]. A gene expression analysis study showed that PTPRF expression is downregulated in a small numbers of adenocarcinoma samples of CRC compared to normal samples; however, no mechanistic studies have been performed [137].

In this study we determined the role of PTPRF in regulating CRC cell growth through modulation of the Wnt signaling pathway. Using primary patient derived colon cancer cells and mouse tumor organoid models, we showed that knockdown of PTPRF inhibited cell proliferation both in 2D cell culture and 3D organoids. Importantly, loss of PTPRF expression inhibited the activation of Wnt signaling *in vitro* and tumorigenesis *in*

vivo. Together, results from our study identified a novel oncogenic function of PTPRF via promoting Wnt signaling upstream of the destruction complex.

3.3 Results

3.3.1 Knockdown of PTPRF inhibits cell proliferation

To determine the functional role of PTPRF in CRC, we silenced PTPRF expression in two CRC cell lines, including HCT116 and patient-derived PT130 [101], using lentivirus-mediated RNAi with two different targeting sequences. As previously described, PTPRF consists of an extracellular domain (E-domain), a single transmembrane domain (TM) and an intracellular phosphatase domain (P-domain) (Figure 3.1A) [40]. The E-domain of PTPRF contains three immunoglobulin (Ig)-like and eight fibronectin type-III motifs, and a post-translational proteolytic cleavage separates the E-domain but it remains attached to the TM domain and the rest of the protein. The P-domain of PTPRF is comprised of a catalytically active D1 domain and a pseudophosphatase D2 domain [138]. The expression of PTPRF was downregulated in both stable knockdown cells as detected by two different antibodies raised against either the E-domain or the P-domain of the protein (Figure 3.1B). In contrast to previous studies performed in other cancer types in which PTPRF has been demonstrated to be a tumor suppressor [132, 133], we found that knockdown of PTPRF significantly decreased growth of both HCT116 and PT130 cells cultured in regular 2D growth conditions (Figure 3.1C) and in 3D Matrigel (Figure 3.1D). Collectively, these results provide the first evidence supporting that PTPRF plays a positive role in promoting cell growth and proliferation in CRC.

3.3.2 PTPRF expression suppresses colony formation in tumor organoids

We next evaluated the effect of silencing PTPRF using intestinal tumor organoids derived from Apc/Kras double mutant mice [102]. Control and PTPRF knockdown tumor organoids grown in 3D Matrigel were generated using lentiviral shRNA. Single cell suspension of Apc/Kras mouse tumor organoids were seeded in 3D Matrigel and the number of colonies (organoids) formed was determined after 6 days (Figure 3.2A). We found that the ability of PTPRF knockdown cells to form colonies in 3D was significantly decreased (Figure 3.2B). Interestingly, while a majority of control tumor cells formed spherical organoids in 3D, increasing numbers of PTPRF knockdown organoids showed branching phenotype (Figure 3.2C). In this tumor organoid model, branching phenotype is associated with decreased stem-like properties as measured by subsequent colony formation assays. Moreover, control and PTPRF knockdown organoids were labeled with EdU to assess the number of proliferating cells. Results showed that the relative levels of EdU positive cells were largely decreased in PTPRF knockdown organoids compared to the control group (Figure 3.2D). Quantitative real time PCR (RT-PCR) analysis demonstrated that the expression of Lgr5 and Ccnd1, a marker of stem cells and cell proliferation, respectively, was decreased in PTPRF knockdown tumor organoids (Figure 3.2E). Additionally, single cells of control and PTPRF knockdown HCT116 cells were cultured in suspension stem cell medium, a condition known to enrich tumor initiating cells [139], and numbers of spheroids (colonies) formed were counted after 6 days. We found that the numbers of spheroids formed were significantly decreased in PTPRF knockdown cells suggesting inhibition of colony formation (Figure 3.3). Taken together, our results suggest that knockdown of PTPRF may decrease tumor formation.

3.3.3 PTPRF suppression reduces Wnt signaling

Since the tumorigenesis process in CRC is largely controlled by Wnt signaling, we determined the effect of PTPRF downregulation on the expression of Wnt target genes. Results from RT-PCR analysis revealed that the levels of AXIN2, TCF7 and CCND1 were significantly decreased in both HCT116 and PT130 PTPRF knockdown cells (Figure 3.4A-B). Similar results were obtained in SW480 cells where silencing PTPRF decreased cell proliferation and Wnt target gene expression (Figure 3.5). Moreover, we determined the effect of silencing PTPRF on the activation of Wnt signaling using TOP-Flash reporter assays in 293T cells. While stimulation with Wnt-conditioned media markedly increased TOP-Flash luciferase activity over time, silencing PTPRF prevented the activation of Wnt signaling (Figure 3.4C). Western blot analysis of 293T cells used for TOP-Flash assays showed ~50% reduction in active β -catenin levels in PTPRF knockdown cells (Figure 3.4D-E). Furthermore, we found that overexpression of PTPRF in 293T resulted in an increase in Wnt activation as measured by TOP-Flash reporter activity (Figure 3.4F). Consistently, the levels of active β -catenin were increased in PTPRF overexpressing cells (Figure 3.4G-H). Together, these results indicate that PTPRF positively regulates Wnt signaling.

3.3.4 PTPRF regulates Wnt signaling at the level upstream of the destruction complex

To begin elucidating the molecular mechanism by which PTPRF regulates Wnt signaling, we treated cells with a GSK3 inhibitor, CHIR99021. As a key member of the β -catenin destruction complex, GSK3 β is responsible for direct phosphorylation of β -catenin

for degradation [140]. Inhibition of GSK3 results in activation of β -catenin-mediated transcription of Wnt target genes circumventing the destruction complex. Indeed, treatment with CHIR99021 increased the expression of Wnt target genes, including AXIN2 and TCF7, in both HCT116 and PT130 control cells. Moreover, GSK3 β inhibitor treatment largely rescued the expression of Wnt target genes in PTPRF knockdown cells (Figure 3.6A-B), suggesting that PTPRF functions upstream of the β -catenin destruction complex. As a control, we showed that silencing PTPRF did not alter GSK3 activity directly (Figure 3.7).

3.3.5 PTPRF interacts with LRP6

We next determined if PTPRF may regulate Wnt signaling at the receptor level. To this end, we evaluated the levels of phosphorylated LRP6, a Wnt co-receptor, as a readout for Wnt signaling activation in control and PTPRF knockdown cells. Results from Western blot analysis showed that when normalized to total LRP6 levels, the expression of phosphorylated LRP6 (at Ser1490) was significantly lower in PTPRF knockdown cells compared to the control in both HCT116 and PT130 cells (Figure 3.8A-B). Additionally, immunofluorescent staining experiments were performed to detect the cellular localization of LRP6 and PTPRF in PT130 cells. Since the antibodies for LRP6 and PTPRF were not sensitive enough to detect endogenous proteins, GFP-tagged LRP6 and RFP-tagged WT PTPRF were either expressed alone or co-expressed in PT130 cells. As shown in Figure 3.8C, the expression of PTPRF-RFP and LRP6-GFP was detected at the cell membrane as well as intracellular vesicles when expressed alone, although relatively higher levels of LRP6-GFP at the plasma membrane were observed compared to PTPRF-RFP. Moreover,

the colocalization of PTPRF-RFP and LRP6-GFP was readily detected in cells co-expressing both proteins (Figure 3.8D and Figure 3.9). Quantitative analysis revealed that the average Pearson's coefficient for PTPRF and LRP6 colocalization was 0.68. Interestingly, increasing localization of LRP6-GFP in large intracellular vesicles was observed in cells co-expressing PTPRF-RFP; however, the presence of LRP-GFP did not change the localization pattern of PTPRF-RFP.

To confirm that PTPRF regulates Wnt signaling at the receptor level, TOP-Flash Wnt reporter activity assays were performed in 293T cells transfected with either vector or Flag-PTPRF and subsequently treated with Pitstop 2 clathrin endocytosis inhibitor. Similar as shown in Fig. 3E, overexpression of PTPRF increased Wnt reporter activity; however, this effect was largely inhibited by treating cells with Pitstop 2, suggesting that PTPRF-mediated activation of Wnt signaling requires the endocytic pathway (Figure 3.10A). Moreover, similar experiments were performed in HCT116 cells using the TOP-Flash reporter. We found that PTPRF-induced Wnt activation was effectively blocked by the treatment with Pitstop 2 (Figure 3.10C). The overexpression of PTPRF protein was confirmed in these cells using Western blot analysis (Figure 3.10B and D).

Furthermore, we determined if PTPRF expression is associated with cancer-related pathways by analyzing gene expression data from the Cancer Genome Atlas (TCGA) colon cancer RNA-seq dataset. Results from the GSEA revealed that PTPRF expression is positively associated with CRC and Wnt signaling pathway (Figure 3.10E). As a control, the expression of PTPRF was also found to positively correlate with the axon guidance pathway, a previous known function of PTPRF. These data support our findings that PTPRF functions to promote tumorigenesis in colon cancer by promoting signaling

through the Wnt pathway. Other pathways associated with PTPRF expression are shown in Table 3.1. To better understand the role of PTPRF in colon cancer cells, we performed RNA-seq analysis in control and PTPRF knockdown PT130 cells. Results from the GSEA showed that PTPRF regulates a number of oncogenic signaling pathways (Table 3.2). Interestingly, the endocytosis pathway and colorectal cancer were also found to be positively enriched with PTPRF whereas the DNA replication and cell proliferation related processes were negatively enriched (Table 3.2). Together, results from these bioinformatic analyses are consistent with the notion that PTPRF expression enhances Wnt and other oncogenic signaling and knockdown of PTPRF inhibits cell proliferation.

3.3.6 Downregulation of PTPRF decreases *in vivo* tumor growth

Given the importance of Wnt signaling in sustaining tumor growth, we investigated the functional effects of PTPRF knockdown in regulating tumorigenesis *in vivo*. Control and PTPRF knockdown HCT116 cells were subcutaneously injected into NSG mice and tumor size was measured 3 times per week for a total of 6 weeks. We found that silencing PTPRF significantly reduced the rate of tumor growth over the follow-up period (Figure 3.11A) and the average weight of tumors derived from PTPRF knockdown cells was nearly three times smaller than of the control tumors (Figure 3.11B). Consistently, the level of phosphorylated LRP6 was significantly lower in PTPRF knockdown tumors (Figure 3.11C-D). Similar to our *in vitro* experiments, results from RT-PCR analysis of tumor tissues revealed that the expression of AXIN2, TCF7, CCND1 and Ki67 was decreased indicating decreased Wnt signaling and cell proliferation (Figure 3.11E). To support the potential oncogenic function of PTPRF, we analyzed the COSMIC database for altered

expression of PTPRF gene in human cancers. Consistently, upregulation of PTPRF gene was commonly detected in various cancer types (between 3-12% of patient samples) whereas downregulation of PTPRF was relatively rare (Table 3.3).

In summary, we demonstrated that downregulation of PTPRF leads to decreased cell proliferation and colony formation in colon cancer cells and 3D tumor organoids. In addition, xenograft tumorigenesis experiments showed that silencing PTPRF expression inhibits tumor growth *in vivo*.

3.4 Discussion

Hyperactivation of Wnt signaling drives tumorigenesis in CRC. Continuous efforts have been focused on determining mechanisms involved in the regulation of Wnt signaling to support tumor initiation, progression and cancer stem cell properties. In this study, we investigated the role of PTPRF, a receptor type PTP, in promoting cell proliferation and tumorigenesis by regulating Wnt activation. While the majority of previous studies define the role of PTPRF through the differential expression of PTPRF mRNA or protein in tumors compared to normal tissue, the underlying mechanisms of postulated PTPRF function in cancer remain largely unknown. Results from our study identified PTPRF as a novel positive regulator that functions upstream of the destruction complex to enhance Wnt signaling in colon cancer cells. Consistent with the role of PTPRF in promoting Wnt signaling, it has been shown previously that double knockout of PTPRF and closely related PTPRS in mice resulted in craniofacial malformations during embryonic development, a hallmark of Wnt signaling deficiency [141].

Although it has long been postulated that signaling events upstream of the destruction complex have limited impact on activating the Wnt pathway in cancer cells with APC or β -catenin mutations, recent studies have indicated that Wnt ligands produced by cancer cells play an important role in sustaining canonical Wnt signaling via a receptor-mediated autocrine mechanism [142]. Increasing evidence suggests that a gradient of Wnt signaling is required to regulate distinct cell functions even in tumors with APC or β -catenin mutations [143, 144]. Given the notion that highest levels of Wnt signaling activation are required to maintain cancer stem cell properties [145, 146], it is attractive to speculate that Wnt-dependent stimulation upstream of the destruction complex is needed to maintain the cancer stem cell population. Previous studies have implicated both caveolin- and clathrin-dependent endocytic pathways in facilitating Wnt-stimulated internalization of LRP6 and the formation of signalosomes [62, 147-149]. Notably, the requirement for clathrin-mediated endocytosis has been shown to promote the activation of Wnt signaling in cells with APC mutations [62]. Consistently, we found in our study that PTPRF colocalizes with LRP6 at the plasma membrane and intracellular vesicles and inhibition of clathrin-mediated endocytosis attenuates PTPRF's effect on activating Wnt signaling. Moreover, results from our RNA-seq analysis suggested that altered PTPRF expression affects pathways involved in endocytosis, endosomal sorting and cytoskeletal rearrangement in addition to its effects on regulating cell proliferation and oncogenic signaling pathways (Table 3.2). However, future studies are needed to address if PTPRF regulates the formation of LRP6-containing signalosomes via an endocytosis-dependent mechanism. Interestingly, the involvement of PTPRF in regulating vesicle trafficking has

recently been demonstrated in the recycling of integrin $\alpha 5\beta 1$ and secretion of fibronectin in endothelial cells [150].

Previous gene expression analysis of PTPRF in different cancer types has yielded seemingly contradictory conclusions depending on the cancer type. For example, studies in breast, gastric and liver cancer have suggested that PTPRF may serve as a tumor suppressor [35, 132, 136]; however, an oncogenic role of PTPRF has also been implicated in breast, prostate, thyroid and non-small cell lung cancer [49, 134, 151-153]. Currently, the mechanisms by which PTPRF regulates cancer phenotypes remain largely unknown. Given the notion that protein phosphatases commonly control multiple different substrates, it is likely that specific effects associated with altered PTPRF expression may depend on the predominant oncogenic pathways important for that particular cancer type. For example, it has been shown that silencing PTPRF expression promotes cell proliferation and tumor development as a result of increased SRC phosphorylation and activity in hepatocellular carcinoma [136]. However, we did not observe any changes in SRC phosphorylation in PTPRF knockdown CRC cells used in our study. In addition, we found that the expression of PTPRD and PTPRS, two closely related members in the PTPRF subfamily, may become upregulated in PTPRF knockdown cells. Both PTPRD and PTPRS have consistently been identified as tumor suppressors in various cancer types. Thus, the compensatory effect among PTPRF subfamily members may add another layer of complexity to the cell-type and cell-context dependent differences in PTPRF functions. Results from our study identify a functional connection between PTPRF and LRP6 in positively regulating Wnt signaling, thus supporting a tumor prompting role of PTPRF in CRC. However, more studies are needed to further determine the molecular mechanisms by which PTPRF regulates Wnt

signaling through LRP6 activation and whether PTPRF functions differently in CRC cells with different mutation background. Given the importance of Wnt signaling in CRC, the identification of PTPRF as a novel oncogenic protein may lead to future translational applications targeting PTPRF.

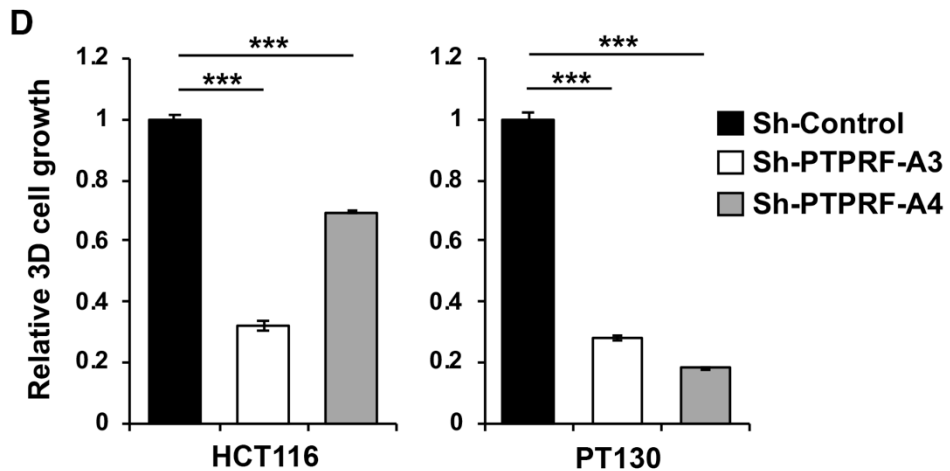
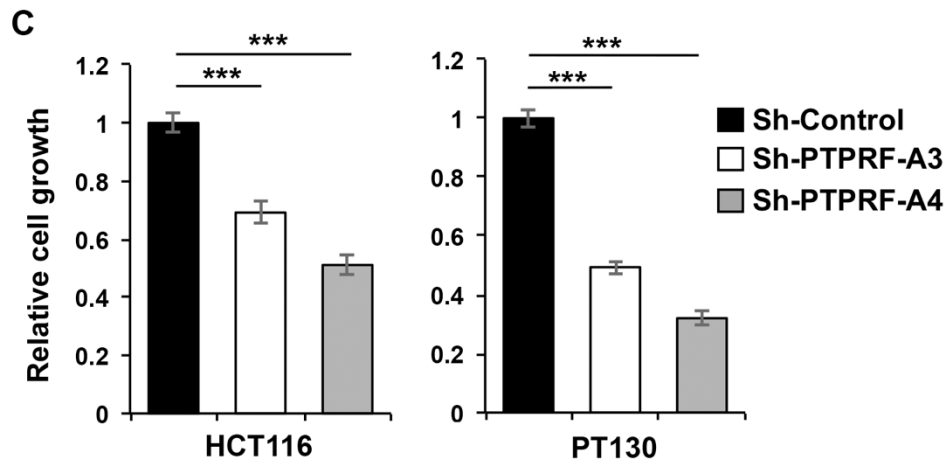
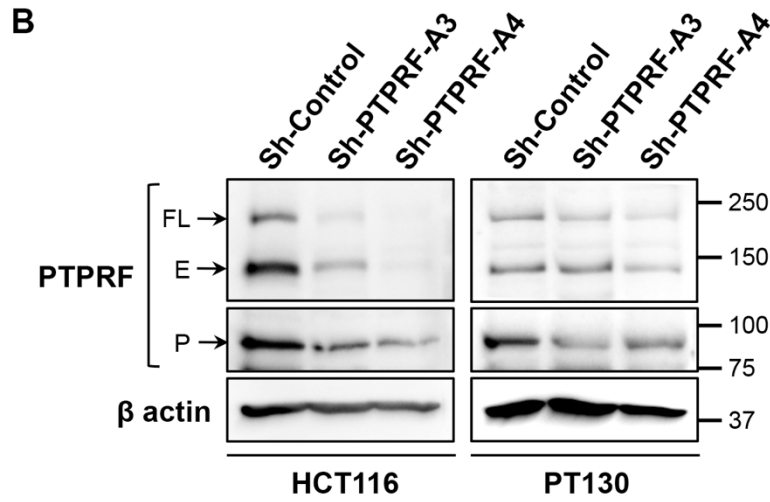
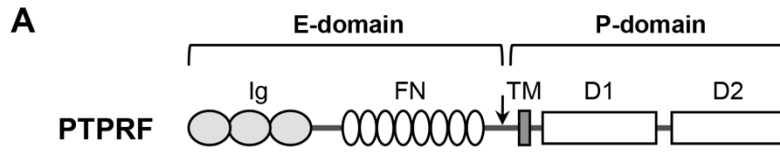


Figure 3.1 Knockdown of PTPRF inhibits cell proliferation in colon cancer cells

(A) A diagram showing the domain structure of PTPRF. The full-length (FL) PTPRF protein contains an extracellular domain (E-domain) consisting of three Ig-like domains and eight fibronectin (FN) domains, a single transmembrane domain, and an intracellular phosphatase domain (P-domain) consisting of a functional D1 phosphatase and a D2 pseudophosphatase domain. The arrow indicates the putative proteolytic cleavage site. (B) The expression of PTPRF was analyzed in stable control and PTPRF knockdown HCT116 and PT130 cells using Western blotting. Two different shRNA targeting sequences (A3 and A4) were used to silence PTPRF in each cell line. β -actin was used as loading controls. The FL protein and E-domain of PTPRF were detected by the anti-LAR mAb whereas the P-domain was detected by the anti-PTPRF mAb. (C) Knockdown of PTPRF decreased the growth of HCT16 and PT130 cells cultured in 2D. Equal number of control and PTPRF knockdown HCT16 and PT130 cells were allowed to grow for 3 and 5 days, respectively, and the relative cell growth was determined using crystal violet staining. Data represent the mean \pm SD (n=3, *** p<0.0001). (D) Knockdown of PTPRF decreased the growth of HCT16 and PT130 cells cultured in 3D Matrigel. Equal number of control and PTPRF knockdown HCT16 and PT130 cells were seeded into 50% Matrigel and allowed to grow for 7 days. The relative cell growth was determined using Cell Titer Glo 3D Viability Assay. Data represent the mean \pm SD (n=3, *** p<0.0001).

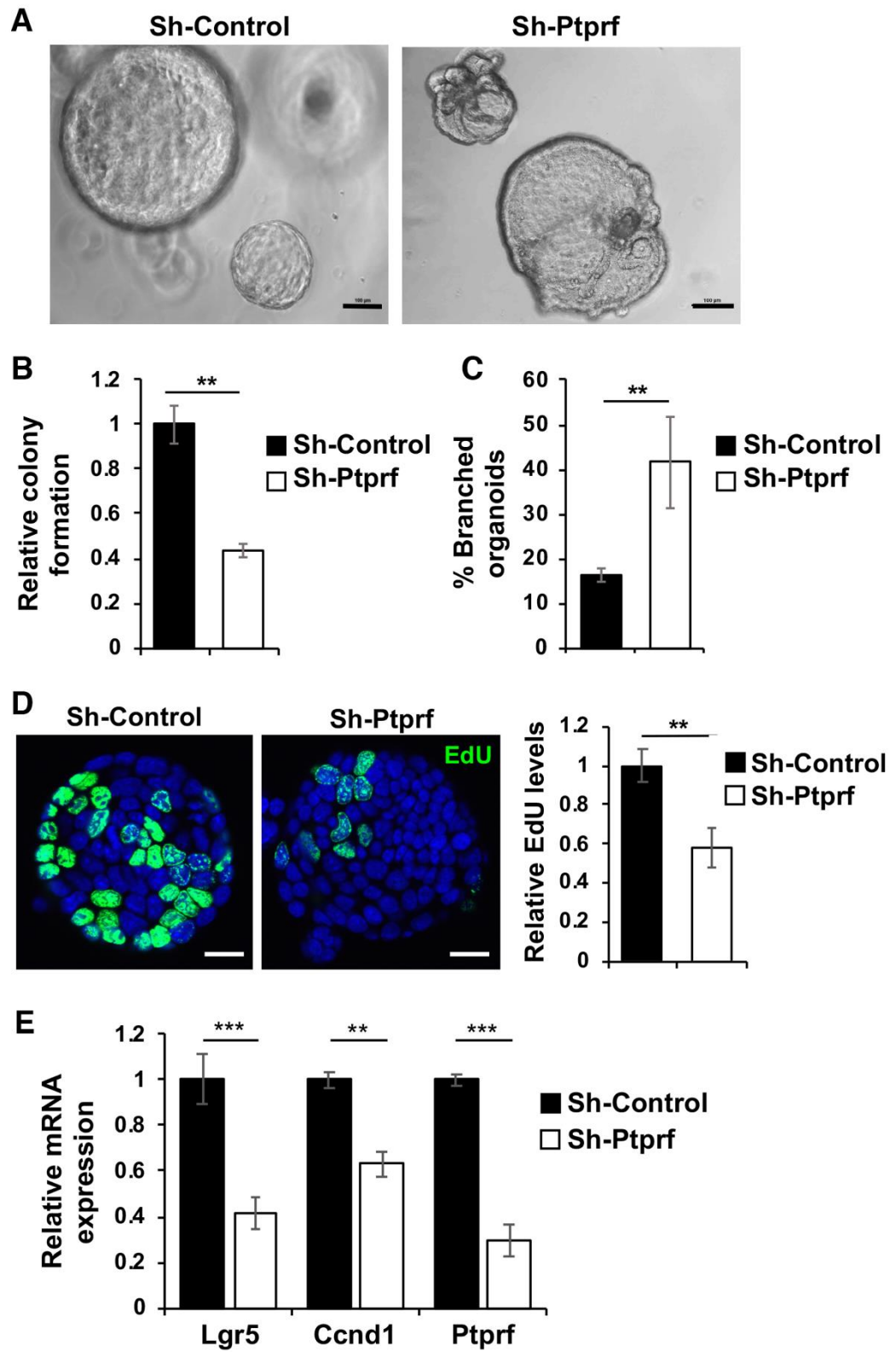


Figure 3.2 Knockdown of PTPRF decreases tumor organoid formation

(A). Single cell suspensions of control and Prprf knockdown mouse Apc/Kras tumor cells were seeded in 3D Matrigel. Representative images of control and Ptprf knockdown tumor organoids are shown after 6 days in culture. Scale bar, 100 μ m. (B) The relative numbers of tumor organoids formed and (C) the percentage of organoids showed branched phenotype were quantified (total 1,000 cells were seeded per group). Data represent the mean \pm SD (n=3, ** p < 0.001). (D) Stable control and Ptprf knockdown tumor organoids grown in 3D Matrigel for 3 days were labeled with EdU to mark proliferating cells. The EdU positive cells were visualized using Click-iT EdU Alexa 488. Scale bar, 50 μ m. The EdU-positive cells in tumor organoids were quantified and compared between two groups. Data represents mean \pm SD (** p<0.001). (E) Control and Prprf knockdown tumor organoids were subseeded and grown in 3D Matrigel for 3 days. The mRNA expression of Ptprf as well as target genes of Wnt/ β -catenin [including Lgr5 and Ccnd1 (cyclin D1)] was determined using qRT-PCR. Data represent the mean \pm SD (n=3, *** p<0.0001 and ** p < 0.001).

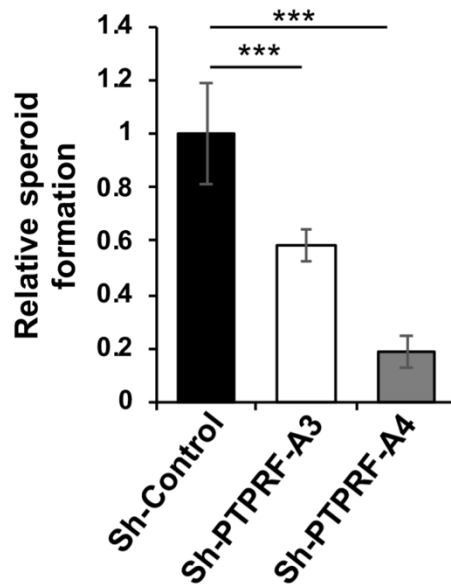


Figure 3.3 Knockdown of PTPRF decreases tumor spheroid formation in suspension culture.

Control and PTPRF knockdown HCT116 cells were seeded as single cells in the stem cell suspension medium and the number of colonies formed was determined after 7 days. Data represent the mean \pm SD (n=3, *** p<0.0001).

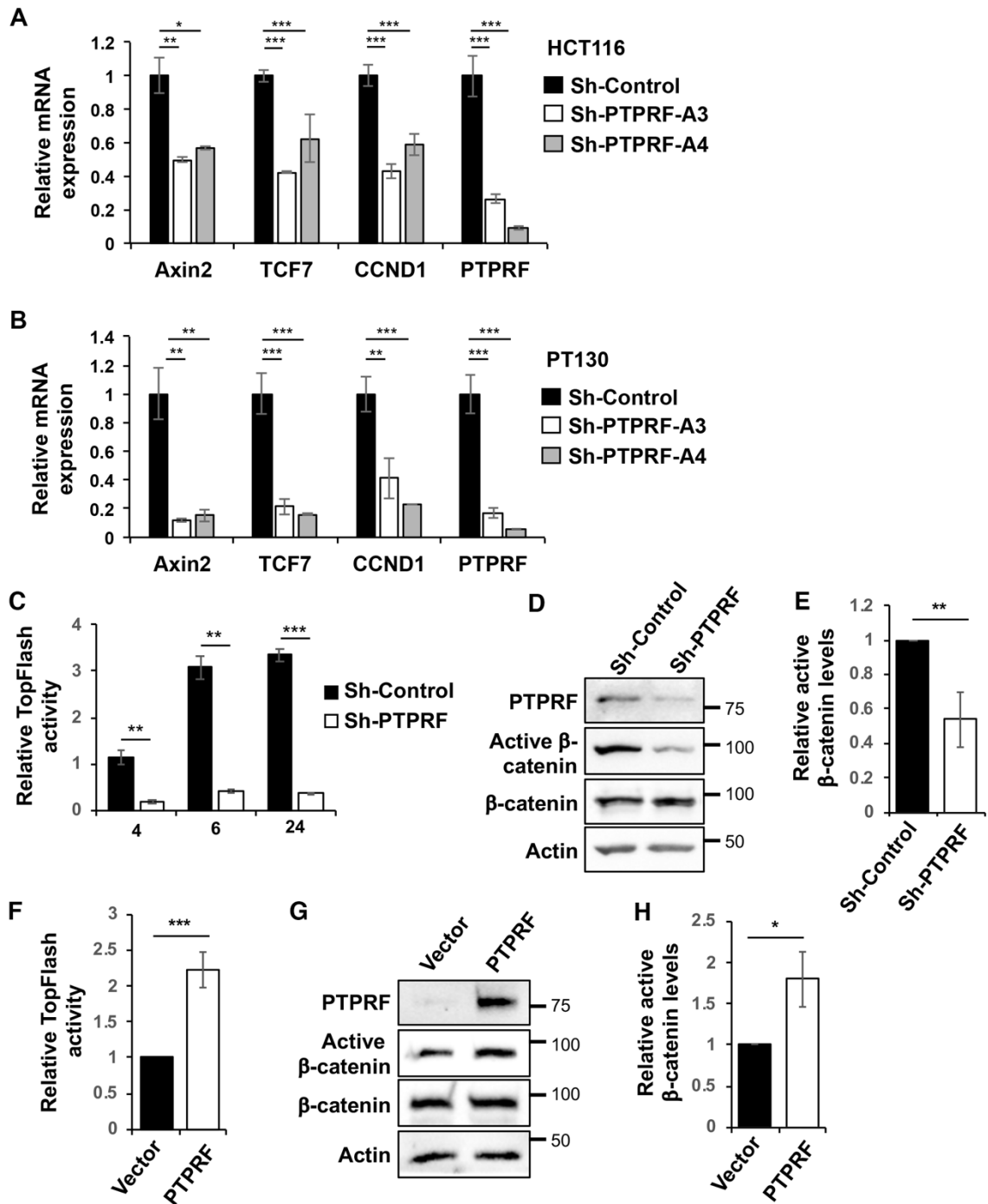


Figure 3.4 The expression of PTPRF positively regulates Wnt signaling.

(A-B) Knockdown of PTPRF reduced the expression of Wnt target genes in HCT16 (A) and PT130 (B) cells. The relative expression of *AXIN2*, *TCF7*, *CCND1* and *PTPRF* mRNA was determined using qRT-PCR in control and PTPRF knockdown cells. Data represent

the mean \pm SD (n=3, *** p<0.0001, ** p < 0.001 and * p < 0.05). (C) HEK293 cells stably expressing the TOP-Flash Firefly luciferase reporter and control Renilla luciferase expression constructs were infected with sh-PTPRF-A3 lentivirus. Cells were then treated with the Wnt3A-conditioned media and the relative luciferase reporter activities were measured after Wnt treatment for 4, 6 and 24 h. Data represent the mean \pm SD (n=3, *** p<0.0001 and ** p < 0.001). (D) Western blot analysis of PTPRF, active β -catenin and total β -catenin in control and PTPRF knockdown cells used in (C). The expression of PTPRF was detected using the anti-PTPRF mAb. (E) The relative levels of active β -catenin were quantified by normalizing to actin and compared to control cells. Data represent the mean \pm SD (n=3, ** p < 0.01). (F) HEK293 cells expressing the Wnt luciferase reporter as described in (C) were transfected with PTPRF. Cells were treated with the Wnt3A-conditioned medium for 6 h and the relative luciferase reporter activities were measured. Data represent the mean \pm SD (n=3, *** p<0.0001). (G) Western blot analysis of PTPRF, active β -catenin and total β -catenin in control and PTPRF overexpressing cells used in (F). The expression of PTPRF was detected using the anti-PTPRF mAb. (H) The relative levels of active β -catenin were determined by normalizing to actin and compared to control cells. Data represent the mean \pm SD (n=3, * p < 0.05).

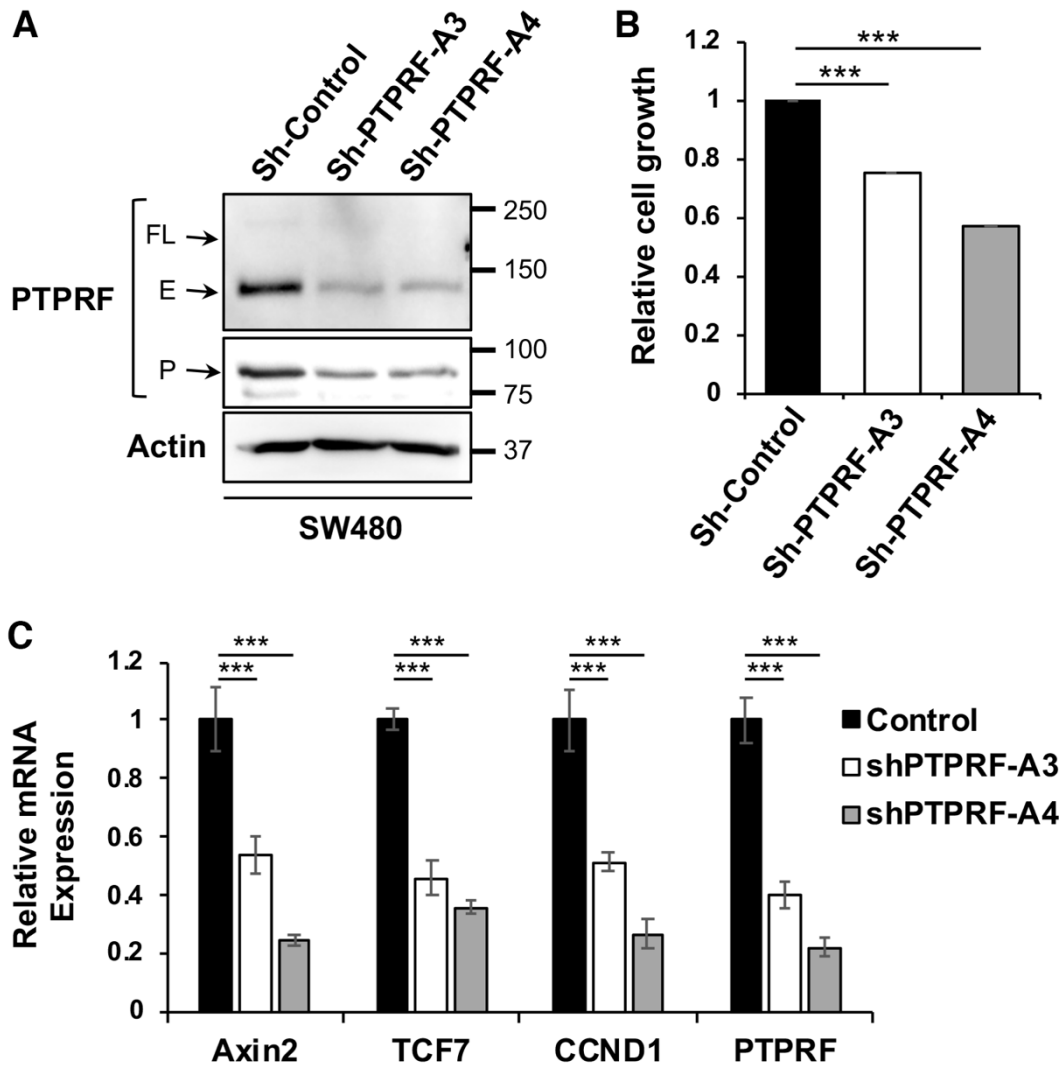


Figure 3.5 Knockdown of PTPRF inhibits cell proliferation and Wnt signaling in SW480 cells.

(A) The expression of PTPRF was analyzed in stable control and PTPRF knockdown SW480 cells using Western blotting. Two different shRNA targeting sequences (A3 and A4) were used to silence PTPRF in each cell line. β -actin was used as loading controls. The FL protein and E-domain of PTPRF were detected by the anti-LAR mAb whereas the P-domain was detected by the anti-PTPRF mAb. (B) Equal number of control and PTPRF knockdown SW480 cells were allowed to grow for 3 days. The relative cell growth was determined using crystal violet staining. Data represent the mean \pm SD (n=3, ***

p<0.0001). (C) Knockdown of PTPRF reduced the expression of Wnt target genes in SW480 cells. The relative expression of *AXIN2*, *TCF7*, *CCND1* and *PTPRF* mRNA was determined using qRT-PCR in control and PTPRF knockdown cells. Data represent the mean \pm SD (n=3, *** p<0.0001).

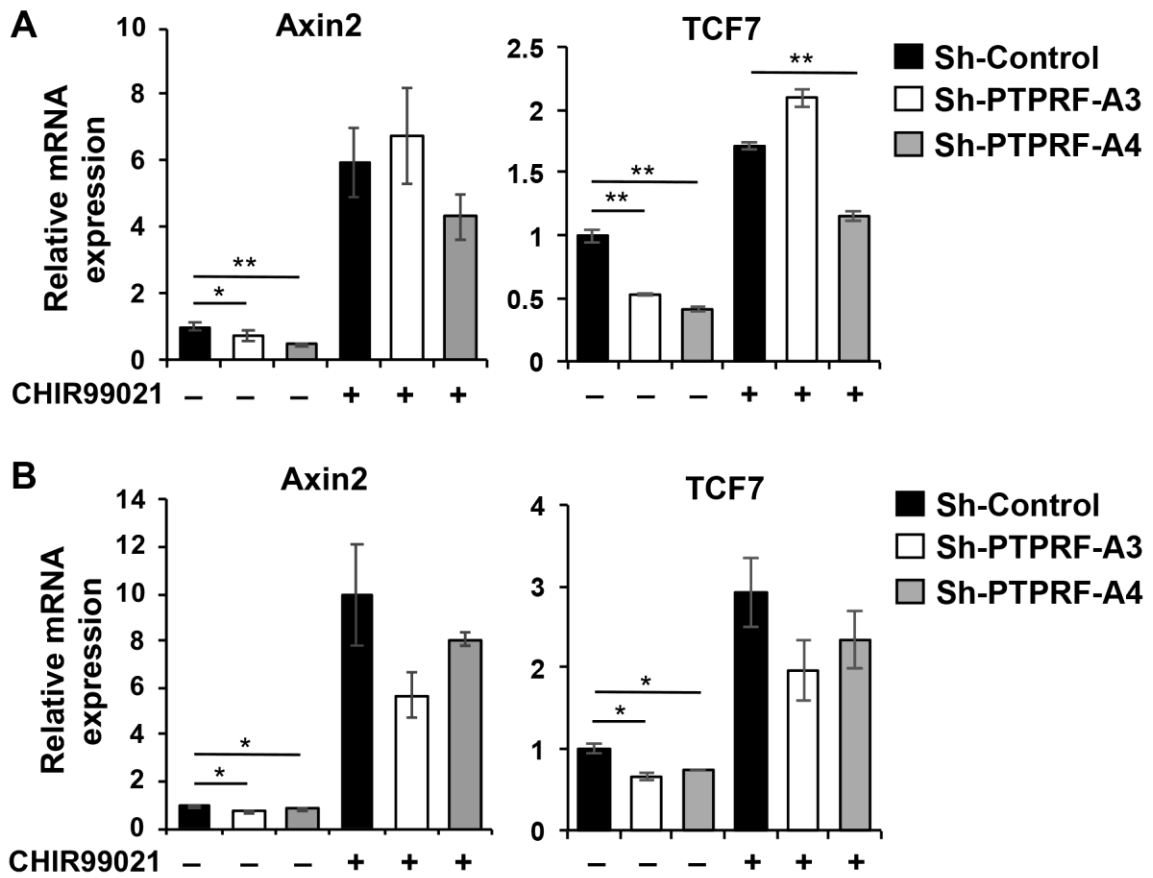


Figure 3.6 PTPRF regulates Wnt signaling at a step upstream of the β -catenin destruction complex.

(A-B) Control and PTPRF knockdown HCT116 (A) and PT130 (B) cells were treated with DMSO or GSK3 inhibitor CHIR99021 (3 μ M) for overnight. The relative expression of *AXIN2* and *TCF7* mRNA was determined using qRT-PCR analysis. Data represent the mean \pm SD (n=3, ** p < 0.001 and * p < 0.05).

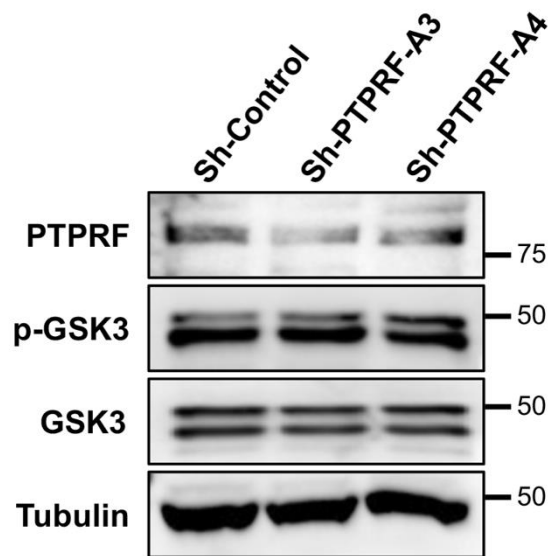


Figure 3.7 The status of GSK3 phosphorylation in PTPRF knockdown.

Cell lysates prepared from sh-control and sh-PTPRF knockdown PT130cells were analyzed for the phosphorylation of GSK3 as well as the expression of total GSK3, PTPRF and tubulin.

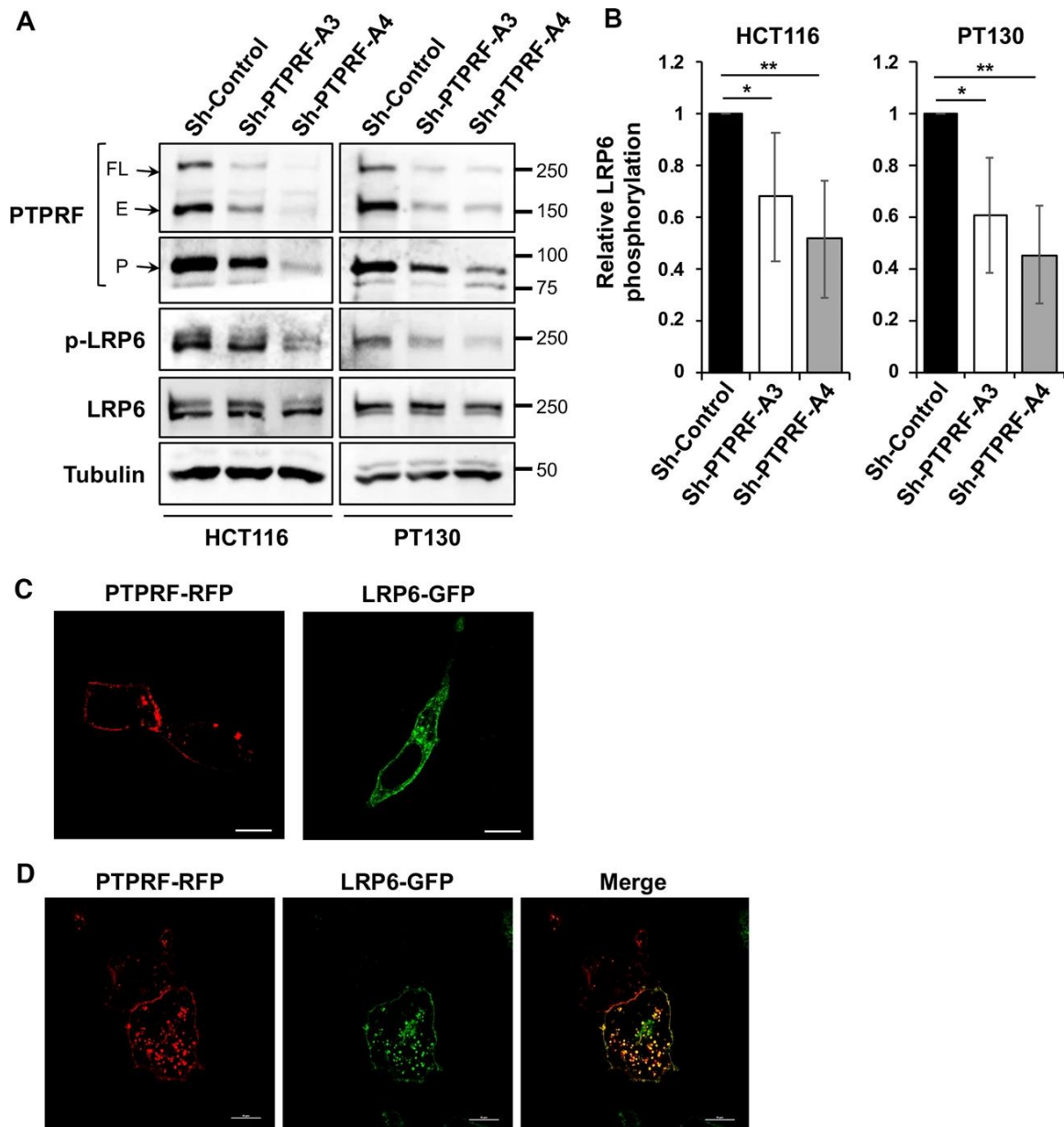


Figure 3.8 PTPRF interacts with LRP6.

(A) Knockdown of PTPRF reduced the phosphorylation of LRP6 in HCT16 and PT130 cells. Cell lysates prepared from control and PTPRF knockdown cells were analyzed for the phosphorylation of LRP6 as well as the expression of total LRP6, PTPRF and tubulin. (B) The levels of LRP6 phosphorylation were quantified by normalizing to total LRP6. Data represent the mean \pm SD (n=3, ** p < 0.001 and * p < 0.05). (C) PT130 cells transfected with PTPRF-RFP or LRP6-GFP expression plasmid alone were fixed and

visualized using confocal microscopy. Scale bar, 10 μm . (D) PT130 cells co-transfected with PTPRF-RFP and LRP6-GFP were fixed and visualized using confocal microscopy. Scale bar, 10 μm . Quantitative analysis of PTPRF and LRP6 colocalization revealed that the average Pearson's coefficient is 0.68 ± 0.14 (mean \pm SD, n=5).

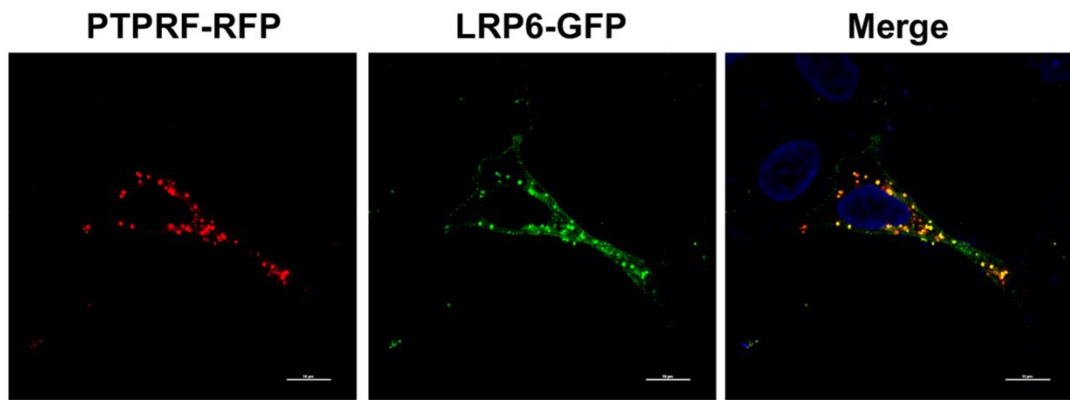


Figure 3.9 Colocalization of PTPRF and LRP6 in colon cancer cells.

PT130 cells co-transfected with PTPRF-RFP and LRP6-GFP were fixed and visualized using confocal microscopy. Cell nuclei were stained with DAPI in the merged image. Scale bar, 10 μm .

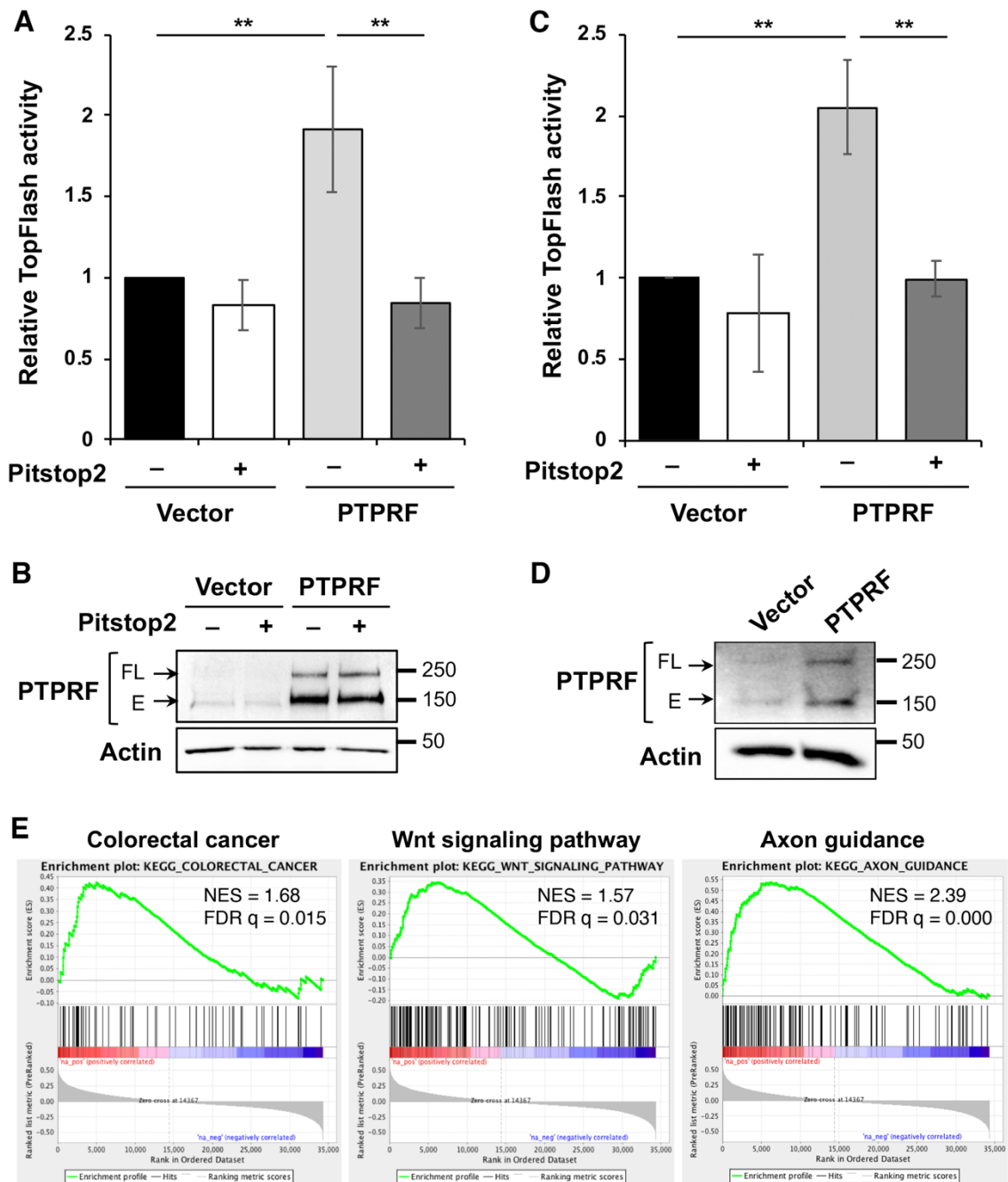


Figure 3.10 PTPRF-mediated activation of Wnt signaling requires clathrin-dependent endocytosis.

(A) HEK293 cells expressing the Wnt luciferase reporter were transfected with vector or WT PTPRF. The cells were stimulated with Wnt-conditioned media in the presence or absence of Pitstop 2 (20 μ M) for 6 h and the relative luciferase reporter activities were

measured. Data represent the mean \pm SEM (n=3, ** p < 0.01). (B) The cells used for TOP-Flash reporter assays were analyzed for the expression of PTPRF. The full-length and E-domain of PTPRF was detected by the LAR antibody. (C) HCT116 cells were transfected with vector or WT PTPRF along with TOP-Flash reporter and Renilla control plasmids as indicated. The cells were treated with Wnt-condition media in the presence or absence of Pitstop 2 (20 μ M) for 6 h and the relative luciferase reporter activities were measured. Data represent the mean \pm SEM (n=3, ** p < 0.01). (D) HCT116 lysates from the reporter assay were analyzed for the expression of PTPRF. The full-length and E-domain of PTPRF was detected by the LAR antibody. (E) The GSEA was performed using the TCGA Colon Adenocarcinoma (COAD) RNA-seq dataset to identify gene sets in the KEGG collections that have positive correlations with PTPRF expression. Enrichment plots showed significant correlation of colorectal cancer (NES = 1.68, FDR q-val = 0.015), the Wnt signaling pathway (NES = 1.57, FDR q-val = 0.031) and the axon guidance pathway (NES = 2.39, FDR q-val = 0.000) with PTPRF expression in colon cancer patients.

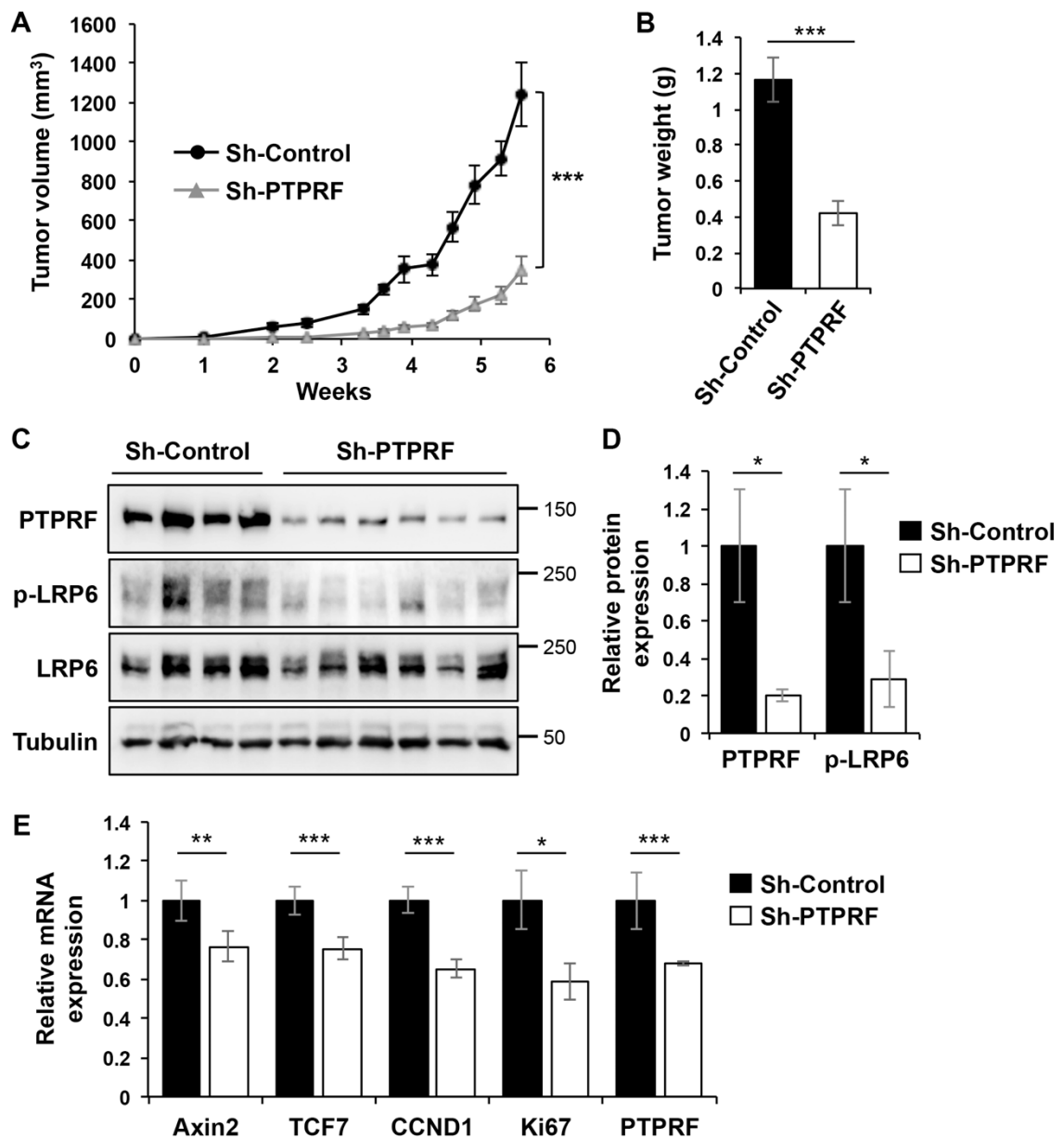


Figure 3.11 Knockdown of PTPRF inhibits xenograft tumor growth and Wnt signaling.

(A) Control and PTPRF knockdown HCT116 cells were injected subcutaneously into NSG mice. The size of the tumors was measured every 3-5 days starting at one week after injection. Data represent the mean \pm SEM (n=6, for sh-control group; and n=10 for sh-PTPRF group, *** p < 0.0001). (B) At the end of the 6-week experiment, tumors were

excised and weighted. Data represent the mean \pm SEM (***) $p < 0.0001$). (C) Tumor tissues from 4 mice in the sh-control group and 6 mice in the sh-PTPRF group were analyzed for the levels of PTPRF, p-LRP6 and total LRP6 using Western blotting. (D) The relative PTPRF expression and LRP6 phosphorylation were quantified by normalizing levels of PTPRF and p-LRP6 to that of tubulin and total LRP6, respectively. Data represent the mean \pm SD (* $p < 0.05$). (E) Tumor tissues from 4 mice in the sh-control group and 6 mice in the sh-PTPRF group were analyzed for the expression of Axin2, TCF7, CCND1, MKI67 (Ki67) and PTPRF using qRT-PCR. Data represent the mean \pm SEM (***) $p < 0.0001$, ** $p < 0.001$ and * $p < 0.05$).

Gene sets that are positively associated with PTPRF expression in TCGA-COAD dataset			
	NAME	NES	FDR.q.val
Cell-cell and cell-ECM interaction	KEGG_AXON_GUIDANCE	2.394	0.000
	KEGG_FOCAL_ADHESION	2.268	0.000
	KEGG_GAP_JUNCTION	2.233	0.000
	KEGG_REGULATION_OF_ACTIN_CYTOSKELETON	2.202	0.000
	KEGG_TIGHT_JUNCTION	2.100	0.000
	KEGG_ADHERENS_JUNCTION	2.065	0.001
	KEGG_LEUKOCYTE_TRANSENDOTHELIAL_MIGRATION	1.976	0.001
	KEGG_ECM_RECEPTOR_INTERACTION	1.721	0.012
	KEGG_CELL_ADHESION_MOLECULES_CAMS	1.538	0.037
Signaling Transduction	KEGG_CALCIIUM_SIGNALING_PATHWAY	2.569	0.000
	KEGG_ERBB_SIGNALING_PATHWAY	2.461	0.000
	KEGG_PHOSPHATIDYLINOSITOL_SIGNALING_SYSTEM	2.517	0.000
	KEGG_NOTCH_SIGNALING_PATHWAY	2.279	0.000
	KEGG_INSULIN_SIGNALING_PATHWAY	2.220	0.000
	KEGG_ENDOCYTOSIS	2.105	0.000
	KEGG_PPAR_SIGNALING_PATHWAY	2.031	0.001
	KEGG_NEUROTROPHIN_SIGNALING_PATHWAY	2.001	0.001
	KEGG_MAPK_SIGNALING_PATHWAY	1.883	0.003
	KEGG_HEDGEHOG_SIGNALING_PATHWAY	1.792	0.007
	KEGG_VEGF_SIGNALING_PATHWAY	1.729	0.011
	KEGG_MTOR_SIGNALING_PATHWAY	1.667	0.017
	KEGG_B_CELL_RECEPTOR_SIGNALING_PATHWAY	1.628	0.022
	KEGG_CHEMOKINE_SIGNALING_PATHWAY	1.609	0.024
KEGG_WNT_SIGNALING_PATHWAY	1.568	0.031	
Cancer	KEGG_ENDOMETRIAL_CANCER	2.495	0.000
	KEGG_ACUTE_MYELOID_LEUKEMIA	2.142	0.000
	KEGG_GLIOMA	2.095	0.000
	KEGG_NON_SMALL_CELL_LUNG_CANCER	2.023	0.001
	KEGG_PROSTATE_CANCER	1.985	0.001
	KEGG_CHRONIC_MYELOID_LEUKEMIA	1.879	0.003
	KEGG_RENAL_CELL_CARCINOMA	1.846	0.004
	KEGG_BASAL_CELL_CARCINOMA	1.824	0.005
	KEGG_COLORECTAL_CANCER	1.682	0.015
	KEGG_THYROID_CANCER	1.677	0.016
	KEGG_PANCREATIC_CANCER	1.624	0.022
KEGG_MELANOMA	1.537	0.037	
Metabolism	KEGG_INOSITOL_PHOSPHATE_METABOLISM	2.535	0.000
	KEGG_STARCH_AND_SUCROSE_METABOLISM	2.553	0.000
	KEGG_ASCORBATE_AND_ALDARATE_METABOLISM	2.262	0.000
	KEGG_RETINOL_METABOLISM	2.266	0.000
	KEGG_FATTY_ACID_METABOLISM	2.277	0.000
	KEGG_VALINE_LEUCINE_AND_ISOLEUCINE_DEGRADATION	2.030	0.001
	KEGG_CITRATE_CYCLE_TCA_CYCLE	1.722	0.012
	KEGG_GLYCOLYSIS_GLUONEOGENESIS	1.642	0.020
	KEGG_SPHINGOLIPID_METABOLISM	1.599	0.026

Gene sets that are negatively associated with PTPRF expression in TCGA-COAD dataset			
	NAME	NES	FDR.q.val
DNA transcription and repair	KEGG_CELL_CYCLE	-2.525	0.000
	KEGG_DNA_REPLICATION	-2.526	0.000
	KEGG_NUCLEOTIDE_EXCISION_REPAIR	-2.418	0.000
	KEGG_RNA_DEGRADATION	-2.353	0.000
	KEGG_SPLICEOSOME	-2.578	0.000
	KEGG_BASAL_TRANSCRIPTION_FACTORS	-2.288	0.000
	KEGG_HOMOLOGOUS_RECOMBINATION	-2.129	0.000
	KEGG_RNA_POLYMERASE	-2.109	0.000
	KEGG_MISMATCH_REPAIR	-2.068	0.000
	KEGG_BASE_EXCISION_REPAIR	-2.032	0.000
	KEGG_PYRIMIDINE_METABOLISM	-2.150	0.000
Protein synthesis and degradation	KEGG_PROTEASOME	-2.753	0.000
	KEGG_PROTEIN_EXPORT	-2.412	0.000
	KEGG_RIBOSOME	-3.085	0.000
	KEGG_AMINOACYL_TRNA_BIOSYNTHESIS	-2.077	0.000

Table 3.1 The Gene Set Enrichment Analysis (GSEA) of PTPRF expression in colon cancer patients.

TCGA Colon Adenocarcinoma (COAD) RNA-seq dataset was first used to identify genes that have positive or negative correlations with PTPRF expression. The GSEA was then performed to determine if PTPRF expression is associated with gene sets in the KEGG collection. The name of the gene sets and the corresponding normalized enrichment score (NES) and false discovery rate (FDR) are listed in the table (the cutoff for significance is set for $FDR < 0.05$).

Gene sets that are positively enriched in the RNA-seq dataset			
	NAME	NES	FDR q-val
Cell-cell and cell-ECM interaction	KEGG_FOCAL_ADHESION	2.910	0.0020
	KEGG_REGULATION_OF_ACTIN_CYTOSKELETON	2.885	0.0017
	KEGG_CELL_ADHESION_MOLECULES_CAMS	2.365	0.0087
	KEGG_ECM_RECEPTOR_INTERACTION	2.305	0.0109
	KEGG_NATURAL_KILLER_CELL_MEDIATED_CYTOTOXICITY	2.235	0.0164
	KEGG_LEUKOCYTE_TRANSENDOTHELIAL_MIGRATION	2.045	0.0320
	KEGG_AXON_GUIDANCE	1.883	0.0524
	KEGG_TIGHT_JUNCTION	1.808	0.0682
Signaling Transduction	KEGG_MAPK_SIGNALING_PATHWAY	2.677	0.0039
	KEGG_ENDOCYTOSIS	2.578	0.0054
	KEGG_TOLL_LIKE_RECEPTOR_SIGNALING_PATHWAY	2.492	0.0059
	KEGG_CYTOKINE_CYTOKINE_RECEPTOR_INTERACTION	2.524	0.0061
	KEGG_NEUROACTIVE_LIGAND_RECEPTOR_INTERACTION	2.061	0.0303
	KEGG_CHEMOKINE_SIGNALING_PATHWAY	2.047	0.0322
	KEGG_JAK_STAT_SIGNALING_PATHWAY	1.978	0.0394
	KEGG_ERBB_SIGNALING_PATHWAY	1.765	0.0784
	KEGG_INSULIN_SIGNALING_PATHWAY	1.681	0.1054
	KEGG_B_CELL_RECEPTOR_SIGNALING_PATHWAY	1.677	0.1056
	KEGG_NEUROTROPHIN_SIGNALING_PATHWAY	1.671	0.1062
	KEGG_VEGF_SIGNALING_PATHWAY	1.631	0.1203
	KEGG_PHOSPHATIDYLINOSITOL_SIGNALING_SYSTEM	1.623	0.1221
	KEGG_MTOR_SIGNALING_PATHWAY	1.551	0.1517
Cancer	KEGG_PANCREATIC_CANCER	2.205	0.0192
	KEGG_GLIOMA	2.181	0.0206
	KEGG_PROSTATE_CANCER	2.026	0.0345
	KEGG_COLORECTAL_CANCER	1.959	0.0416
	KEGG_SMALL_CELL_LUNG_CANCER	1.887	0.0526
	KEGG_CHRONIC_MYELOID_LEUKEMIA	1.794	0.0725
	KEGG_ENDOMETRIAL_CANCER	1.688	0.1028
	KEGG_NON_SMALL_CELL_LUNG_CANCER	1.632	0.1208
	KEGG_MELANOMA	1.544	0.1547
	KEGG_BLADDER_CANCER	1.475	0.1865

Gene sets that are negatively enriched in the RNA-seq dataset			
	NAME	NES	FDR q-val
DNA transcription and repair	KEGG_SPLICEOSOME	-4.799	0.0000
	KEGG_CELL_CYCLE	-2.879	0.0001
	KEGG_DNA_REPLICATION	-2.599	0.0006
	KEGG_BASE_EXCISION_REPAIR	-2.372	0.0037
	KEGG_HOMOLOGOUS_RECOMBINATION	-2.136	0.0128
	KEGG_MISMATCH_REPAIR	-1.713	0.0796
	KEGG_RNA_DEGRADATION	-2.121	0.0134
Protein synthesis and degradation	KEGG_RIBOSOME	-7.428	0.0000
	KEGG_AMINOACYL_TRNA_BIOSYNTHESIS	-2.941	0.0000
	KEGG_PROTEASOME	-1.629	0.1042
Metabolism	KEGG_CITRATE_CYCLE_TCA_CYCLE	-2.964	0.0000
	KEGG_PYRIMIDINE_METABOLISM	-2.111	0.0142
	KEGG_PROPANOATE_METABOLISM	-1.968	0.0295
	KEGG_ONE_CARBON_POOL_BY_FOLATE	-1.880	0.0421
	KEGG_ARGININE_AND_PROLINE_METABOLISM	-1.852	0.0478
	KEGG_PURINE_METABOLISM	-1.765	0.0673
	KEGG_ALANINE ASPARTATE AND GLUTAMATE METABOLISM	-1.681	0.0892
KEGG_PENTOSE_PHOSPHATE_PATHWAY	-1.655	0.0967	

Table 3.2 Top pathways identified by GSEA based on the RNA-seq analysis of control and sh-PTPRF cells.

Total RNA was prepared from control and sh-PTPRF PT130 cells and subjected to RNA-seq analysis and the KEGG gene sets enriched in PTPRF knockdown cells were determined by the GSEA. The name of the gene sets and the corresponding normalized enrichment score (NES) and false discovery rate (FDR) are listed in the table. The cutoff for significance is set for $FDR < 0.25$.

Tissue	Gene Expression		Tested
	% Up Regulated	% Down Regulated	
Breast	4.89	1.18	1104
Central nervous system	3.59	3.16	697
Cervix	10.42	0	307
Endometrium	5.32	0.17	602
Hematopoietic and lymphoid	3.62	0	221
Kidney	4.17	5.17	600
Large intestine	3.77	0.16	610
Liver	3.49	0	373
Lung	3.71	0.20	1019
Oesophagus	3.20	0	125
Ovary	12.03	0.75	266
Pancreas	3.91	0	179
Prostate	3.01	1.41	498
Skin	4.23	0	473
Soft tissue	6.46	0	263
Stomach	11.58	0.35	285
Thyroid	1.95	0.19	513
Upper aerodigestive tract	2.87	0	522
Urinary tract	6.13	0	408

Table 3.3 The tissue distribution of altered PTPRF gene expression in human cancers.

The table was derived from the COSMIC data as of June 2020 showing the tissue distribution of the percentage of samples with altered PTPRF gene expression. The number of samples tested include samples from the targeted and whole genomes/exome resequencing.

CHAPTER 4. NEDD4L PROMOTES THE UBIQUITINATION AND INTERNALIZATION OF PTPRF TO INHIBIT WNT SIGNALING

Ashley T. Skaggs, Dylan Rivas, Sumati Hasani, Tianyan Gao. NEDD4L promotes the ubiquitination and internalization of PTPRF to inhibit Wnt Signaling. (2022) JBC. *In Revision*

4.1 Abstract

Acting together with protein tyrosine kinases, protein tyrosine phosphatases (PTPs) play an important role in maintaining the balance of a large number of signaling pathways. PTPRF belongs to a family of receptor-type PTPs. Our previous studies have identified PTPRF as an oncogenic phosphatase by enhancing the activation of Wnt signaling in colorectal cancer. However, little is known on how the expression and localization of PTPRF is regulated. In this study, we show that NEDD4L, an E3 ubiquitin ligase, controls PTPRF protein stability and membrane localization. Overexpression of NEDD4L decreases the half-life of PTPRF whereas knockdown of NEDD4L has the opposite effect. Interestingly, NEDD4L utilizes the K29 and K63 linkage to ubiquitinate PTPRF, a process that also relies on the phosphatase activity of PTPRF. In addition, NEDD4L-dependent ubiquitination promotes PTPRF internalization and trafficking to multivesicular bodies where it colocalizes with HRS. However, treating cells with endocytosis inhibitors has no effect on PTPRF ubiquitination, suggesting that NEDD4L-mediated PTPRF ubiquitination occurs at the plasma membrane. Functionally, by removing PTPRF from the membrane NEDD4L blocks the ability of PTPRF to enhance Wnt activation. Taken together, our study identifies NEDD4L-dependent ubiquitination of PTPRF as a novel mechanism that fine-tunes the regulation of Wnt signaling.

4.2 Introduction

Protein phosphorylation defines one of the most important regulatory mechanisms in cell signaling. A precise control of the balance between phosphorylation and dephosphorylation is crucial for living organisms to maintain normal physiological functions. While protein kinases have been extensively studied in efforts of developing therapeutically relevant inhibitors, significant knowledge gaps exist on the opposing actions of protein phosphatases. PTPs are classified into four families based on their catalytic mechanisms and substrate specificities [7, 154]. Protein tyrosine phosphatase receptor type F, PTPRF, belongs to the class I R2A subfamily of PTPs that strictly dephosphorylate phosphotyrosine residues. PTPRF contains a large extracellular domain (E-domain) with three immunoglobulin (Ig)-like and eight fibronectin type-III motifs, a single transmembrane domain and two tandem phosphatase domains (named D1 and D2) in the intracellular region. The D1 domain in PTPRF is catalytically active whereas the D2 domain is considered a pseudo-phosphatase without phosphatase activity; and the D1 and D2 domain together is often referred to as the P-domain [155, 156]. Like all tyrosine phosphatases in the R2A subfamily, PTPRF is post-translationally cleaved to produce a separate E domain that remains attached to the rest of the protein via non-covalent interaction [40, 51]. Developmental biology studies using *Drosophila* and mouse models have demonstrated that PTPRF is involved in regulating axon guidance [16, 157], cell polarity [32] and craniofacial bone development [141]. We recently identified PTPRF as an oncogenic phosphatase that functions upstream of the β -catenin destruction complex to enhance Wnt signaling in colon cancer [51]. However, little is known about how the expression of PTPRF at the protein level is regulated.

Protein ubiquitination is an important post-translational modification that serves as a signal for protein degradation, receptor endocytosis and trafficking, protein-protein interaction and other cellular processes [158]. NEDD4L is a HECT domain E3 ligase that is known for its ability to ubiquitinate membrane proteins and regulate their internalization and degradation [96]. For example, NEDD4L has been shown to promote the ubiquitination of epithelial Na⁺ channel (ENaC) resulting in the internalization and downregulation of channel proteins [97, 159, 160]. Moreover, recent studies demonstrate that NEDD4L controls the ubiquitination and degradation of DVL2 [161] and LGR5 [162], two key components of the Wnt pathway, to inhibit Wnt signaling.

In this study, we discovered that NEDD4L functions as a E3 ubiquitin ligase to regulate the localization and degradation of PTPRF. The NEDD4L-mediated ubiquitination removes PTPRF from the plasma membrane and prevents PTPRF from activating Wnt signaling. Together, our study identified PTPRF as a novel substrate of NEDD4L which adds another level of complexity in the regulation of Wnt pathway.

4.3 Results

4.3.1 The expression of PTPRF is regulated by NEDD4L

Given the notion that PTPRF and NEDD4L have opposite roles in regulating Wnt signaling, we tested if NEDD4L is involved in negatively modulating PTPRF expression. To this end, we first generated PTPRF knockout (KO) 293T cells using CRISPR/Cas9. As shown in Figure 4.1A, PTPRF was detected by antibodies against either the E- or P-domain of the protein in parental 293T cells but not in one of the PTPRF KO cell lines. To

determine the effect of NEDD4L on PTPRF expression, PTPRF KO cells were transfected with PTPRF in combination with WT or catalytically inactive NEDD4L/DD mutant. Indeed, co-expression of NEDD4L significantly reduced PTPRF expression whereas NEDD4L/DD mutant had no effect (Figure 4.1B-C), suggesting that NEDD4L-mediated regulation of PTPRF requires its E3 ligase activity. Moreover, we silenced NEDD4L expression using two lentiviral shRNAs (B10 and B11) in 293T cells. Consistently, the expression of endogenous PTPRF was significantly increased in both sh-NEDD4L cell lines (Figure 4.1D-E). Furthermore, the effect of NEDD4L expression on regulating PTPRF protein stability was assessed using cycloheximide (CHX) chase experiments. We found that overexpression of NEDD4L decreased, whereas knockdown of NEDD4L increased, the half-life of PTPRF protein (Figure 4.1F-G). Overall, these results provide the first evidence supporting a direct role of NEDD4L on regulating PTPRF stability.

4.3.2 NEDD4L controls PTPRF ubiquitination

We next determined if NEDD4L promotes PTPRF ubiquitination. PTPRF KO cells were transfected with PTPRF-Flag and NEDD4L (WT or DD mutant) in combination with HA-tagged ubiquitin (HA-Ub). Results from analyzing levels of PTPRF ubiquitination in cell lysates revealed that the expression of WT NEDD4L, but not the E3 ligase activity deficient mutant NEDD4L/DD, increased PTPRF ubiquitination (Figure 4.2 A-B). The major ubiquitinated species detected by the HA antibody was ~10-20 kDa larger than the predicated molecular weight of the P-domain of PTPRF (Figure 4.2A). This likely represents a modified PTPRF species with 2-3 ubiquitin molecules added to the protein. To better understand which intracellular domain of PTPRF is required for NEDD4L-

mediated ubiquitination, we expressed phosphatase domain deletion mutants of PTPRF (including Δ D1 and Δ D2) along with NEDD4L and HA-Ub in PTPRF KO cells. Intriguingly, deletion of the phosphatase-active D1 domain largely abolished the ubiquitination of PTPRF whereas PTPRF- Δ D2 was similarly ubiquitinated (Figure 4.2C). The major ubiquitinated species of PTPRF- Δ D2 showed a comparable ~10-20 kDa molecular weight shift over the truncated P-domain of PTPRF, suggesting that deletion of D2 domain did not alter the pattern of PTPRF ubiquitination. Collectively, these results indicate that NEDD4L-mediated ubiquitination requires the D1 phosphatase domain of PTPRF.

NEDD4L is known to ubiquitinate substrates via K29-linked ubiquitin [161, 163]. Additionally, K48- and K63-linkage have been associated with NEDD4L-mediated ubiquitination [163]. To determine the type of ubiquitin linkage that NEDD4L uses to modify PTPRF, we expressed a set of ubiquitin mutants, including HA-tagged K29-, K48- or K63-only ubiquitin, in which the ubiquitin chain formation can only occur on the indicated lysine while all other lysine residues are mutated to arginine. In addition to WT ubiquitin, NEDD4L-mediated PTPRF ubiquitination was observed in cells expressing either K29- or K63-only ubiquitin whereas NEDD4L was unable to attach K48-only ubiquitin to PTPRF, suggesting that NEDD4L utilizes K29 and K63 linkages to ubiquitinate PTPRF (Figure 4.2D). To confirm findings obtained with these Ub mutants, we examined PTPRF ubiquitination by using another set of Ub mutants, including K29R, K48R and K63R, in which only the indicated lysine residue is mutated to arginine. Consistently, NEDD4L-mediated PTPRF ubiquitination was partially decreased in cells expressing K29R-Ub or K63R-Ub but not in cells expressing K48R-Ub (Figure 4.3). Taken

together, these results suggest that NEDD4L targets the phosphatase domain of PTPRF via K29-and K63-linked ubiquitination.

4.3.3 NEDD4L-mediated ubiquitination of PTPRF relies on its phosphatase activity

Since we found that NEDD4L ubiquitinates PTPRF in the D1 phosphatase domain, we next investigated how the phosphatase activity of PTPRF affects its stability. Interestingly, PTPRF-C/S mutant was consistently expressed at a higher level compared to WT PTPRF when cells were transfected with the same amount of expression plasmids (Figure 4.4A). Next, we assessed the stability of PTPRF-C/S using CHX chase experiments. Note that the amount of PTPRF-C/S expression plasmid used was reduced to allow similar levels of WT and C/S mutant protein expression prior to CHX treatment. Indeed, the rate of WT PTPRF degradation was faster compared to C/S mutant suggesting that lack of catalytic activity renders PTPRF more stable (Figure 4.4B). Moreover, we found that the level of NEDD4L-stimulated ubiquitination was reduced in PTPRF-C/S mutant (Figure 4.4 C-D), thus indicating that the phosphatase activity is important for NEDD4L-mediated modification of PTPRF.

Furthermore, we examined if NEDD4L-mediated ubiquitination alters the localization of WT and C/S mutant PTPRF. PTPRF KO cells were rescued with the expression of RFP-tagged WT or C/S mutant PTPRF along with NEDD4L and localization of PTPRF was examined using confocal microscopy. When expressed alone, both WT and C/S mutant PTPRF localized primarily to the plasma membrane (Figure 4.4E). However, co-expression with NEDD4L resulted in translocation of WT PTPRF to large intracellular

vesicles where it co-localized with NEDD4L (Figure 4.4E). This effect of NEDD4L on promoting internalization of PTPRF was significantly attenuated towards PTPRF-C/S as it largely remained on the plasma membrane whereas NEDD4L showed diffused cytoplasmic localization (Figure 4.4E). Quantitative analysis showed that the percentage of cells with intracellular puncta of PTPRF was markedly higher in cells co-expressing WT PTPRF and NEDD4L compared to PTPRF-C/S and NEDD4L co-expressing cells (Figure 4.4D). Taken together, our results suggest that NEDD4L preferentially ubiquitinates catalytically active PTPRF and the ubiquitination of PTPRF leads to internalization of the phosphatase into intracellular vesicles.

4.3.4 NEDD4L-mediated ubiquitination promotes endocytosis of PTPRF via the caveolin pathway

Previous studies have extensively characterized that the ubiquitination of receptor tyrosine kinases induces receptor endocytosis via both clathrin-dependent and independent pathways [164]. However, the mechanisms underlying the trafficking of receptor type tyrosine phosphatases have yet to be investigated. Since co-expression of NEDD4L triggers PTPRF internalization, we further analyzed the relationship between ubiquitination and intracellular trafficking of PTPRF. To visualize the localization of ubiquitinated PTPRF, we co-expressed YFP-tagged ubiquitin and PTPRF along with WT or NEDD4L/DD mutant. Interestingly, co-localization of PTPRF, YFP-Ub and WT NEDD4L was clearly observed in large intracellular vesicles, whereas PTPRF remained at the membrane with limited co-localization with YFP-Ub in cells co-expressing NEDD4L/DD mutant (Figure 4.5). Taken together with our finding that NEDD4L/DD is

unable to induce PTPRF ubiquitination (Figure 4.2A), the results here support the notion that ubiquitination of PTPRF is closely coupled with internalization.

Next, we treated cells expressing PTPRF and NEDD4L with nystatin or pitstop 2 (PS2), inhibitors of caveolin- or clathrin-dependent endocytosis, respectively, and analyzed the localization of PTPRF using confocal microscopy. Consistent with results shown in Figure 3E, the expression of NEDD4L stimulated the formation of intracellular puncta where PTPRF and NEDD4L were colocalized in DMSO treated cells. In contrast, PTPRF largely remained at the plasma membrane in cells treated with nystatin despite the co-expression of NEDD4L; however, PS2 treatment was less effective at blocking PTPRF internalization (Figure 4.6A). Quantitative results indicated that caveolin-mediated endocytosis is mainly responsible for NEDD4L-triggered PTPRF internalization as the percentage of cells with co-localized PTPRF-NEDD4L puncta was significantly decreased (Figure 5B). Furthermore, we determined if treatment with nystatin or PS2 alters PTPRF ubiquitination. Intriguingly, the level of PTPRF ubiquitination remained unchanged upon either treatment (Figure 4.6C), indicating that NEDD4L-mediated ubiquitination likely occurs at the plasma membrane prior to PTPRF internalization. Collectively, these results confirm that NEDD4L-induced ubiquitination is required for PTPRF endocytosis.

4.3.5 NEDD4L removes PTPRF from the plasma membrane to inhibit Wnt signaling

To better understand the nature of intracellular vesicles containing ubiquitinated PTPRF, we next determined if internalized PTPRF co-localizes with endosome markers. Since ubiquitinated membrane proteins are often sorted to multivesicular bodies (MVBs)

[165, 166], we expressed CFP-tagged HRS, a marker of MVBs, with PTPRF-RFP and NEDD4L in PTPRF KO cells and monitored their cellular localization. In the absence of NEDD4L co-expression, PTPRF was localized at the plasma membrane with limited colocalization with HRS (Figure 4.7A, left panel). However, overexpression of NEDD4L significantly enhanced the colocalization of PTPRF with HRS (Figure 4.7A, right panels). To confirm the requirement of PTPRF ubiquitination in promoting its trafficking to MVBs, we examined the co-localization of PTPRF- Δ D1 and PTPRF- Δ D2 mutants with HRS. Both PTPRF- Δ D1 and PTPRF- Δ D2 were primarily localized to the plasma membrane when expressed alone (Figure 4.7B-C, left panels). Interestingly, while co-expression of NEDD4L had little effect on removing PTPRF- Δ D1 from the plasma membrane, colocalization of PTPRF- Δ D2, NEDD4L and HRS in large intracellular vesicles was readily observed (Figure 4.7B-C, right panels). Quantitative analysis of Pearson's coefficient indicated that NEDD4L stimulates the colocalization of HRS with WT and PTPRF- Δ D2 but not with PTPRF- Δ D1 (Figure 4.7D). Taken together with our findings that the D1 domain is required for NEDD4L to ubiquitinate PTPRF (Figure 4.2C), these results suggest that NEDD4L-mediated ubiquitination allows for the trafficking of PTPRF to MVBs.

We have shown previously that PTPRF positively regulates Wnt signaling upstream of the destruction complex [51]. Here we examined the effect of NEDD4L-induced PTPRF internalization and degradation on Wnt signaling activation. Results from Wnt reporter assays showed that rescuing the expression of PTPRF significantly increased Wnt signaling in PTPRF KO cells (Figure 4.8A). Although NEDD4L has been shown to promote the degradation of DVL2 and LGR5 [161, 167], overexpression of either WT or

NEDD4L/DD mutant did not significantly alter Wnt reporter activities in PTPRF KO cells (Figure 4.8A). Importantly, co-expression of NEDD4L completely abolished PTPRF-stimulated increase of Wnt reporter activities whereas NEDD4L/DD mutant had no effect (Figure 4.8A). The expression of PTPRF and NEDD4L was confirmed using western blot analysis (Figure 4.8B). Collectively, our results demonstrate that NEDD4L-mediated PTPRF ubiquitination occurs at the plasma membrane and this ubiquitination event removes PTPRF from the plasma membrane; and subsequent internalization and degradation of PTPRF blocks its ability to enhance Wnt signaling (Figure 4.8C).

4.4 Discussion

Protein phosphorylation is one of the most common post-translational modifications involved in regulating cell signaling. The balance between phosphorylation and dephosphorylation is tightly controlled by the action of protein kinases and phosphatases. Compared to protein kinases, the function and regulation of protein phosphatases are largely understudied. Here we describe a novel mechanism by which the expression and localization of PTPRF is regulated. Previous studies have demonstrated that the ubiquitination and internalization cell surface receptors are critical in controlling the amplitude and duration of signaling downstream of receptor tyrosine kinases [164, 165]. To our knowledge, our study is the first to show that similar regulatory mechanisms can be utilized to regulate receptor tyrosine phosphatases. Specifically, we establish that NEDD4L-mediated ubiquitination of PTPRF triggers its internalization and degradation, a stepwise process that resembles how NEDD4L controls the expression of other membrane substrates such as ENaC [96]. Moreover, the finding that NEDD4L uses K29- and K63-linked ubiquitin to modify PTPRF is consistent with previously reported roles of these two

types of ubiquitin linkages in regulating receptor endocytosis and trafficking [158]. Interestingly, K29-linked ubiquitination of DVL2 and Axin2, two key components in the Wnt pathway, has been shown to negatively regulate Wnt signaling via degradation-dependent and -independent mechanisms [161, 168]. In addition, we find that ubiquitinated PTPRF is transported to MVBs where it colocalizes with NEDD4L and HRS. Since ubiquitinated membrane proteins in MVBs can be sorted into lysosome for degradation or recycle back to the membrane, additional studies are needed to determine the fate of ubiquitinated PTPRF beyond MVBs.

Intriguingly, we show that the phosphatase inactive mutant PTPRF is more stable compared to WT phosphatase. The PTPRF-C/S mutant is less insensitive to NEDD4L-induced ubiquitination and internalization. We reason that the phosphatase-inactive mutant may adopt a different confirmation that prevents the access of NEDD4L. However, more studies are needed to determine how the phosphatase activity of PTPRF affects its protein stability. Unlike most tyrosine kinase receptors, the existence of endogenous ligands for receptor tyrosine phosphatases is largely unknown. It has been shown that the E-domain of PTPRF interacts with the glycosaminoglycan chains of syndecan with high affinity [169]. Given the functional connection between PTPRF and Wnt signaling, it is of particular interest to determine if the presence of syndecan or Wnt ligand alters NEDD4L-mediated ubiquitination of PTPRF in future studies.

The Wnt pathway is known to be modulated by protein ubiquitination at multiple steps in order to control signaling propagation. In addition to well-characterized ubiquitination-mediated degradation of β -catenin in the destruction complex, Frizzled and LGR5 receptors have been shown to be ubiquitinated and subsequent degraded by E3

ligases such as RNF43/ZNRF3 and NEDD4L [162, 170]. Moreover, the identification of tankyrase- and RNF146-dependent ubiquitination of Axin has led to the development of tankyrase inhibitors for cancer therapies [171]. Given that the E3 ligase function of NEDD4L regulates DVL2 and LGR5 in addition to PTPRF, it is of particular interest for future studies to determine how Wnt stimulation dictates the selection of substrates downstream of NEDD4L. In summary, our study on identifying PTPRF as a new substrate of NEDD4L provides another ubiquitination-dependent mechanism that involves removal of a positive regulator from the plasma membrane to downregulate Wnt signaling.

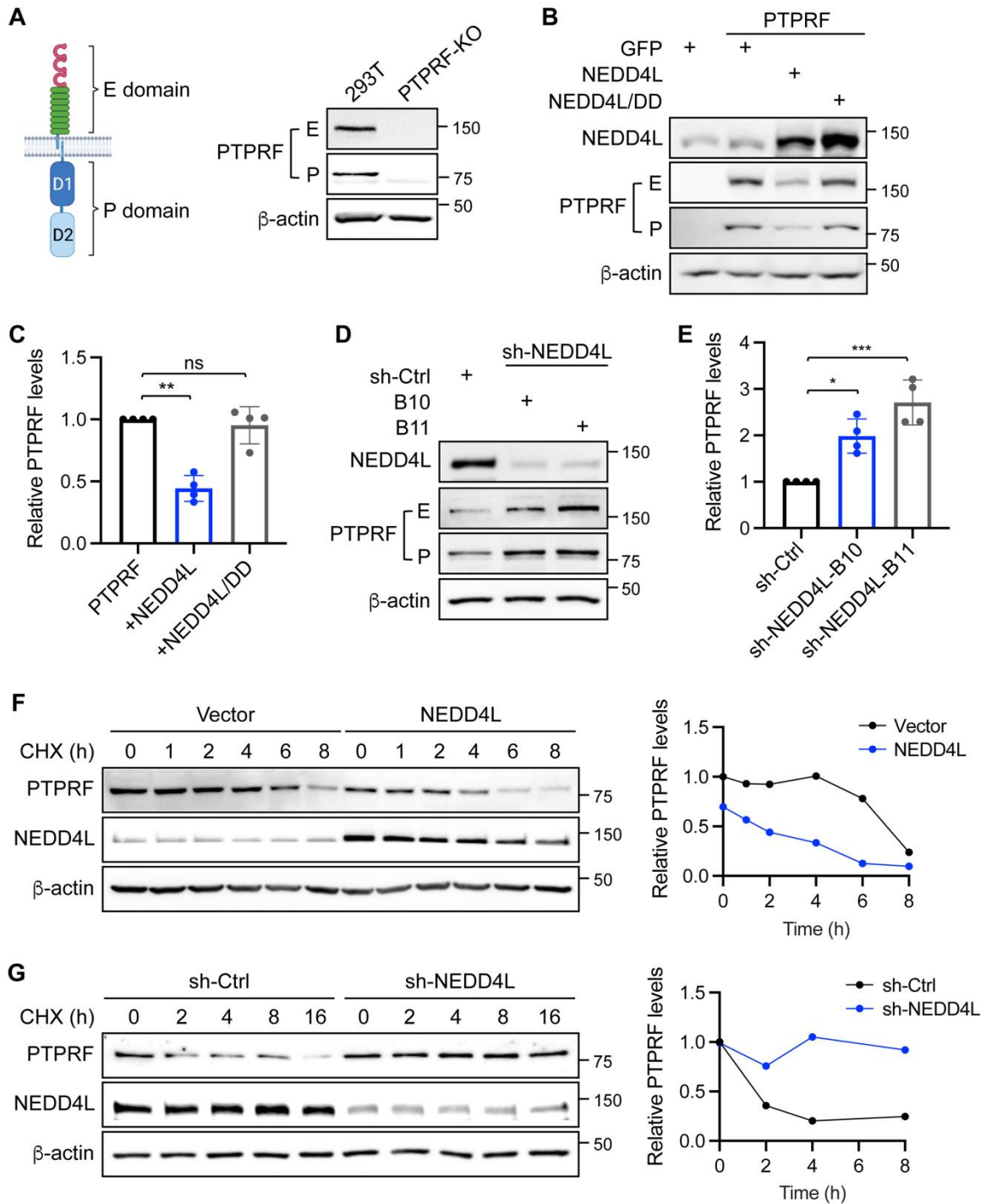


Figure 4.1 The expression of PTPRF is regulated by NEDD4L.

(A) The expression of PTPRF can be detected using antibodies against either the extracellular domain (E-domain) or the intracellular phosphatase domain (P-domain). The P-domain is consisted of a catalytically active D1 phosphatase domain and a

pseudophosphatase D2 domain. Representative western blots showed lack of PTPRF expression in one of the PTPRF KO clonal 293T cell lines. (B) PTPRF KO 293T cells were transfected with GFP vector, HA-NEDD4L or HA-NEDD4L/DD along with PTPRF. Cell lysates were analyzed for the expression of PTPRF, NEDD4L and β -actin using western blot. (C) Relatively levels of PTPRF expression were quantified by normalizing to β -actin. Data were presented as mean \pm SD (n = 4, ** p<0.01). (D) Knockdown of NEDD4L increased PTPRF expression in 293T cells. Cell lysates prepared from control (sh-Ctrl) and two NEDD4L knockdown cell lines (B10 and B11) were analyzed for the expression of PTPRF, NEDD4L and β -actin using western blot. (E) Relative levels of PTPRF were quantified by normalizing to β -actin. Data represented mean \pm SD (n = 4, * p<0.05 and ** p<0.01). (F) PTPRF KO cells were transfected with PTPRF-Flag together with either vector or HA-NEDD4L. Cells were treated with CHX (20 μ g/mL) and chased for 0-8 h. The expression of PTPRF, NEDD4L and β -actin was analyzed using western blot. Quantitative results of normalized PTPRF expression were shown on the right. (G) Control (sh-Ctrl) and NEDD4L knockdown cells were treated with CHX and chased for 0-16 h. Quantitative results of normalized PTPRF expression were shown on the right.

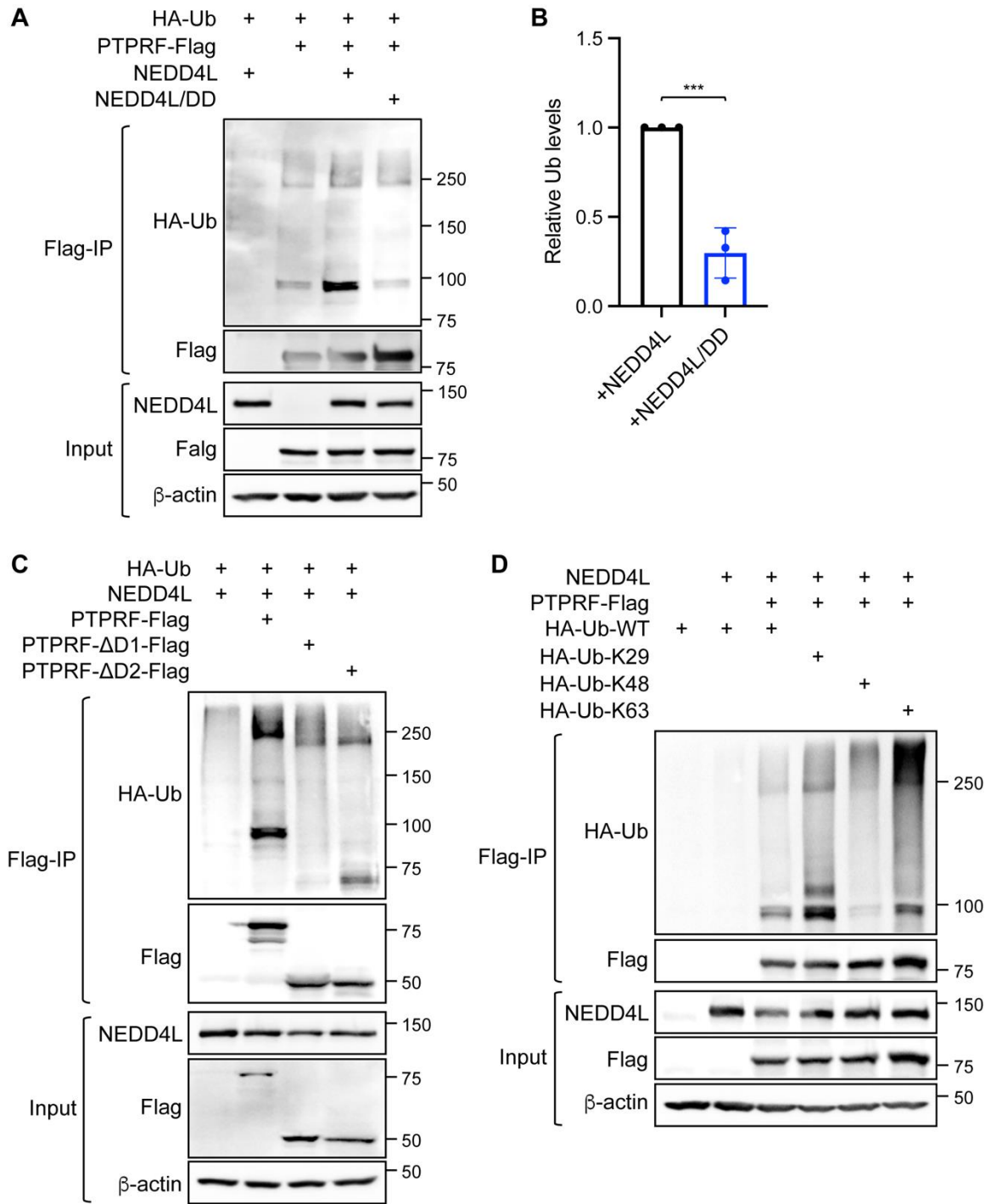


Figure 4.2 NEDD4L controls PTPRF ubiquitination

(A) PTPRF KO cells were transfected with PTPRF-Flag and HA-Ub together with either His-NEDD4L or His-NEDD4L/DD. The Flag-tagged PTPRF was immunoprecipitated using Flag antibody conjugated beads. The levels of PTPRF ubiquitination were detected

using the HA antibody. Cell lysates were used to show the expression of NEDD4L, PTPRF-Flag and β -actin in the input. (B) Relative levels of PTPRF ubiquitination were quantified by normalizing HA-Ub to PTPRF-Flag in immunoprecipitates. Data represent mean \pm SD (n = 3, *** p<0.001). (C) PTPRF KO cells were transfected with HA-Ub and His-NEDD4L along with PTPRF-Flag, PTPRF- Δ D1-Flag or PTPRF- Δ D2-Flag. Cell lysates were immunoprecipitated with Flag antibody conjugated beads. The ubiquitination and expression of WT, Δ D1 and Δ D2 PTPRF proteins were detected as described in (A). (D) PTPRF KO cells were transfected with PTPRF-Flag and His-NEDD4L together with one of ubiquitin expression constructs, including HA-Ub (WT), HA-Ub-K29, HA-Ub-K48 and HA-Ub-K63. The ubiquitination of PTPRF with different linkages was detected as described in (A). Cell lysates were used to show the expression of NEDD4L, PTPRF-Flag and β -actin in the input.

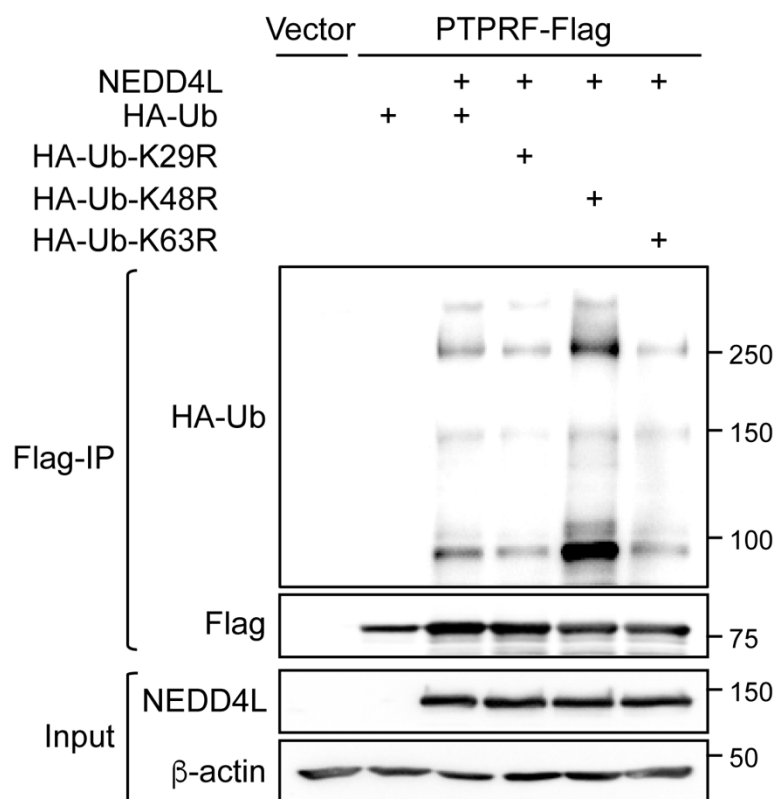


Figure 4.3 NEDD4L-mediated ubiquitination of PTPRF uses the K29 and K63 linkage.

PTPRF KO cells were transfected with PTPRF-Flag and His-NEDD4L together with one of ubiquitin constructs, including HA-Ub (WT), HA-Ub-K29R, HA-Ub-K48R and HA-Ub-K63R. Un-transfected cells and cells transfected with HA-Ub (WT) alone were included as controls. The ubiquitination of PTPRF with different linkages was detected in immunoprecipitates as described in Figure 2. Cell lysates were used to show the expression of NEDD4L and β -actin in the input.

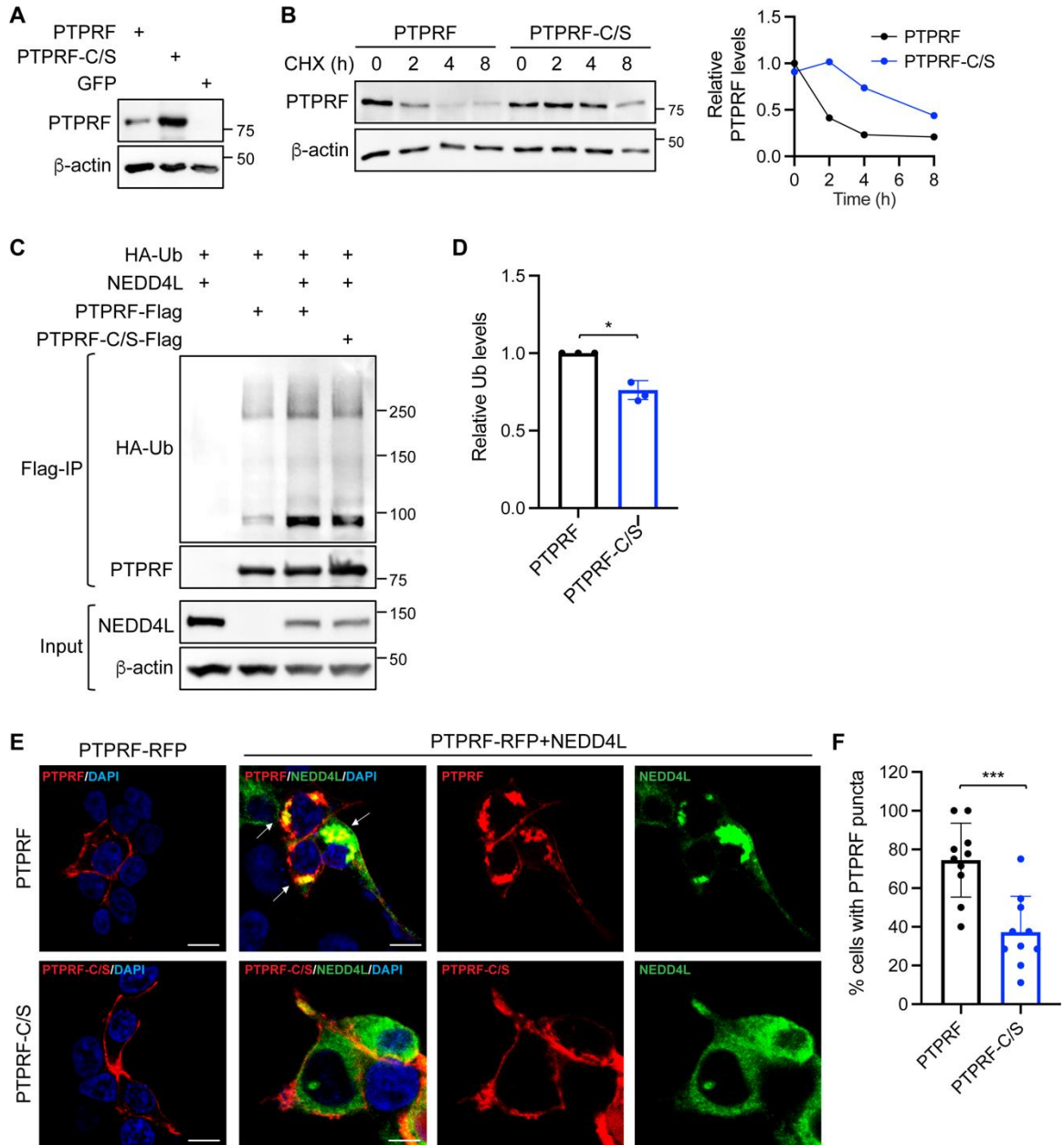


Figure 4.4 The phosphatase activity of PTPRF promotes its ubiquitination and degradation.

(A) PTPRF KO cells transfected with WT PTPRF, PTPRF-C/S, or GFP were analyzed for the expression of PTPRF and β -actin. (B) PTPRF KO cells transfected with PTPRF-Flag or PTPRF-C/S-Flag were treated with CHX (20 μ g/mL) and chased for 0-8 h. Protein lysates were analyzed using western blot and quantitative results of normalized PTPRF expression were shown on the right. (C) PTPRF KO cells were transfected with HA-Ub

and His-NEDD4L together with PTPRF-Flag or PTPRF-C/S-Flag. WT and C/S mutant PTPRF were immunoprecipitated using Flag antibody conjugated beads, and PTPRF ubiquitination was detected using the HA antibody. The expression of NEDD4L and β -actin was detected in the input using western blot. (D) Relative levels of PTPRF ubiquitination were obtained by normalized HA-Ub to PTPRF in the immunoprecipitates. Data represent mean \pm SD (n = 3, * p<0.05). (E) PTPRF KO cells were transfected as the following: PTPRF-RFP, PTPRF-C/S-RFP, PTPRF-RFP + HA-NEDD4L, and PTPRF-C/S-RFP + HA-NEDD4L. The localization of PTPRF and NEDD4L was detected via RFP (red) or staining with the NEDD4L antibody (green), respectively. DAPI was used to stain nuclei. Arrows indicate intracellular puncta with colocalized PTPRF-RFP and NEDD4L. Scale bar, 10 μ m. (F) Images taken from PTPRF-RFP + HA-NEDD4L and PTPRF-C/S-RFP + HA-NEDD4L co-transfected cells were scored for percentage of cells with PTPRF puncta. Data represent mean \pm SD (n=10, *** p<0.001).

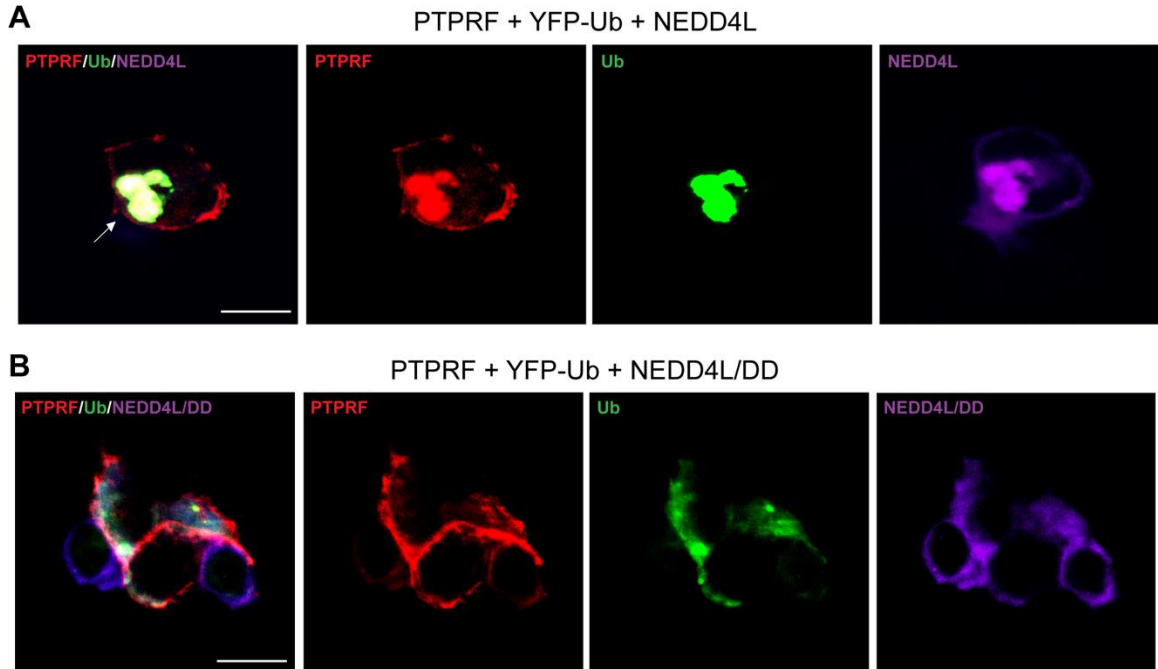


Figure 4.5 NEDD4L-mediated ubiquitination removes PTPRF from the plasma membrane.

(A-B) PTPRF KO cells were transfected with PTPRF-RFP + YFP-Ub in combination with HA-NEDD4L or HA-NEDD4L/DD. The localization of PTPRF, Ub and NEDD4L was detected via RFP (red), YFP (green) and staining with the NEDD4L antibody (Cy5, purple), respectively. An arrow indicates a large intracellular punctum with colocalized PTPRF-RFP, YFP-Ub and NEDD4L. Scale bar, 10 μ m.

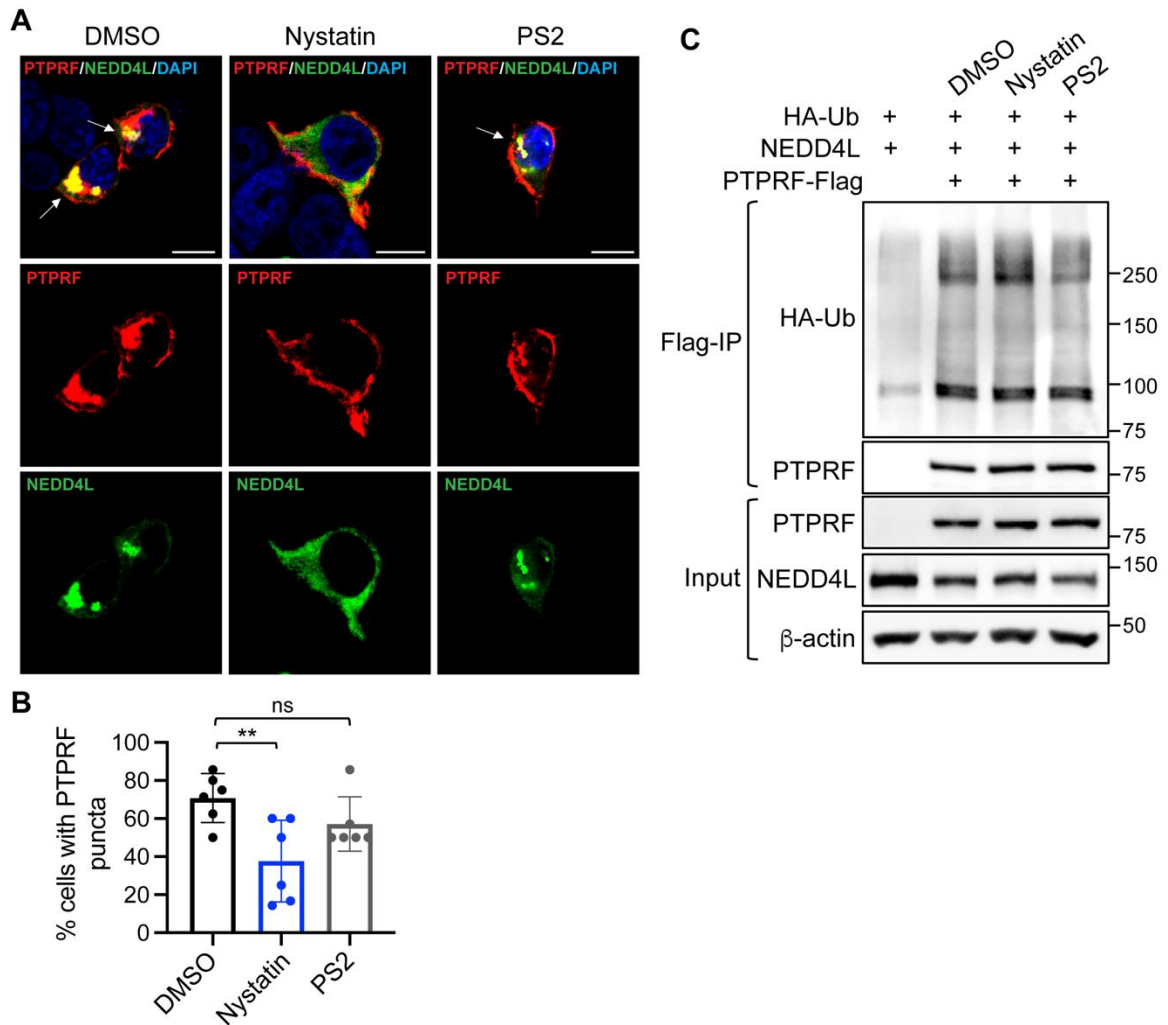


Figure 4.6 The ubiquitination of PTPRF triggers caveolin-mediated internalization. (A) PTPRF KO cells transfected with PTPRF-RFP and HA-NEDD4L were treated with DMSO, nystatin, or PS2 for 2 h. The localization of PTPRF and NEDD4L was detected via RFP (red) and staining with the NEDD4L antibody (green), respectively. DAPI was used to stain nuclei. Arrows indicate intracellular puncta with colocalized PTPRF-RFP and NEDD4L. Scale bar, 10 μ m. (B) The percentage of cells with PTPRF puncta was quantified as described in Methods. Data represent mean \pm SD ($n = 6$, ** $p < 0.01$). (C) PTPRF KO cells transfected with PTPRF-Flag, HA-Ub and His-NEDD4L were treated with DMSO, Nystatin, or Pitstop2 (PS2) for 2 h. Cells transfected with HA-Ub and His-NEDD4L were included as a control. The ubiquitination of PTPRF was detected in immunoprecipitates

using the HA antibody. The expression of PTPRF, NEDD4L and β -actin was detected in the input using western blot.

HRS and NEDD4L was detected via RFP (red), CFP (blue) and staining with the NEDD4L antibody (green), respectively. DAPI was used to stain nuclei in cells expressing PTPRF- Δ D1-RFP alone. Scale bar, 10 μ m. (C) PTPRF KO cells were transfected with PTPRF- Δ D2-RFP or PTPRF- Δ D2-RFP + CFP-HRS + HA-NEDD4L. The localization of PTPRF- Δ D2, HRS and NEDD4L was detected via RFP (red), CFP (blue) and staining with the NEDD4L antibody (green), respectively. DAPI was used to stain nuclei in cells expressing PTPRF- Δ D2-RFP alone. Arrow indicate intracellular puncta with colocalized PTPRF- Δ D2-RFP, CFP-HRS and NEDD4L. Scale bar, 10 μ m. (D) Colocalization of WT and mutant PTPRF-RFP and CFP-HRS was determined using Pearson's coefficient as calculated by NIS-elements AR software (Nikon). Data represent mean \pm SD (n = 20, * p<0.05 and **** p<0.0001).

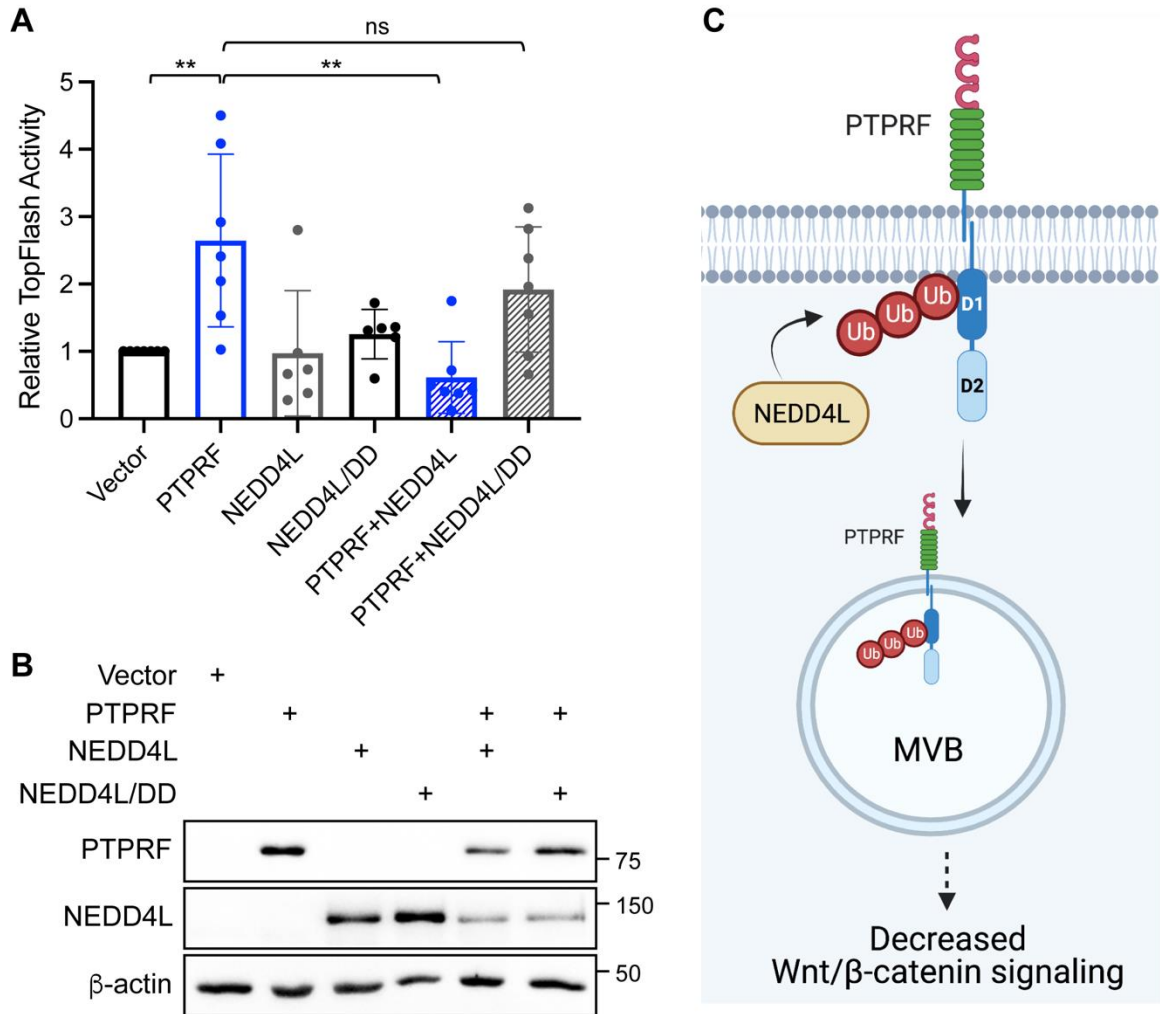


Figure 4.8 NEDD4L-mediated degradation of PTPRF decreases Wnt signaling.

(A-B) PTPRF KO cells were transfected with the TopFlash Wnt reporter along with a combination of expression plasmids as indicated. Subsequently, the cells were stimulated with Wnt3A conditioned media for 8 h. Cell lysates were analyzed for the relative Wnt reporter activities using luciferase assays (A) and the expression of PTPRF and NEDD4L using western blot (B). (C) Results from our study indicate that PTPRF is ubiquitinated at the plasma membrane by NEDD4L and subsequently internalized to MVBs via a caveolin-dependent mechanism. Functionally, ubiquitination and internalization of PTPRF blocks PTPRF-dependent activation of Wnt signaling.

CHAPTER 5. PTPRF REGULATES WNT SIGNALING AND INTESTINAL STEM CELL RENEWAL VIA DEPHOSPHORYLATION OF CAVEOLIN-1

5.1 Abstract

PTPRF, a receptor type protein tyrosine phosphatase, functions as a positive regulator in the Wnt pathway at the level upstream of the destruction complex. Our previous studies have shown that PTPRF-mediated activation of Wnt signaling requires its phosphatase activity in colon cancer cells; however, no substrates of PTPRF have been identified. Here we describe a novel substrate that mediates PTPRF-dependent Wnt activation. While knockout of PTPRF decreased Wnt activation as shown by TopFlash reporter assays, re-expression of WT but not phosphatase activity deficient mutant PTPRF rescued Wnt reporter activity and LRP6 phosphorylation. Additionally, we found that PTPRF dephosphorylated Tyr14 (Y14) of caveolin-1 (Cav1) by interacting with the substrate. Results from confocal microscopy revealed that Wnt stimulation induced the formation of the Wnt signalosome at the plasma membrane where PTPRF and Cav1 colocalized. Moreover, the expression of Cav1/Y14F mutant blocks the effect of PTPRF on enhancing LRP6 phosphorylation. Functionally, by crossing *Ptprf* knockout mice to the *Lgr5-EGFP-IRES-creERT2* (*Lgr5-EGFP*) model, we show that the proliferation and self-renewal ability of intestinal crypt cells are decreased in *Ptprf* KO mice. Consistently, the number of intestinal stem cells and the expression of stem cell genes downstream of Wnt signaling were significantly reduced. Overall, our study demonstrates that PTPRF promotes Wnt activation likely through dephosphorylation of Cav1 to prolong the signaling lifetime of Wnt signalosomes. The PTPRF-deletion induced deficiency in intestinal stem cells highlights the importance of PTPRF as a novel co-regulator of the Wnt pathway to fine tune the level of activation.

5.2 Introduction

Protein Tyrosine Phosphatase Receptor Type F (PTPRF) is a single-pass transmembrane phosphatase that is important for cell adhesion, neuronal development, and Wnt signaling. PTPRF is a member of the class IIA RPTPs which contain extracellular fibronectin type 3 (FN3) and immunoglobulin-like (Ig-like) domains, and 2 intracellular phosphatase domains (D1 & D2). The D1 phosphatase domain is active and more proximal to membrane, and the D2 domain is deficient in phosphatase activity (pseudophosphatase domain). PTPRF is cleaved post-translationally at the transmembrane region giving rise to the final protein consisting of an extracellular (E) subunit and an intracellular phosphatase domain (P) subunit that are non-covalently bound at the membrane [14]. PTPRF has been most studied for its role in cell adhesion via its extracellular domain binding to HSPGs. However, few substrates of PTPRF have been identified to date. Studies from the 1990's identified the insulin receptor [36-39] and EGFR [36] showing changes in tyrosine phosphorylation with silencing of PTPRF. Most recently, EphA2 was identified as a substrate of PTPRF to control cell migration [5].

PTPRF has been implicated as a positive activator of the Wnt signaling pathway [22, 51]. The Wnt/ β -catenin pathway is a highly conserved ligand-activated receptor pathway important in embryonic development and growth of tissues. When Wnt ligand is not present, β -catenin is targeted for proteasomal degradation a destruction complex composed of Axin, adenomatous polyposis coli (APC), GSK3 β , and CK1 α . This complex phosphorylates β -catenin which is a signal for β -TrCP mediated ubiquitination and proteasomal degradation to keep intracellular levels low. When Wnt ligand is present, it binds its receptors Frizzled (Fzd), a 7-pass transmembrane receptor and LRP5/6, a single-

pass transmembrane co-receptor. This heterodimeric complex induces a conformational change leading to phosphorylation of a series of Ser residues in the C-terminus of LRP6 (including Ser1490). Binding of Axin to phosphorylated LRP6 recruits additional effector proteins such as Dishevelled (Dvl) to the destruction complex, inhibiting its ability to phosphorylate β -catenin so it is not degraded. This allows cytosolic levels of β -catenin to accumulate where it translocates to the nucleus to bind TCF/LEF to activate the transcription of Wnt target genes, such as *Myc*, *CCND1*, *Lgr5*, and *Axin2*, that are important for cell proliferation and differentiation [54, 56].

Regulation of the Wnt/ β -catenin pathway is under tight control because of its importance in development and growth of tissues. One of the main regulatory mechanisms is the internalization of Wnt-Fzd-LRP6 receptor complex via the Wnt signalosome, controlling both the number of receptors available at the plasma membrane and the level of activation. Upon binding of Wnt ligand, the formation of a Wnt-Fzd-LRP6 complex and the recruitment of Dvl and Axin results in a multiprotein complex known as the Wnt signalosome [172]. This helps lead to increased downstream signaling and internalization of receptors via caveolin-mediated endocytosis [63, 64]. While caveolin is required for signalosome formation in normal cells [63, 64], clathrin-mediated endocytosis has been shown to promote the activation of Wnt signaling in cells with APC mutations [62]. More recently, the phosphorylation status of caveolin has been shown to influence its ability to internalize. Specifically, Tyr14 (Y14) on Cav1 has been shown to be phosphorylated by Src kinase and phosphorylation of Y14 leads to increased internalization of caveolae pits [69-72, 173]. However, the effect of caveolin phosphorylation at Y14 has not been studied in the context of the Wnt pathway or signalosome formation.

Intestinal epithelial cells are the most highly replicative cell population in the human body, turning over every 3-5 days [75]. The intestine is composed of the crypt base and villi that extend out into lumen to absorb nutrients and increase surface area. At the crypt base resides the intestinal stem cells (ISCs), a highly replicative and self-renewing stem cell population that can give rise to all epithelial cell types in the intestine. The cells proliferate and differentiate from the crypt base up the villus axis to replace cells at the villus tip. A large body of evidence indicates that the highest levels of Wnt signaling near the crypt base is required for the self-renewal and proliferation of ISCs [174, 175]. Dysregulation of the Wnt/ β -catenin pathway leads to the development of human diseases such as cancer and neurological disorders.

In this study, we investigated the mechanisms by which PTPRF regulates Wnt signaling. We found that PTPRF activates the Wnt pathway in a phosphatase-dependent manner by controlling the phosphorylation of Cav1. PTPRF-mediated dephosphorylation of Cav1-Y14 leads to prolonged signalosome retention at the plasma membrane, enhanced pLRP6 and downstream Wnt activation. Using PTPRF KO mouse model, we showed that PTPRF functions as a positive regulator of the Wnt pathway *in vivo* to enhance intestinal stem cell function. Together, our study identifies the role of PTPRF in activating the Wnt pathway by controlling Wnt signalosome formation and internalization.

5.3 Results

5.3.1 PTPRF activates Wnt signaling in a phosphatase dependent manner

Our previous study has shown that PTPRF promotes Wnt signaling at the level upstream of the destruction complex [51] (& chapter 4). Here we further investigated the mechanisms of PTPRF-mediated Wnt activation by focusing at the plasma membrane. Using PTPRF KO cell lines (described in chapter 4) we showed that loss of PTPRF expression led to a reduction in the Wnt signaling activation as measured by TopFlash reporter assays (Figure 5.1A-B). Next, we rescued PTPRF KO cells by re-expressing WT or PTPRF C/S mutant to determine if the phosphatase activity is required. Interestingly, while the expression of WT PTPRF rescued the Wnt reporter activity, phosphatase-deficient mutant failed to increase Wnt activation (Figure 5.1C).

Next, we determined the effect of PTPRF expression on Wnt-induced activation of LRP6 by monitoring the phosphorylation of LRP6 at S1490. Indeed, re-expression of PTPRF increases pLRP6 in a phosphatase-dependent manner after Wnt stimulation for 8 h (Figure 5.1D). Furthermore, we found that PTPRF expression increased the amplitude and duration of Wnt-induced LRP6 phosphorylation in rescued PTPRF KO cells (Figure 5.1E). Consistently, the levels of LRP6 phosphorylation were markedly decreased upon Wnt treatment in PTPRF KO cells compared to 293T parental cells (Figure 5.1F). Together, these results provide the evidence supporting the role of PTPRF in activating Wnt signaling using a phosphatase-dependent mechanism.

5.3.2 PTPRF interacts with LRP6

LRP6 is known to undergo spontaneous internalization from the membrane via the clathrin endocytosis pathway [56, 61]. Previously, we have shown that PTPRF and LRP6 colocalize in CRC cancer cells in intracellular vesicles under basal conditions [51]. To detect the localization of PTPRF and LRP6 in 293T cells, we rescued PTPRF KO cells with RFP-tagged PTPRF and stained for endogenous LRP6. Indeed, PTPRF and LRP6 colocalized in intracellular vesicles under basal conditions (Figure 5.2A). To identify the pathway by which PTPRF and LRP6 are internalized, PTPRF KO cells expressing PTPRF-RFP and LRP6-GFP were co-stained with EEA1 antibody to label early endosomes. Although majority of PTPRF-RFP and LRP6-GFP localized to the plasma membrane and large intracellular vesicles, we found that EEA1 positive vesicles contain both PTPRF and LRP6 (Figure 5.2B).

Next, we address the question if Wnt treatment stimulates PTPRF internalization. To this end, we expressed PTPRF-RFP together with CFP-tagged HRS to mark multi-vesicle body (MVB) in PTPRF KO cells. Cells were placed on ice for 30 min to stop internalization, then stimulated with Wnt3A condition media at 37°C for 0-4 h. We found that PTPRF was initially localized at the plasma membrane; and PTPRF gradually internalized to HRS positive vesicles following Wnt treatment for 2 h. However, with 4 h of Wnt treatment, increasing amount of PTPRF re-localized to the membrane (Figure 5.2C). Collectively, these results suggest 1) PTPRF colocalizes with LRP6 basally in intracellular vesicles likely due to constitutive internalization and recycling of these membrane receptor proteins; 2) only a small amount of PTPRF and LRP6 are found in

early endosomes; and 3) endocytosis of PTPRF can be triggered by Wnt stimulation thus further establishing a mechanistic connection between PTPRF and the Wnt pathway.

5.3.3 PTPRF dephosphorylates Y14 of Cav1 to enhance Wnt signaling

To date, only a few substrates of PTPRF have been identified, none being involved in the Wnt pathway. Since PTPRF-mediated Wnt activation is phosphatase-dependent (Figure 5.1C), we searched for potential substrates in the Wnt pathway that are known to be phosphorylated at tyrosine residues. Given the involvement of Cav1 in LRP6 endocytosis [63] and fact that it is phosphorylated at Y14, we investigated the hypothesis that PTPRF activates Wnt signaling by regulating caveolin-mediated Wnt signalosome formation. To determine if Cav1 is a substrate, PTPRF KO cells were transfected with Flag-Cav1 together with vector, WT or PTPRF-C/S mutant. Indeed, when WT PTPRF was overexpressed, there was a significant reduction in the level of Cav1-Y14 phosphorylation compared to vector transfected cells; however, expression of PTPRF-C/S mutant had no effect on Cav1-Y14 dephosphorylation (Figure 5.3A, B). Next, we examined the interaction between Cav1 and PTPRF. Interestingly, Wnt stimulation increased the interaction between PTPRF and Cav1 as well as LRP6 (Figure 5.3C). Moreover, using a tyrosine mutant at Y14 (Y14F) to mimic the effect of PTPRF dephosphorylation, we showed that the interaction between this mutant and PTPRF was increased without Wnt treatment (Figure 5.3C). To visualize the association of PTPRF and Cav1, PTPRF-RFP and Cav1-EGFP were co-expressed in PTPRF KO cells. Prior to Wnt stimulation, PTPRF was predominately localized at the plasma membrane whereas Cav1 has mixed intracellular vesicle and plasma membrane localization. A limited colocalization of PTPRF

and Cav1 was observed in small puncta along the membrane (Figure 5.3D). However, upon 2 h Wnt stimulation, the number and size of membrane localized puncta containing both Cav1 and PTPRF were increased (Figure 5.3D, insert). Additionally, colocalization of PTPRF and Cav1 was also seen in larger intracellular vesicles upon Wnt treatment (Figure 5.3D). A similar intracellular localization pattern of PTPRF was observed in Figure 5.2C where it internalized into HRS+ MVB vesicles in Wnt treated cells. Taken together, our results identify Cav1 as a novel substrate of PTPRF and Wnt stimulation increases the interaction and co-localization of the two proteins into Wnt signalosomes at the plasma membrane.

To further determine the functional effect of PTPRF-mediated dephosphorylation of Cav1, PTPRF KO cells were transfected with the Topflash Wnt reporter together with PTPRF and Cav1 separately or in combination. Our preliminary data showed that while PTPRF increased Wnt activation, Cav1 expressed by itself had no significant effect on altering Wnt reporter activity. Interestingly, co-expression of PTPRF with Cav1 further increased Wnt activation (Figure 5.4A). In addition, PTPRF KO cells transfected with WT or Cav1-Y14F mutant along with either WT or PTPRF-C/S mutant were analyzed for LRP6 phosphorylation upon treating with Wnt3A condition media. Consistent with results shown in Figure 5.2, re-expression of PTPRF increased pLRP6 levels in a phosphatase dependent manner in the context of WT Cav1 (Figure 5.4B). However, the expression of Cav1-Y14F alone was able to increase pLRP6 levels in the absence of PTPRF and the co-expression of WT or PTPRF-C/S had no additional effect on LRP6 phosphorylation (Figure 5.4B). Furthermore, we compared the location of Cav1-EGFP in 293T parental or PTPRF KO cells. In the presence of endogenous PTPRF, Cav1 containing puncta were observed at the

plasma membrane; in contrast, a majority of Cav1-positive puncta were intracellularly localized in PTPRF KO cells (Figure 5.4C). Taken together, these data suggest that PTPRF increases pLRP6 levels through dephosphorylation and membrane retention of Cav1 to enhance the signalosome formation and Wnt activation.

5.3.4 Deletion of PTPRF inhibits cell proliferation in mouse intestine

Given the role of Wnt signaling in maintaining the homeostasis of intestinal epithelium, we investigate the functional importance of PTPRF-dependent Wnt activation *in vivo* using a whole body PTPRF KO mouse model. To determine the effect of PTPRF deletion, we isolated intestinal tissues and crypt cells from WT and PTPRF KO mice for IHC, western blot, RT-qPCR and colony formation analysis (Figure 5.5A). To assess the stemness of intestinal crypts, we seeded freshly isolated crypt cells in 3D Matrigel for primary colony formation assays. Deletion of the PTPRF gene significantly reduced the ability of intestinal crypt cells to form organoids, a process mediated by functionally active intestinal stem cells (Figure 5.5B). Additionally, the proliferation of isolated crypt cells was decreased in PTPRF KO mice as shown by reduced expression of CCND1 and Ki67 genes using RT-qPCR analysis (Figure 5.5C). Furthermore, the rate of cell proliferation was assessed using immunofluorescence staining with the Ki67-Cy5 antibody in frozen intestinal tissues from WT and PTPRF KO mice. Quantitative analysis of the number of proliferative (Ki67⁺) cells per crypt showed decreased cell proliferation in the crypt of PTPRF KO mice (Figure 5.5D). Consistent with the role of PTPRF as a positive regulator in the Wnt pathway, our initial results demonstrate that PTPRF plays an important role in intestinal epithelial cell proliferation.

5.3.5 Deletion of PTPRF decreases the stemness and Wnt signaling in intestinal epithelial cells

To examine the effect of PTPRF-loss on modulating intestinal stem cell properties, we analyzed the expression of the *Lgr5* gene, a stem cell marker, using RNA *in-situ* hybridization. Consistently, the expression of *Lgr5* gene was exclusively observed at the crypt base (Figure 5.6A). The number of individual *Lgr5* copies/cell were quantified using HALO software; and the results showed that PTPRF KO mice displayed significantly fewer *Lgr5* copies per cell compared to WT mice (Figure 5.6B). In addition, the expression of other stem cell-associated genes (including *Ascl2*, *Sox9*, *Olfm4*, *Bmi1*) was significantly decreased whereas *Krt20*, a marker of intestinal epithelial cell differentiation, was increased in PTPRF KO mice (Figure 5.6C).

Furthermore, we crossed PTPRF KO mice to the LGR5-EGFP mouse model, which allows us to visualize and quantify the number of *Lgr5*⁺ stem cells *in vivo* (Figure 5.6D-E). The *Lgr5*-EGFP⁺ stem cells were readily detected at the crypt base in frozen sections using confocal microscopy (Figure 5.6D). To better quantify the number of *Lgr5*-EGFP⁺ cells, we isolated single cells from the crypts of WT and PTPRF KO mice and subjected them to FACS analysis. Among EpCAM⁺ intestinal epithelial cells, the percentage of *Lgr5*-EGFP⁺ cells were quantified. Interestingly, PTPRF KO mice had significantly fewer stem cells compared to WT mice (Figure 5.6E). Together, these data indicate that loss of PTPRF inhibits intestinal stem cell function *in vivo*.

One of the most importance signaling pathways involved in intestinal stem cell self-renewal and differentiation is the Wnt/ β -catenin pathway. To further determine how PTPRF-loss affects Wnt activation, we found that the phosphorylation of LRP6 and the

expression of Myc protein, a transcriptional target of Wnt, were significantly decreased in PTPRF KO mice compared to WT mice (Figure 5.7A-B). Consistent with decreased Wnt signaling, the expression of Wnt target genes, including Tcf7, Myc, and Lgr5, was significantly decreased in the crypts of PTPRF KO mice using RT-qPCR analysis (Figure 5.7C). Finally, to determine if activation downstream of the destruction complex can rescue the defect seen in PTPRF KO intestinal stem cells, we treated crypt cells with a GSK3 β inhibitor (CHIR99021) in colony formation assays to bypass the need for Wnt activation at the receptor level. We found that the ability of PTPRF KO crypts to form new organoids was restored to the same level as that of WT crypts following GSK3 β inhibitor treatment (Figure 5.7D). Collectively, these findings suggest that PTPRF-loss disrupts the self-renewal and proliferation of intestinal stem cells by inhibiting Wnt signaling upstream of the destruction complex.

Taken together, our *in vitro* and *in vivo* data support the function of PTPRF as a positive Wnt activator/regulator. The PTPRF-mediated dephosphorylation of Cav1 prolongs the retention of Wnt signalosome at the plasma membrane, allows for increased receptor clustering and pLRP6 accumulation, which ultimately leads to increased downstream β -catenin signaling and intestinal stem cell function (Figure 5.8). Overall, this study is the first to identify a role for a tyrosine phosphatase in the Wnt pathway, which sheds more light on how the endocytic pathway controls Wnt signalosome functions at the level of membrane receptors.

5.4 Discussion

The signalosome serves as a site for Wnt receptor clustering which can regulate signal amplification, maintenance, termination or inhibition [176]. The ability to regulate signal transduction at the membrane level is very important in tissue development and stem cells, as too much or too little pathway activation can lead to detrimental effects. In this study, we identified PTPRF as a novel regulator of the Wnt signaling pathway through the regulation of caveolin-mediated signalosome formation at the plasma membrane. PTPRF dephosphorylates Cav1 to attenuate its ability to internalize, which results in increased pLRP6, signalosome assembly and downstream β -catenin signaling. The identification of PTPRF as a co-regulator of the Wnt pathway provide a new mechanism that fine-tunes signaling activation at the receptor level.

Protein kinases have been extensively studied for their regulatory functions in the Wnt pathway, mainly GSK3 β and CK1 α for their phosphorylation of β -catenin and LRP6 [177]. However, no previous studies have explored the role of a tyrosine phosphatase in the Wnt pathway. Cav1 is known to be phosphorylated at Y14 by Src family of tyrosine kinases [178]; and this phosphorylation regulates the formation caveolae and endocytosis of certain membrane receptors [179, 180]. Although tyrosine phosphorylated Cav1 has been shown to regulate various cellular processes, including cancer cell migration and invasion, sensitivity to chemotherapy drugs, ROS-induced cell death and endothelial cell function [181-184], the functional importance of Cav1 phosphorylation at Y14 in modulating Wnt signaling has not been investigated. Here, we provide the first evidence supporting Cav1 as a new substrate of PTPRF in regulating the Wnt pathway. Although we have shown that the expression of WT but not phosphatase mutant PTPRF decreases

Cav1 phosphorylation at Y14 site, additional experiments are needed to confirm that Cav1 is a direct substrate. Moreover, it is of particular importance for future studies to determine if Cav1-Y14F mutant alters the time course of localization and phosphorylation of LRP6. Additional questions to be addressed include 1) how does Wnt stimulation regulate the endocytosis of PTPRF; 2) what is the role of Cav1/Cav1 phosphorylation in controlling the trafficking of PTPRF; and 3) how does PTPRF regulate the internalization and recycling of LRP6 and Fzd receptors both basally and upon Wnt stimulation? In addition, it has been shown that LRP6 can be phosphorylated by Src and Fer at multiple tyrosine residues (including Y1460, Y1517 and Y1520) in the intracellular domain and tyrosine phosphorylation of LRP6 inhibits Wnt signaling by decreasing signalosome formation and LRP6 endocytosis [185]. Given the close interaction between PTPRF and LRP6 and the notion that tyrosine mutations in LRP6 increases Wnt activation [186], PTPRF may regulate LRP6 phosphorylation in addition to Cav1. We have generated the necessary reagents and tools to tackle these questions in the future.

Using PTPRF KO mice, our study is the first to determine the functional significance of PTPRF in intestinal homeostasis *in vivo*. However, the main limitation of our study is that the phenotypes observed in our study may not be intestinal stem cell specific as a conventional whole-body KO mouse model is used. More recently, we have obtained a conditional *Ptprf*-flox mouse model [187] from the Jackson Laboratory (*Ptprf*^{tm1.1Sud/J}). The potential effect of PTPRF deletion in intestinal stem cells can be examined specifically by crossing the *Ptprf*-flox mouse model to *Lgr5*-EGFP-Cre mice used in our current study.

Overall, by combining *in vitro* biochemical and cell biology assays, *ex vivo* intestinal organoids and *in vivo* PTPRF KO mouse models, our study identifies a novel role of PTPRF in regulating Wnt signaling and intestinal stem cell function by controlling the phosphorylation of Cav1 and the signaling lifetime of Wnt signalosome. Future studies will focus on dissecting the functional interplay among Wnt signalosome components and PTPRF and tissue-specific contribution of PTPRF to intestinal homeostasis.

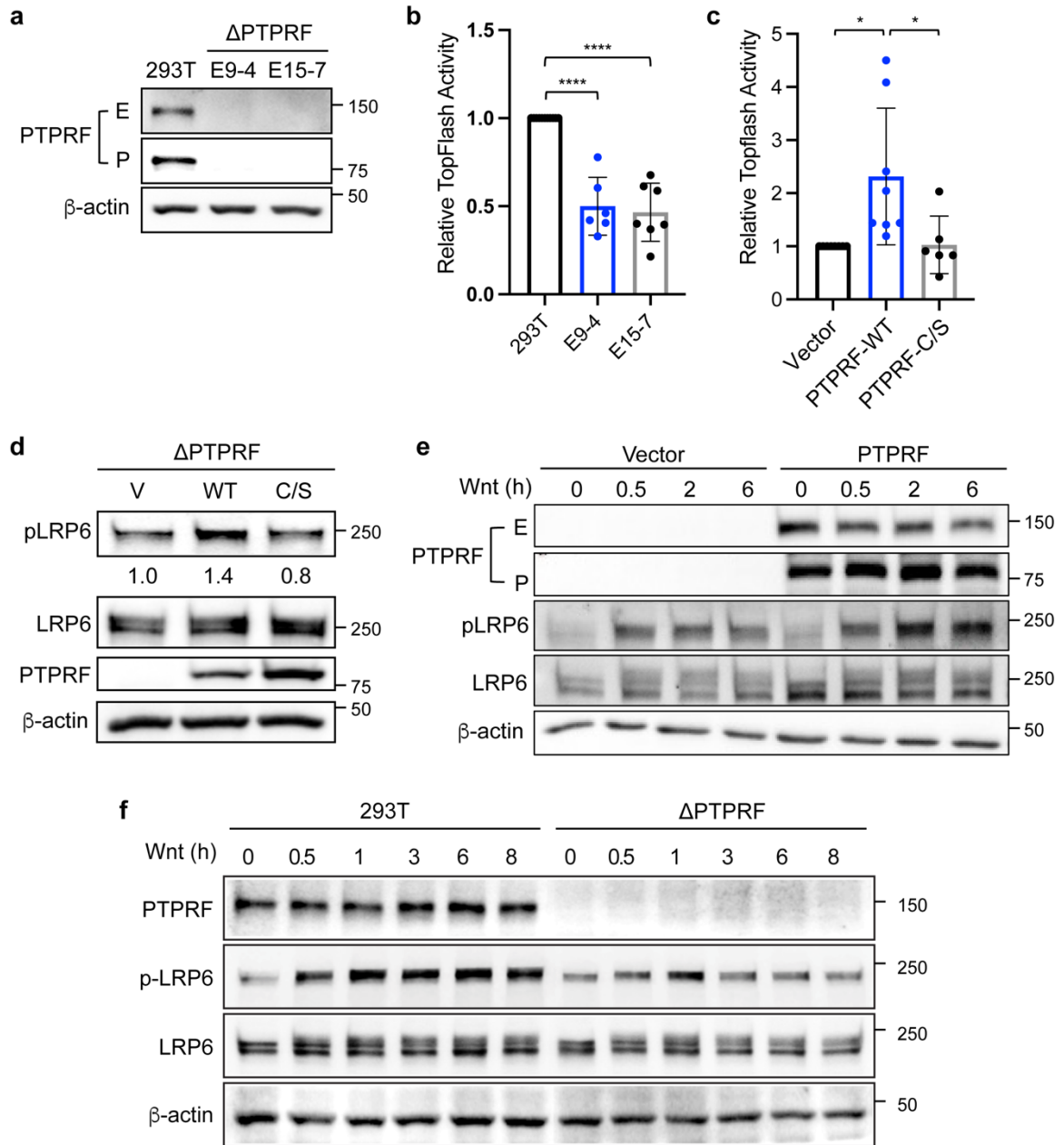


Figure 5.1 PTPRF activates Wnt signaling in a phosphatase dependent manner.

(A) 293T ΔPTPRF (PTPRF-KO) cells were generated using CRISPR/Cas9 with gRNAs targeting exon 9 or 15 of PTPRF (E9-4 & E15-7). Cell lysates were analyzed for the expression of PTPRF and β-actin using western blot. PTPRF was detected using antibodies specific for the extracellular E and intercellular P domain, respectively. (B) 293T or PTPRF KO cells were transfected with the TopFlash Wnt reporter. Subsequently, the cells were

stimulated with Wnt3A conditioned media for 8 h. Cell lysates were analyzed for the relative Wnt reporter activities using luciferase assays. Data were presented as mean \pm SD (n = 6, **** p<0.0001). (C-D) PTPRF KO cells were transfected with the TopFlash Wnt reporter along with vector (V), WT PTPRF, or PTPRF-C/S mutant. Subsequently, the cells were stimulated with Wnt3A conditioned media for 8 h. Cell lysates were analyzed for the relative Wnt reporter activities using luciferase assays (C) and the level of phospho-LRP6 (pLRP6 at S1490) and total protein expression of LRP6, PTPRF and β -actin using western blot (D). (E) PTPRF KO cells transfected with vector or WT PTPRF were subsequently treated with Wnt3A condition media for indicated times. Cell lysates were analyzed for the expression of PTPRF, pLRP6, LRP6, and β -actin using western blot.

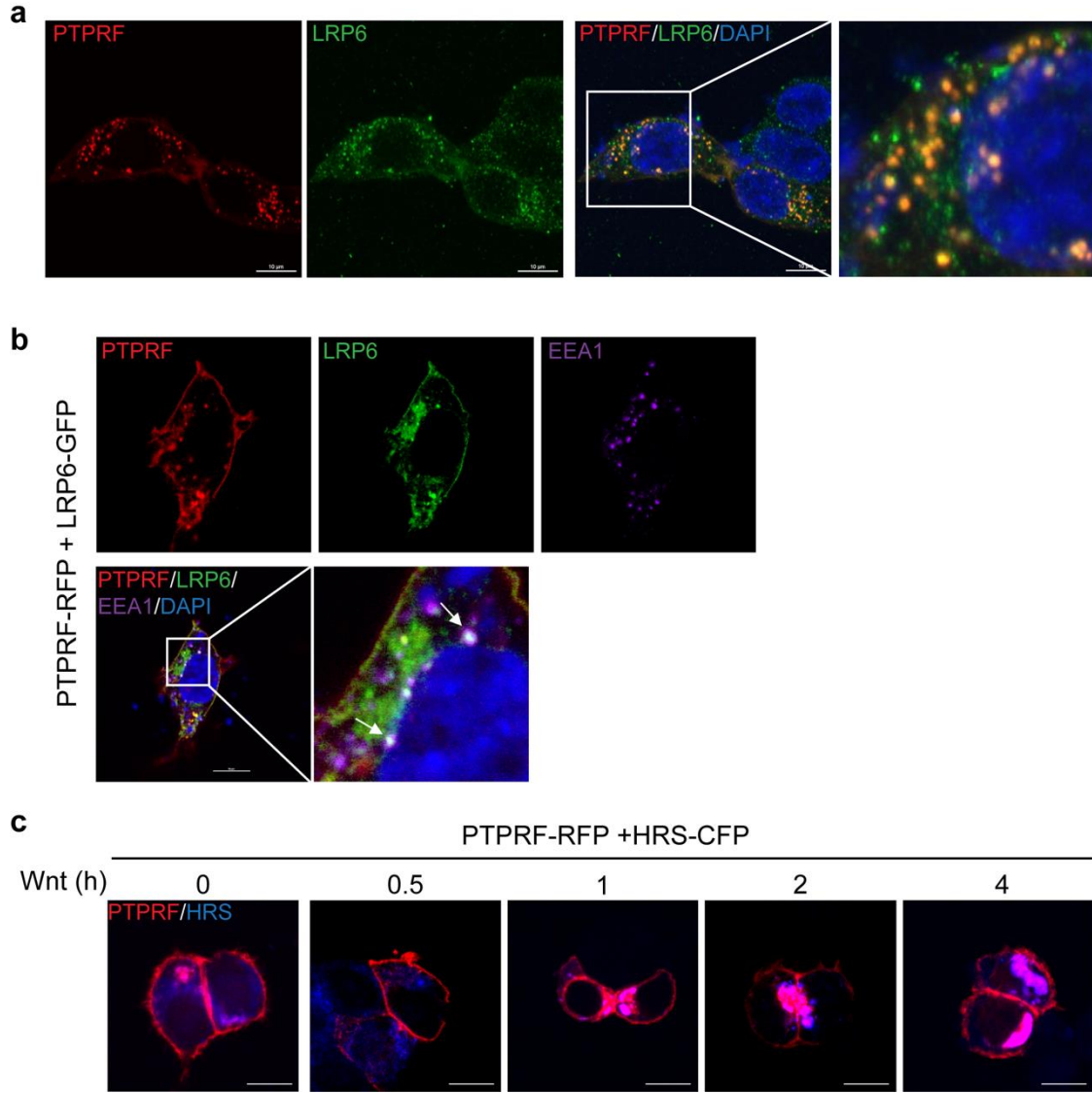


Figure 5.2 Localization of PTPRF and LRP6 basally and upon Wnt stimulation.

(A) PTPRF KO cells were transfected with PTPRF-RFP. The localization of PTPRF and endogenous LRP6 were detected via RFP (red) and staining with the LRP6 antibody (FITC, green), respectively. DAPI was used to stain nuclei (blue). Scale bar, 10 μ m. (B) PTPRF KO cells were transfected with PTPRF-RFP and LRP6-GFP. The localization of PTPRF, LRP6, and EEA1 were detected via RFP (red), FITC (green), and staining with the EEA1 antibody (Cy5, purple), respectively. DAPI was used to stain nuclei (blue). Scale bar, 10 μ m. (C) PTPRF KO cells were transfected with PTPRF-RFP and HRS-CFP. Cells were

placed on ice for 30 min prior to Wnt3A treatment for indicated times at 37°C. The localization of PTPRF and HRS were detected via RFP (red) and CFP (blue), respectively.

Scale bar, 10 μm .

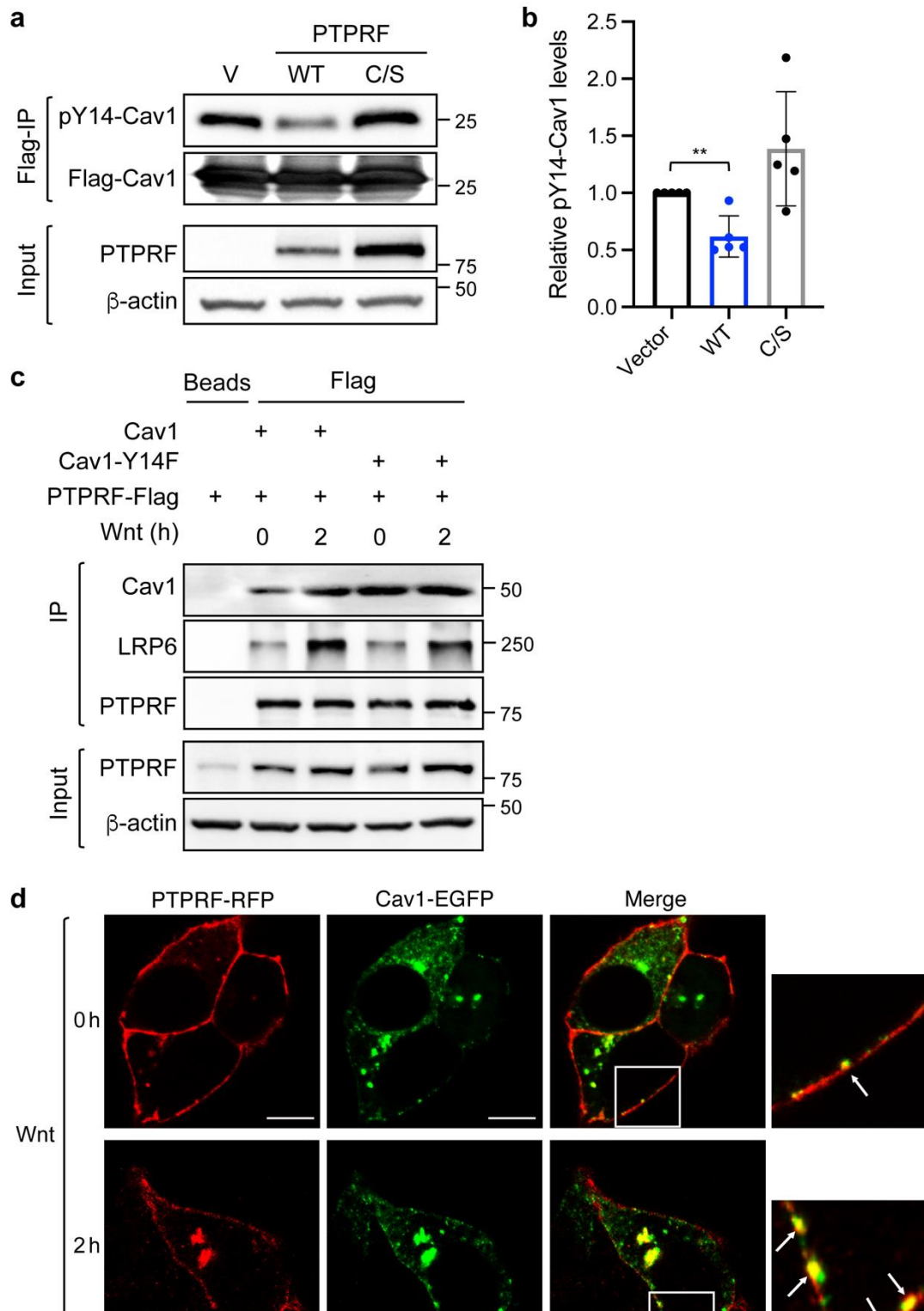


Figure 5.3 PTPRF dephosphorylates Y14 of Cav1.

(A) PTPRF KO cells were transfected with Flag-Cav1 along with vector, WT PTPRF, and PTPRF-C/S mutant. Cell lysates were immunoprecipitated using Flag antibody conjugated

beads. The level of pY14-Cav1 and total Cav1 in the immunoprecipitate was detected using the pY14-CAV and Flag antibodies, respectively. The expression of PTPRF and β -actin in the input were analyzed using western blot. (B) Relative levels of pY14-Cav1 were quantified by normalizing pY14-Cav1 to total Cav1 in immunoprecipitates. Data represent mean \pm SD (n = 4, ** p<0.01). (C) PTPRF KO cells transfected with PTPRF-Flag along with vector, WT Cav1-EGFP, and CAV1-Y14F-EGFP mutant were treated with Wnt3A condition media for 0-2 h. Cell lysates were immunoprecipitated using Flag antibody conjugated beads. The presence of Cav1, LRP6 and PTPRF in the immunoprecipitate was detected using the Cav1, LRP6 and Flag antibodies, respectively. The expression of PTPRF and β -actin in the input were analyzed using western blot. (D) PTPRF KO cells transfected with PTPRF-RFP and Cav1-EGFP were serum starved overnight and placed on ice for 30 min. Cells were fixed after incubation on ice or treated with Wnt3A condition media at 37°C for 2 h. The localization of PTPRF and Cav1 were detected via RFP (red) and GFP (green), respectively. Scale bar, 10 μ m.

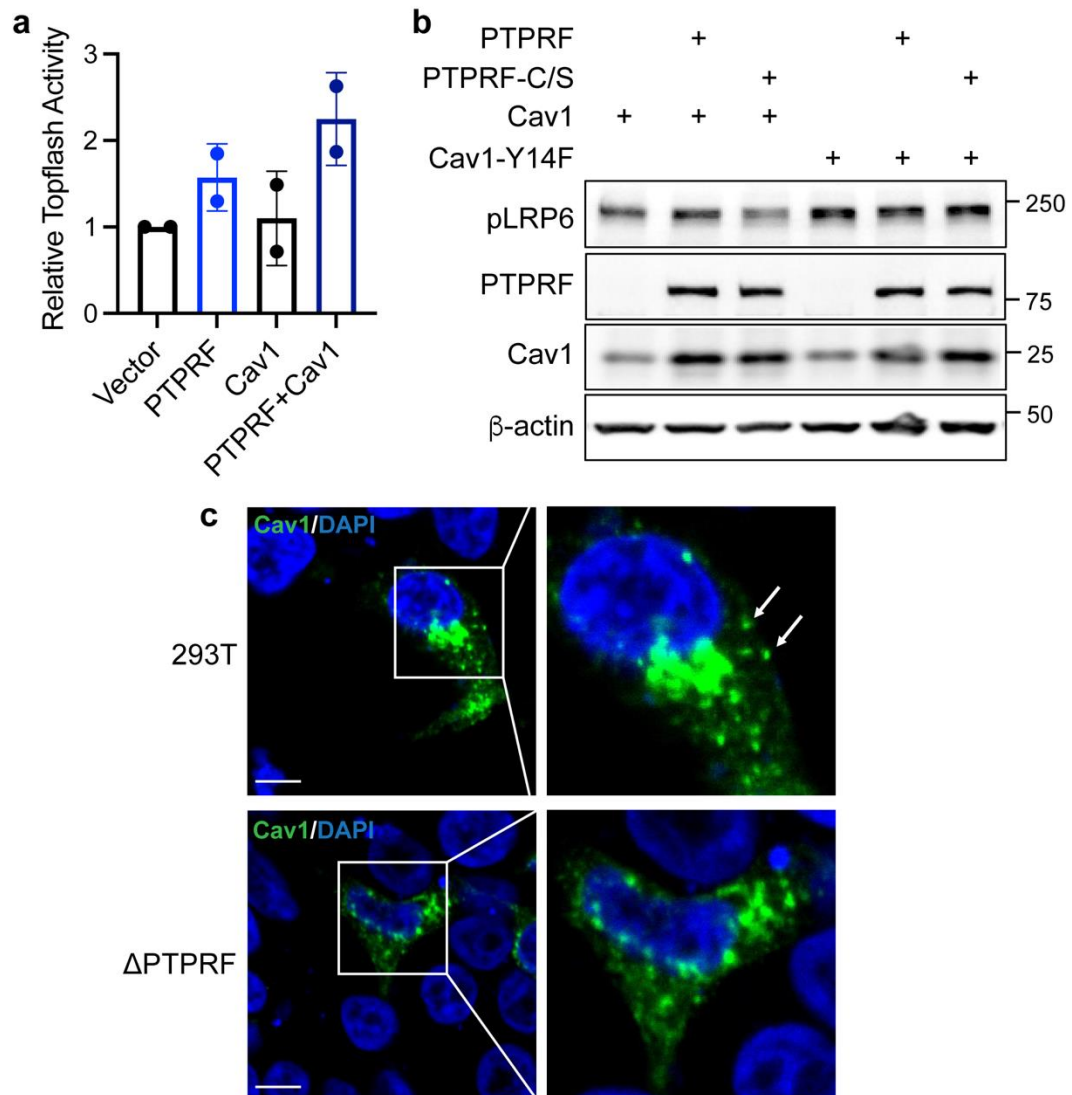


Figure 5.4 The dephosphorylation of Cav1-Y14F increases Wnt signaling and membrane localization.

(A) PTPRF KO cells were transfected with the TopFlash Wnt reporter along with vector, PTPRF, Flag-Cav1, or Flag-Cav1-Y14F. Subsequently, the cells were stimulated with Wnt3A conditioned media for 8 h. Cell lysates were analyzed for the relative Wnt reporter activities using luciferase assays. Data were presented as mean \pm SD (n = 2). (B) PTPRF KO cells were transfected with WT Cav1 or CAV1-Y14F mutant together with vector, WT PTPRF, or PTPRF-C/S. Subsequently, the cells were stimulated with Wnt3A conditioned media for 6 h. Cell lysates were analyzed for the expression of PTPRF, pLRP6 (S1490),

Cav1, and β -actin using western blot. (C) 293T or PTPRF KO cells were transfected with Cav1-EGFP. The localization of Cav1 was visualized via EGFP. DAPI was used to stain nuclei (blue). Scale bar, 10 μ m.

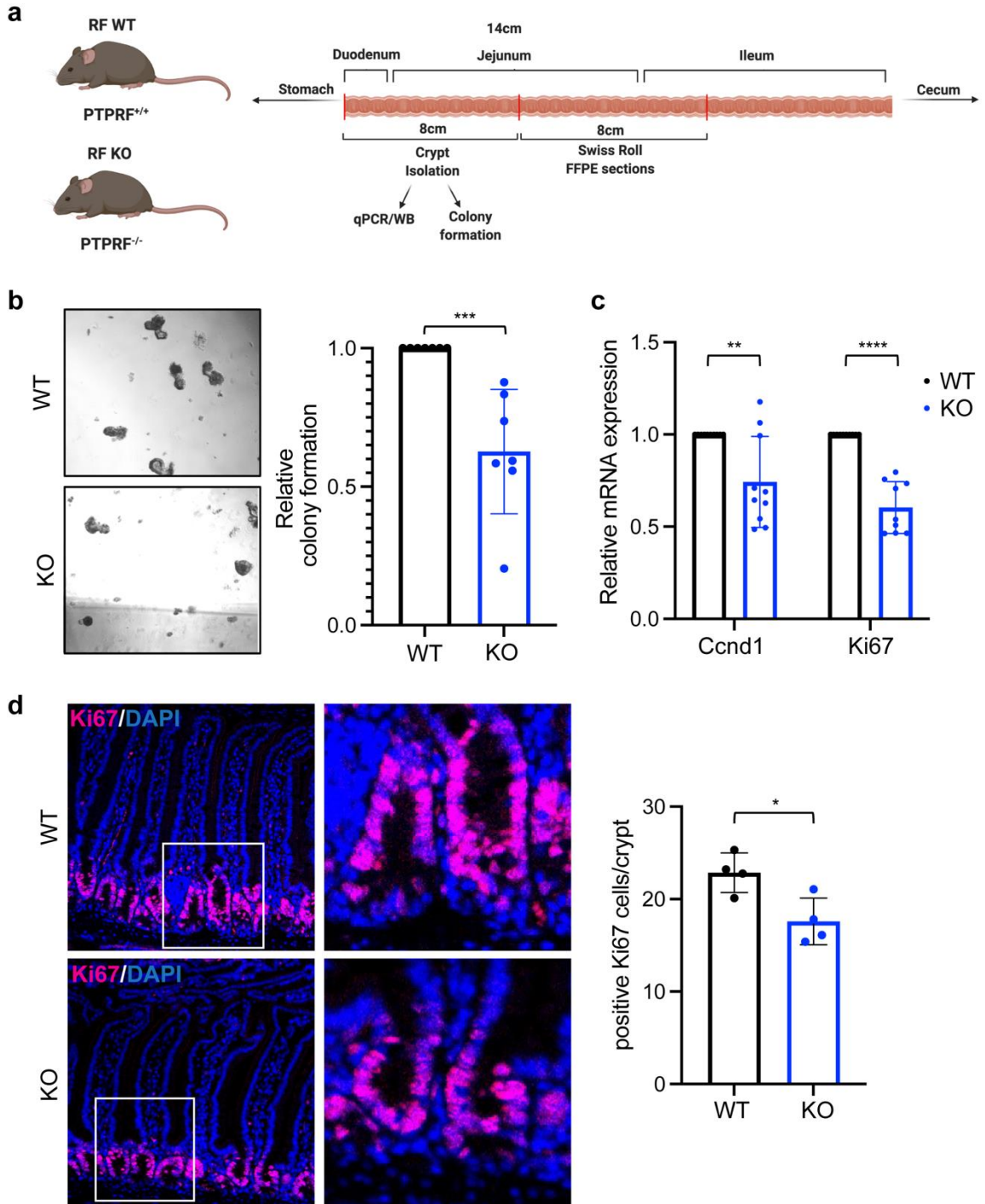


Figure 5.5 Knockout of PTPRF decreases the proliferation and colony formation of intestinal epithelial cells.

(A) Cohorts of WT and conventional PTPRF KO mice (*Ptprf*^{-/-}) of 8-week old were used for the analysis of intestinal phenotypes. The first proximal 8 cm of small intestine tissues were used for crypt isolation and subsequent colony formation and protein/RNA analysis,

whereas the next 8 cm was used for tissue analysis. (B) Freshly isolated crypts were seeded into 48-well plates in triplicates. Three days later, the number of organoids formed were counted and normalized to day 0. Representative images of intestinal organoids formed from crypt cells isolated from WT and KO mice are shown on the left. Scale bar, 100 μ m. Data were presented as mean \pm SD (n = 7, *** p<0.001). (C) The expression of cell proliferation markers, including CCND1 and Ki67, was analyzed in isolated crypt cells using RT-qPCR. Data were presented as mean \pm SD (n = 10, **** p<0.0001 and ** p<0.01). (D) Frozen tissue sections were stained with the Ki67-Cy5 antibody. Scale bar, 100 μ m. The number of Ki67-positive cells per crypt were quantified. Data were presented as mean \pm SD (n = 4, * p<0.05).

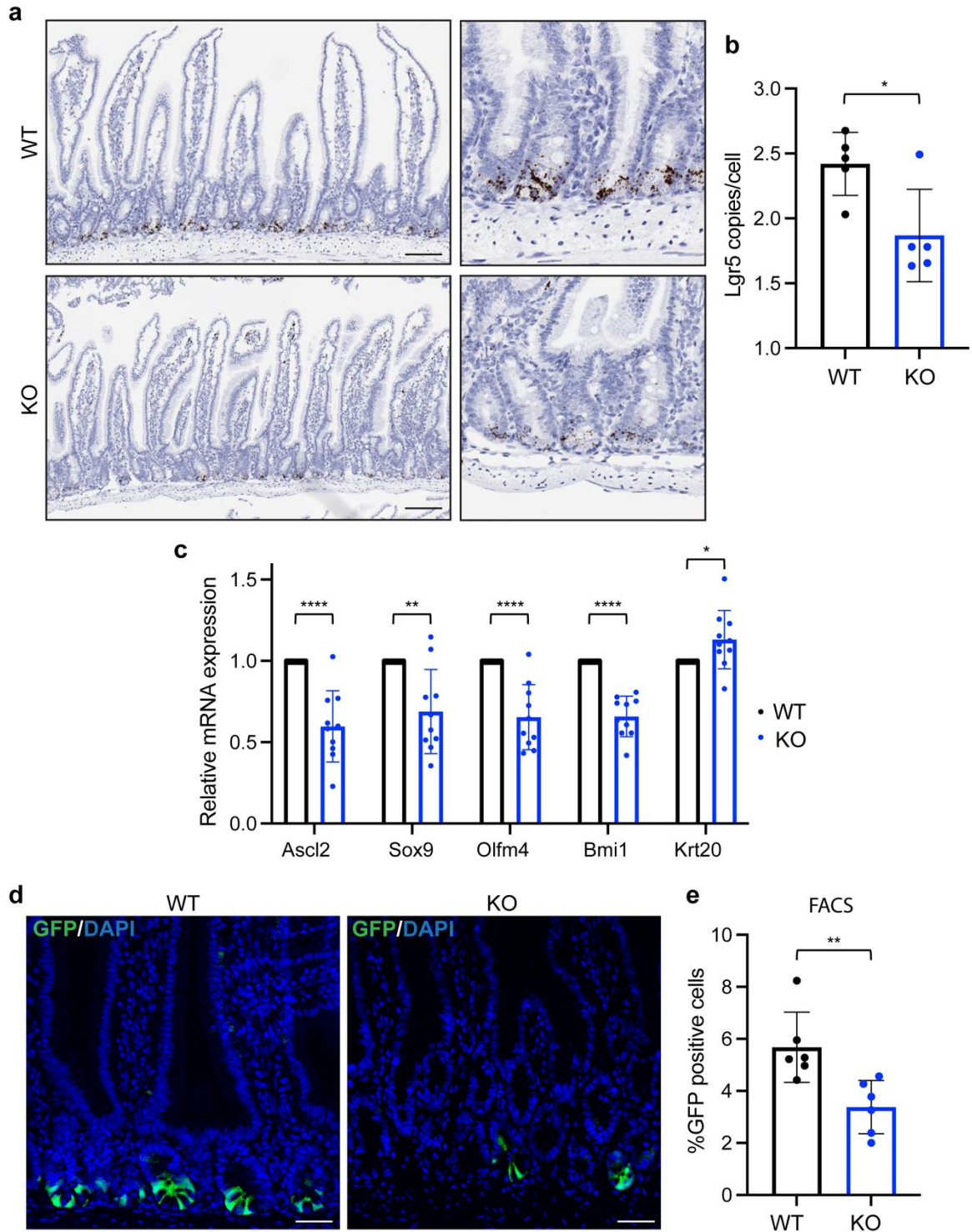


Figure 5.6 Knockout of PTPRF decreases the stemness of intestinal stem cells.

(A) FFPE sections prepared from WT and PTPRF KO mice were analyzed for the expression of Lgr5 mRNA using the RNAscope in situ hybridization (ISH) technology.

Representative images showing the localization of *Lgr5* mRNA in crypt-base stem cells. Scale bar, 100 μ m. (B) The number of individual mRNA copies per cell was quantified using HALO software (Indica labs). Data represent the mean \pm SD (n=5, * p < 0.05). (C) The relative expression of genes associated with intestinal stem cells, including *Ascl2*, *Sox9*, *Olfm4*, and *Bmi1*, as well as *Krt20*, a marker of differentiated epithelial cells, were determined using RT-qPCR in WT and PTPRF KO crypts. Data represent the mean \pm SD (n=10, **** p<0.0001, ** p < 0.01 and * p < 0.05). (D) Frozen sections of WT or PTPRF KO mice that were crossed with *Lgr5*-EGFP mice were visualized for EGFP expression using confocal microscopy. DAPI was used to stain nuclei. Scale bar, 100 μ m. (E) Single cells isolated from crypts of WT or PTPRF KO mice were stained with the Epcam-APC antibody and analyzed using FACS. The percentage of *Lgr5*-EGFP⁺ cells in the Epcam⁺ cell population was determined. Data were presented as mean \pm SD (n = 6, ** p<0.01).

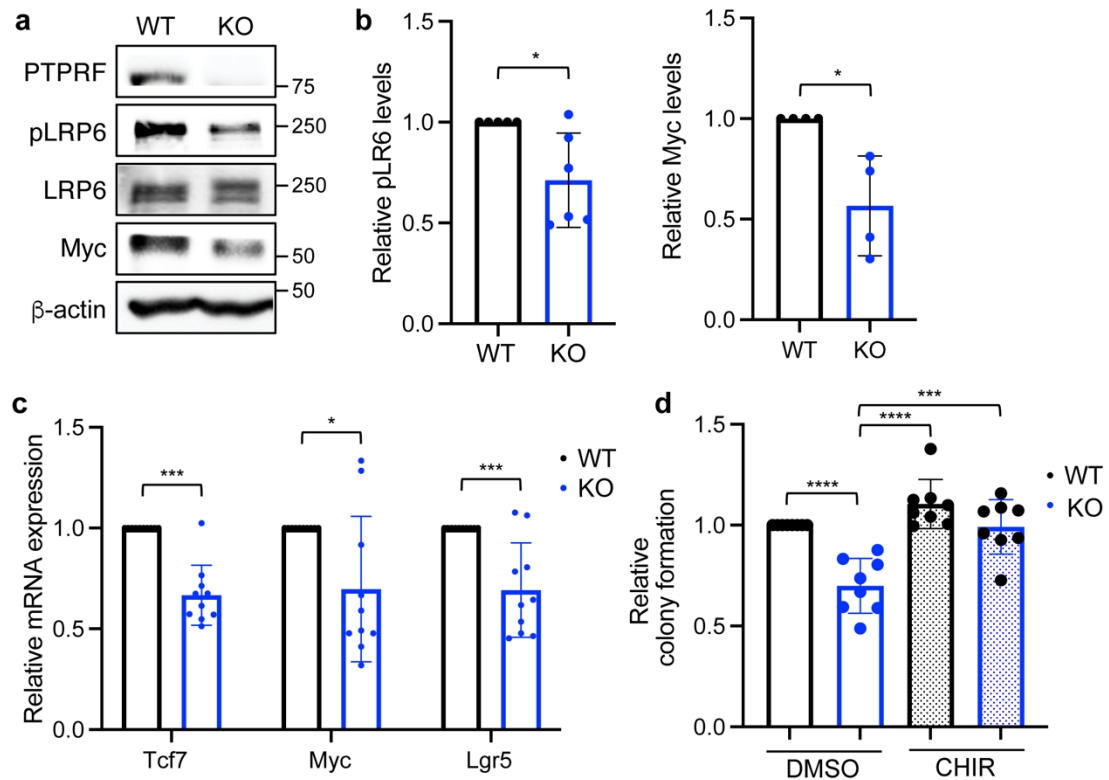


Figure 5.7 Knockout of PTPRF decreases Wnt signaling in vivo.

(A) Western blot analysis of Wnt pathway markers in intestinal crypts isolated from WT and PTPRF KO mice. The expression of PTPRF, pLRP6, LRP6, Myc and β -actin was detected using the corresponding antibodies. (B) Relative levels of LRP6 phosphorylation and Myc expression were quantified by normalizing pLRP6 to total LRP6 and Myc to β -actin, respectively. Data were presented as mean \pm SD (n = 6 for pLRP6 and n=4 for Myc, * p<0.05). (C) The relative expression of Wnt target genes, including *Tcf7*, *Myc*, and *Lgr5*, were determined using RT-qPCR in WT and PTPRF KO crypts. Data represent the mean \pm SD (n=10, *** p<0.001 and * p < 0.05). (D) The relatively colony formation efficiency was determined using intestinal crypts isolated from WT and PTPRF KO mice. The crypt cells were incubated with DMSO or CHIR99021. The number of organoids formed was counted after 3 days normalized to WT crypts treated with DMSO. Data were presented as mean \pm SD (n = 7, **** p<0.0001 and *** p < 0.001).

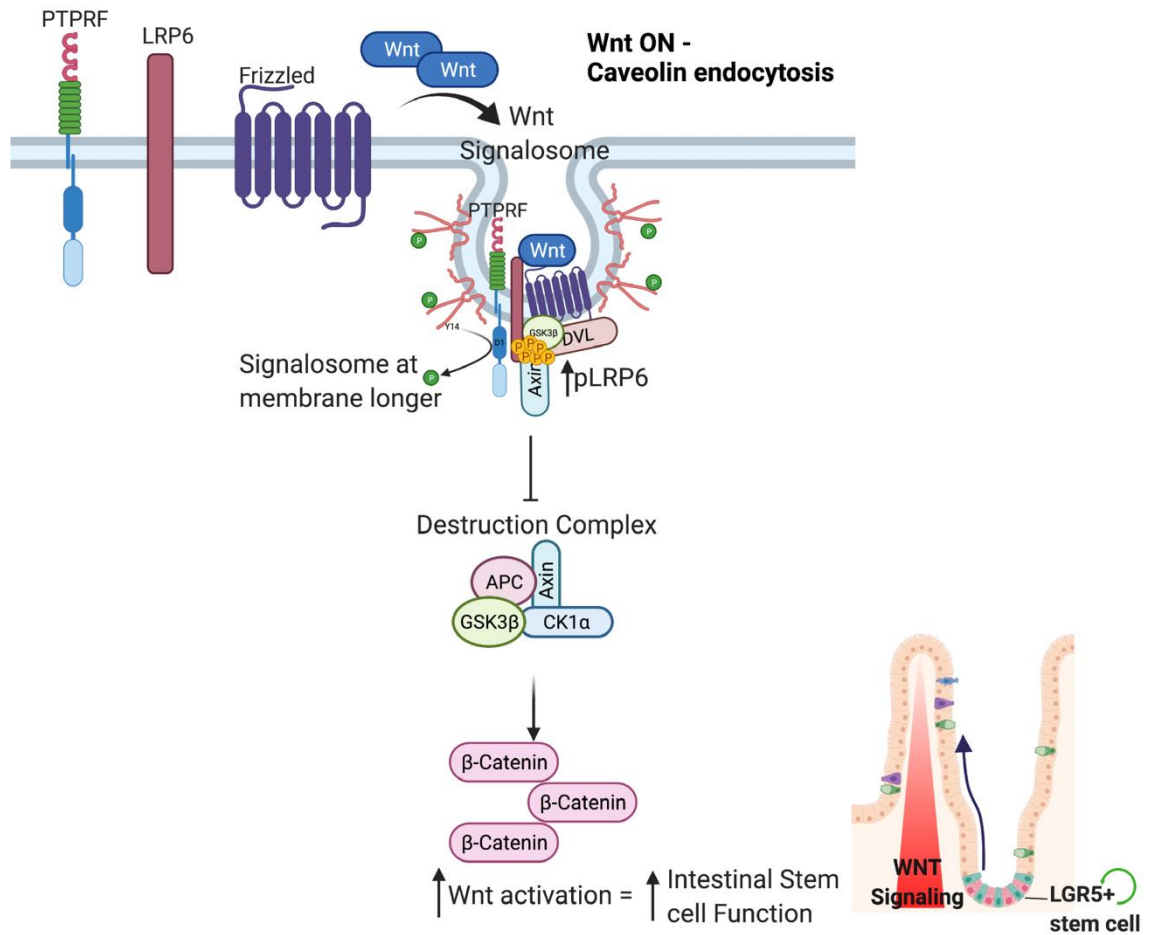


Figure 5.8 The molecular mechanism underlying PTPRF-mediated regulation of the Wnt pathway.

Results from our study suggest that the membrane localized PTPRF interacts with LRP6 and Cav1 basally. Upon Wnt stimulation, PTPRF together with LRP6 (and potentially Fzd receptors as well) are trafficked to the Wnt signalosome where the interaction between PTPRF/LRP6/Cav1 increases. PTPRF dephosphorylates Y14 of Cav1 to prolong the signaling lifetime of Wnt signalosome by preventing caveolin-mediated internalization of signalosome components. As a consequence, PTPRF functions upstream of the destruction complex to sustain Wnt signaling and intestinal stem cell function.

CHAPTER 6. DISCUSSION AND FUTURE DIRECTIONS

6.1 Overall Summary

Previous studies on PTPRF have established its importance as a receptor tyrosine phosphatase in neuronal development and cell adhesion signaling [16-18, 26, 32]. As the founding member of the receptor IIA family, most of studies on PTPRF have been conducted in the 1980's - early 2000's. Since then, only a limited number of publications have attempted to investigate the function of PTPRF beyond its involvement in neuronal development and it remains largely elusive whether its phosphatase activity is required for the regulation of cellular signaling. Additionally, the lack of understanding on PTPRF substrates represents a significant knowledge gap. The aim of this dissertation was to better characterize PTPRF in colorectal cancer, understand how PTPRF itself is regulated, and identify the molecular mechanisms by which PTPRF regulates Wnt activation and intestinal stem cells.

Briefly, Chapter 3 established that PTPRF functions as an oncogenic phosphatase in colorectal cancer by acting as a Wnt signaling activator at a step above the destruction complex. This study provided the initial evidence supporting a role of PTPRF in the Wnt signaling pathway. Chapter 4 determined the regulation of PTPRF expression by protein ubiquitination. We found that PTPRF is ubiquitinated by E3 ligase NEDD4L at the plasma membrane, which removes PTPRF from the membrane to inhibit its ability to promote Wnt activation. This chapter confirmed the importance of membrane localized PTPRF in Wnt activation and provided a first example of how ubiquitination and internalization control the signaling lifetime of a receptor type protein tyrosine phosphatase. Finally, Chapter 5 identified Cav1 as a novel substrate of PTPRF, in which PTPRF regulates the signalosome

assembly and retention at the membrane to enhance the duration and amplification of Wnt signaling by dephosphorylating Y14 of Cav1. Functional studies of PTPRF KO mice showed that they had decreased intestinal proliferation and stemness due to decreases in Wnt signaling (Figure 6.1). This is only the 4th reported/published substrate for PTPRF, and the first identified specific to the Wnt pathway. Our *in vivo* study using mouse models is also the first to characterize the role of PTPRF in intestinal homeostasis. Together, this dissertation provides new insights into the function and regulation of PTPRF under both physiological and pathological conditions.

Overall, this dissertation establishes the role of PTPRF in positively regulating Wnt signaling. When I joined Dr. Gao's lab, this project was first started based on the bioinformatic analysis of TCGA colorectal cancer data showing that the expression of PTPRF is positively associated with Wnt signaling. Our subsequent studies discovered oncogenic properties of PTPRF in colorectal cancer, identified NEDD4L as a novel regulator of PTPRF, and Cav1 as a novel substrate of PTPRF. This dissertation project allowed me to focus on a single phosphatase, but examine it in many different contexts: cancer, normal stem cells, and molecular mechanisms underlying the regulation of the phosphatase. This breadth of studies significantly improves our current understanding of PTPRF and how it is involved in the Wnt signaling pathway.

6.1.1 Additional Mechanisms Underlying PTPRF-mediated Regulation of Wnt Signaling

Although we have identified PTPRF-mediated dephosphorylation of Cav1 as a mechanism in Wnt regulation, our studies do not rule out the possibility that other

substrates might be involved in PTPRF's phosphatase dependent activation of the Wnt pathway. While examining the literature for potential substrates in the Wnt pathway, we identified three other Wnt components, including GSK3 β , DVL2 and LRP6, that can be phosphorylated at tyrosine residues. I will briefly discuss what are known about how tyrosine phosphorylation of these proteins is involved in regulating Wnt signaling. GSK3 β , a key regulator in the Wnt pathway, is known to be phosphorylated at Tyr216, which results in ~5-fold increase in its kinase activity [188]. Although dephosphorylation of GSK3 β Y216 may lead to decreased kinase activity, it has been shown recently that Y216 phosphorylation recruits E3 ligase β -TrCP to GSK3 β and subsequent monoubiquitination of GSK3 β and inhibition of β -catenin degradation [189]. As a consequence, increased GSK3 β -Y216 signaling axis via FAK and PYK2-mediated phosphorylation of Y216 is required for APC-driven intestinal tumorigenesis [189]. In this regard, GSK3 β is unlikely to a direct substrate of PTPRF as such dephosphorylation would be inconsistent with the positive role of PTPRF in Wnt signaling. However, it is still interesting to address if PTPRF expression regulates Y216 phosphorylation particularly in the GSK3 β population that is recruited to the signalosome.

Moreover, another study has demonstrated that Src family kinases function as positive regulators of Wnt/ β -catenin signaling by inducing tyrosine phosphorylation at multiple sites in Dvl2 (including Y18, Y27 and Y275) [190]. Src binds to Dvl2 upon Wnt stimulation to promote Wnt activation. In addition, inhibition of Src activity by silencing Src gene or using Src inhibitors, as well as the expression of Y18F mutant of Dvl2, attenuate Wnt reporter activities. Since tyrosine phosphorylation of Dvl2 (and Src family

kinases) enhances Wnt signaling activation, the effect of PTPRF in this pathway is unlikely to be mediated through these proteins.

Additionally, previous studies have shown that Src-stimulated tyrosine phosphorylation of LRP6 serves as a negative regulatory mechanism in Wnt signaling by disrupting signalosome formation [185, 191]. Given the notion that LRP6 interacts with PTPRF, and they internalize together (Figure 3.8 & Figure 5.2), it is possible that PTPRF may dephosphorylate pY-LRP6 to sustain Wnt signalosome formation and downstream signaling activation, in addition to its role in dephosphorylating Cav1 as described in this dissertation. Both Cav1 and LRP6 could serve as substrates for PTPRF and act synergistically to mediate PTPRF-dependent regulation of signalosome formation.

Studies in this dissertation focus on exploring the role of PTPRF as an active phosphatase in regulating the canonical Wnt signaling pathway. However, the extracellular domain of PTPRF may also be involved by binding to syndecans. Earlier developmental biology studies have identified the glycosaminoglycan chains of syndecan as a ligand for PTPRF to control the axon guidance process [21]. Interestingly, it has been shown recently that the heparan sulfate chain containing syndecan-1 promotes aberrant Wnt activation in multiple myeloma [192]. Syndecan-1 is identified as a Wnt signalosome component to increase the binding of Wnt and R-spondin ligands to cancer cells. Thus, PTPRF may be anchored to membrane subdomains where Wnt receptors and co-receptors are enriched by binding to syndecans. Given the reported role of both PTPRF and syndecans in regulating the non-canonical/PCP pathway, it is of particular interest to determine if the phosphatase activity of PTPRF is required in the non-canonical Wnt pathway.

6.1.2 A Potential Role of PTPRF in Notch Signaling

In the analysis of gene expression in isolated WT and PTPRF KO crypts, we found that deletion of PTPRF gene results in a decrease in the Notch signaling pathway in addition to Wnt target genes (Figure 6.2). The balance between Wnt and Notch pathway controls the lineage specification of intestinal stem cells. A decrease in Notch signaling (Figure 6.2A) may lead to a shift to favor secretory precursor cells. We found in our study that the number of goblet cells, a major type of secretory cells in the intestine, is decreased as assessed by Alcian blue staining (Figure 6.2B). This phenotype might be associated with downregulation of both Wnt and Notch signaling in PTPRF KO mice.

The Notch signaling pathway is also regulated by endocytosis mechanisms [193]. In this dissertation, we only investigated how PTPRF-dependent endocytosis regulates the Wnt pathway; however, our findings that both Wnt and Notch signaling pathways are decreased in PTPRF KO mice may reveal a potentially general role of PTPRF in regulating endocytosis of membrane receptors in various signaling pathways. The balance between the Wnt and Notch pathways allows the differentiation of intestinal stem cells to give rise to all intestinal epithelial cell types. The role of PTPRF in regulating different signaling pathways in the intestinal crypt needs to be further explored.

6.1.3 Limitations

At the time of this study, the only available mouse model to study PTPRF was a whole body KO generated in 1997 [24]. This model utilized traditional embryonic gene editing resulting in every cell in the mouse lacking PTPRF. While this was a good model

for the time, a conditional *Ptprf*-flox mouse model [187] became available through the Jackson Laboratory (*Ptprf*^{tm1.1Sud/J}). Together with the *Lgr5*-EGFP-IRES-CreERT2 model, this *Ptprf*-flox mouse model can be used to generate intestinal stem cell-specific inducible KO model. This model will allow us to specifically interrogate the effect of PTPRF-loss in intestinal stem cells and the differentiation of stem cells into various cell populations. Using the whole-body KO, every cell in the intestine lacks PTPRF, making the differences in lineage differentiation difficult to decipher. Studies in this dissertation showed a clear defect in stem cell renewal, proliferation and Wnt signaling when PTPRF is deleted *in vivo*; however, future studies are needed to dissect the functional contribution of PTPRF-loss using stem cell specific KO model.

Although our experiments showed that knockout of PTPRF alone is sufficient to decrease Wnt activation in intestinal crypts, it is possible that the redundant function of other RIIA subfamily RPTPs, including PTPRD and PTPRS may compensate for the loss of PTPRF. Original studies on the whole-body PTPRF KO mouse revealed that mice lacking PTPRF grow normally; however, female mice show defects in mammary gland development during the gestation period and minor defects in cholinergic innervations of the hippocampal dentate gyrus [194-196]. This lack of major defects observed in PTPRF KO mice may be due to the overlapping functions of RIIA RPTP members. Indeed, double knockout of both PTPRF and PTPRS is embryonic lethal. However, future studies are needed to better understand the potential common and specific functions of all three RIIA members in regulating intestinal homeostasis.

Lastly, to connect the *in vitro* and *in vivo* data in Chapter 5, studies are needed to determine if the level of pY14-Cav1 is increased in PTPRF KO mouse crypts. Attempts

were made to address this question, in which Cav1 was immunoprecipitated from crypt lysates and levels of pY14-Cav1 were analyzed using the phospho-Y14 specific antibody. However, our results were inconclusive due to insufficient sensitivity of the antibody (both Cav1 antibodies are specific for human Cav1 isoform with much reduced sensitivity against mouse Cav1). To circumvent this problem, it may be necessary to overexpress Cav1 in WT and PTPRF KO organoids once isolated from mice using lentivirus-mediated transduction. The organoids can be treated with Wnt and monitored for Y14 phosphorylation of Cav1.

6.1.4 Translational Implications

As the main signaling driver of colorectal cancer, the Wnt pathway has been targeted for drug development with limited success. For example, inhibitors targeting Wnt secretion (PORCN), Tankyrase or β -catenin-mediated transcription, and antibodies targeting frizzled receptors have attracted significant attention and excitement. However, many of these inhibitors have not been successful in the clinic due to their side effects [197] (including gastrointestinal toxicity), again highlighting the importance of Wnt signaling in maintaining tissue homeostasis. New emphasis is being placed on identifying additional regulators of the Wnt pathway that could serve as potential drug targets. By providing mechanistic insights into PTPRF-dependent regulation of Wnt signaling, our findings will help identify new therapeutic strategies for treating Wnt-driven diseases by using PTPRF as a target.

Traditionally, protein kinases have been well studied and are good targets for pharmacological inhibition. The development of specific phosphatase inhibitors has been considered more difficult, the discovery of oncogenic phosphatases and recent advancements in developing allosteric inhibitors of protein phosphatases have led to renewed enthusiasm. Additionally, PROTAC-based technology, tagging a substrate with E3 ligase to target for degradation, or small molecule inhibitors that block the formation of a phosphatase holoenzyme have also gained traction [198]. These innovative approaches provide the stage for future new drugs targeting protein phosphatases.

6.2 Future Directions

The model shown in Figure 6.1 summarizes our current understanding of PTPRF's role in Wnt signaling. We propose the following experiments to further validate and expand the knowledge. Firstly, it is needed to test how the tyrosine phosphorylation of LRP6 and Cav1 affects canonical Wnt activation in the context of PTPRF. Identifying if LRP6 is a substrate for PTPRF would strengthen the role of PTPRF as a phosphatase in regulating the Wnt pathway. The tools needed to study pY-LRP6 at specific sites were not available at the time of this study and the detection of endogenous LRP6 phosphorylation using a phospho-Tyr antibody has not been successful. Additionally, the effect of Tyr phosphorylation mutants of LRP6 on affecting LRP6 trafficking in the context of PTPRF expression needs to be determined. In addition, it is unclear whether the interaction between PTPRF and LRP6 or Cav1 requires the presence of additional scaffolding proteins such as Dvl2/3 or Axin. Experiments can be carried out to determine if PTPRF-mediated regulation of Wnt signaling is LRP6 and or Dvl2/3 dependent.

Secondly, the time course of cellular colocalization of Cav1 (WT and Y14 mutants), LRP6 and PTPRF upon Wnt stimulation needs to be determined. In Chapter 5, we observed that PTPRF and Cav1 are co-localized to signalosome-like membrane microdomains; however, attempts to identify LRP6 in the same complex were unsuccessful due to issues with antibody sensitivity. A recent study reported the generation of GFP-tagged Wnt3a that replicates similar levels of Wnt activation as untagged Wnt ligand [199]. We have recently acquired the expression plasmid and will use the GFP-Wnt3a conditioned media to visualize the formation and trafficking of receptor complex/signalosome. The co-localization of PTPRF and Cav1 with GFP-Wnt3a positive signalosome can be examined as well. This method of staining will also be used to visualize the time course of PTPRF internalization upon Wnt3a treatment using live cell imaging. Moreover, studies of the cellular colocalization of Cav1 (WT and Y14 mutants), LRP6 and PTPRF upon Wnt stimulation and corresponding Wnt reporter activities will reveal the functional interplay among these proteins.

Lastly, we are in the process of generating inducible PTPRF KO mice by crossing newly acquired PTPRF-flox mouse model to Lgr5-EGFP-IRES-CreERT2 and ROSA26-tdTomato mice (PTPRF^{f/f}/Lgr5-EGFP/Td). These mice express EGFP in Lgr5⁺ intestinal stem cells and a single tamoxifen injection allows Cre-mediated recombination in Lgr5⁺ cells which will also be marked with tdTomato fluorescence. We will be able to trace the fate of Lgr5⁺ cells *in vivo*. Furthermore, we will utilize the scRNA-seq technology to identify different intestinal epithelial populations in mice [200]. Single cell suspensions of intestinal crypts will be prepared from WT and PTPRF KO mice and EpCAM⁺ cells will be selected using FACS sorting. In subsequent analysis, by comparing the percentage of

different intestinal epithelial cell populations, we will determine if PTPRF deletion decreases Lgr5⁺ cell numbers and increases any particular differentiated cell populations. Ultimately, these experiments will allow us to determine the mechanisms by which PTPRF-loss induces functional defects in the intestinal epithelium.

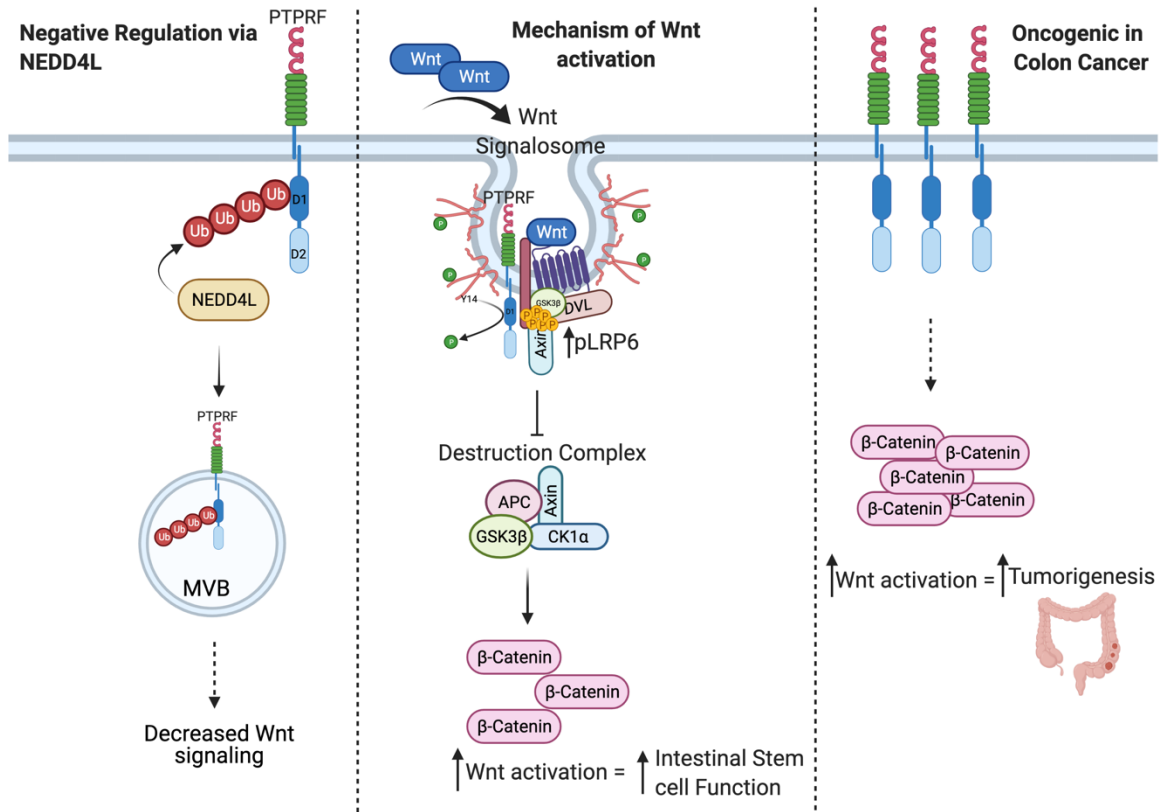


Figure 6.1 Summary Diagram of PTPRF function in Wnt signaling

Overview of PTPRF role in Wnt signaling explored in this dissertation. (Left) PTPRF regulation by NEDD4L-mediated ubiquitination and internalization. (Middle) PTPRF mechanism of action on the Wnt pathway through dephosphorylation of Y14 on Cav1. (Right) PTPRF is oncogenic in colorectal cancer through activation of the Wnt pathway.

Created with BioRender.com

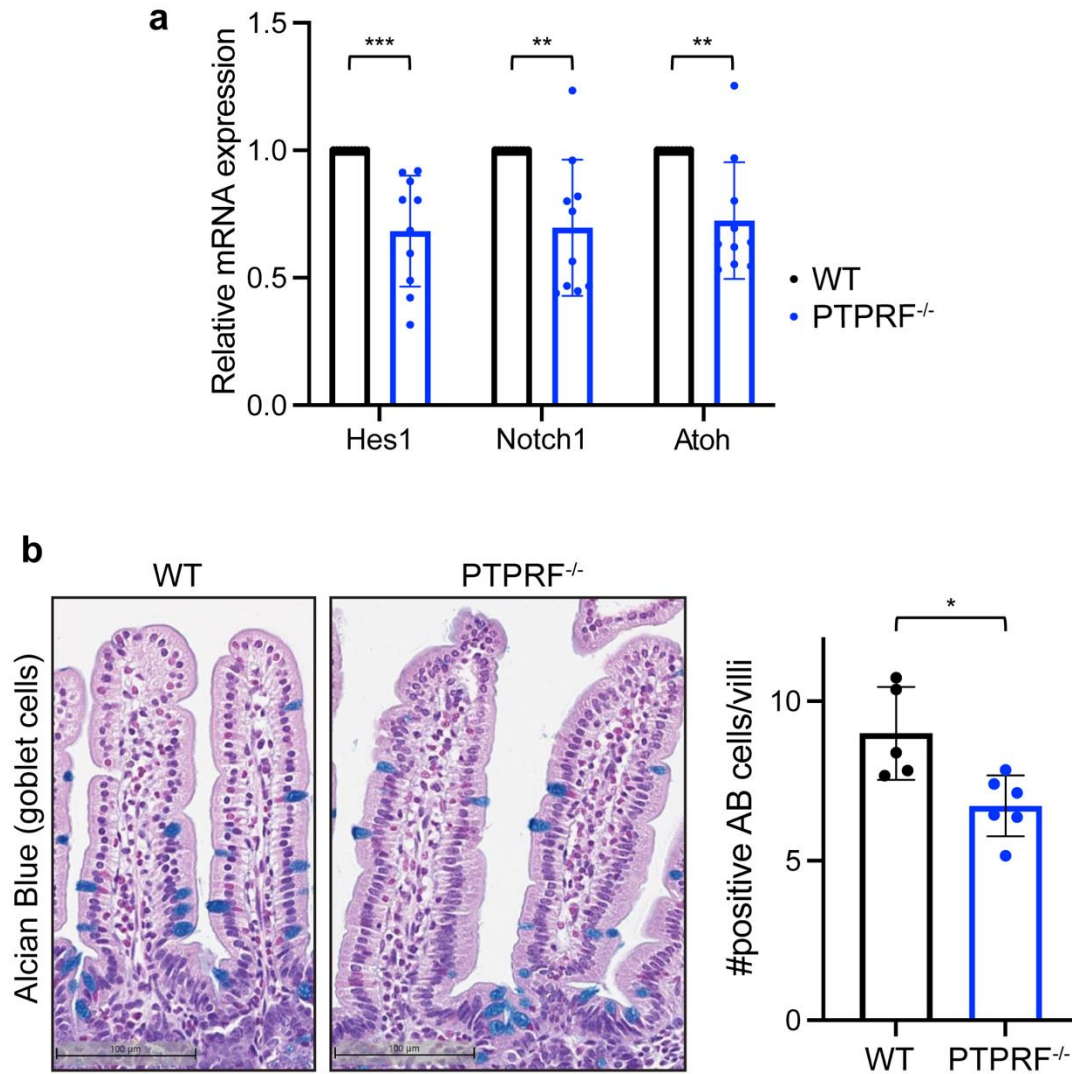


Figure 6.2 Decrease in Notch signaling in PTPRF KO mice

(A) qPCR for Notch target genes from WT or *Ptprf* KO mice crypts. (B) Alcian Blue staining for FFPE sections of WT or PTPRF KO proximal intestine. The number of positive cells per villi were quantified.

REFERENCES

1. Hunter, T., *Tyrosine phosphorylation: thirty years and counting*. Current opinion in cell biology, 2009. **21**(2): p. 140-6.
2. Eckhart, W., M.A. Hutchinson, and T. Hunter, *An activity phosphorylating tyrosine in polyoma T antigen immunoprecipitates*. Cell, 1979. **18**(4): p. 925-933.
3. Tonks, N.K., *Protein tyrosine phosphatases - From housekeeping enzymes to master regulators of signal transduction*. 2013. p. 346-378.
4. Zhao, S., D. Sedwick, and Z. Wang, *Genetic alterations of protein tyrosine phosphatases in human cancers*. Oncogene, 2015. **34**(30): p. 3885-94.
5. Lee, H. and A.M. Bennett, *Receptor protein tyrosine phosphatase-receptor tyrosine kinase substrate screen identifies EphA2 as a target for LAR in cell migration*. Mol Cell Biol, 2013. **33**(7): p. 1430-1441.
6. Tonks, N.K. and B.G. Neel, *From Form to Function: Signaling by Protein Tyrosine Phosphatases*. Cell, 1996. **87**(3): p. 365-368.
7. Alonso, A., et al., *Protein tyrosine phosphatases in the human genome*. Cell, 2004. **117**(6): p. 699-711.
8. Hendriks, W.J.A.J., et al., *Protein tyrosine phosphatases in health and disease*. The FEBS journal, 2013. **280**(2): p. 708-30.
9. Lee, H., et al., *Mining the function of protein tyrosine phosphatases in health and disease*. Semin Cell Dev Biol, 2015. **37**: p. 66-72.
10. Coles, C.H., E.Y. Jones, and A.R. Aricescu, *Extracellular regulation of type IIa receptor protein tyrosine phosphatases: mechanistic insights from structural analyses*. Seminars in Cell & Developmental Biology, 2015. **37**: p. 98-107.
11. Streuli, M., et al., *A new member of the immunoglobulin superfamily that has a cytoplasmic region homologous to the leukocyte common antigen*. The Journal of experimental medicine, 1988. **168**(5): p. 1523-30.
12. Nikolaienko, R.M., B. Agyekum, and S. Bouyain, *Receptor protein tyrosine phosphatases and cancer*. Cell Adhesion & Migration, 2012. **6**(4): p. 356-364.
13. Takahashi, H. and A.M. Craig, *Protein tyrosine phosphatases PTP δ , PTP ζ , and LAR: Presynaptic hubs for synapse organization*. 2013, Elsevier. p. 522-534.
14. Chagnon, M.J., N. Uetani, and M.L. Tremblay, *Functional significance of the LAR receptor protein tyrosine phosphatase family in development and diseases*. Biochemistry and Cell Biology, 2004. **82**(6): p. 664-675.
15. Nam, H.-J., et al., *Crystal Structure of the Tandem Phosphatase Domains of RPTP LAR*. Cell, 1999. **97**(4): p. 449-457.
16. Dunah, A.W., et al., *LAR receptor protein tyrosine phosphatases in the development and maintenance of excitatory synapses*. Nature Neuroscience, 2005. **8**(4): p. 458-467.
17. Tian, S.-S., P. Tsoulfas, and K. Zinn, *Three receptor-linked protein-tyrosine phosphatases are selectively expressed on central nervous system axons in the Drosophila embryo*. Cell, 1991. **67**(4): p. 675-685.
18. Desai, C.J., et al., *Receptor Tyrosine Phosphatases Are Required for Motor Axon Guidance in the Drosophila Embryo*. Cell, 1996. **84**(4): p. 599-609.
19. Johnson, K.G. and D. Van Vactor, *Receptor Protein Tyrosine Phosphatases in Nervous System Development*. Physiological Reviews, 2003. **83**(1): p. 1-24.

20. Desai, C., E. Popova, and K. Zinn, *A Drosophila receptor tyrosine phosphatase expressed in the embryonic CNS and larval optic lobes is a member of the set of proteins bearing the "HRP" carbohydrate epitope*. The Journal of Neuroscience, 1994. **14**(12): p. 7272-7283.
21. Fox, A.N. and K. Zinn, *The heparan sulfate proteoglycan Syndecan is an in vivo ligand for the Drosophila LAR receptor tyrosine phosphatase*. Current Biology, 2005. **15**(19): p. 1701-1711.
22. Stewart, K., et al., *Inactivation of LAR family phosphatase genes Ptprs and Ptprf causes craniofacial malformations resembling Pierre-Robin sequence*. Development (Cambridge, England), 2013. **140**(16): p. 3413-22.
23. Uetani, N., et al., *Maturation of ureter-bladder connection in mice is controlled by LAR family receptor protein tyrosine phosphatases*. The Journal of clinical investigation, 2009. **119**(4): p. 924-35.
24. Schaapveld, R.Q.J., et al., *Impaired Mammary Gland Development and Function in Mice Lacking LAR Receptor-like Tyrosine Phosphatase Activity*. 1997. p. 134-146.
25. Borck, G., et al., *Homozygous truncating PTPRF mutation causes athelia*. Hum Genet, 2014. **133**(8): p. 1041-1047.
26. Sarhan, A.R., et al., *LAR protein tyrosine phosphatase regulates focal adhesions via CDK1*. Journal of Cell Science, 2016. **129**(15): p. 2962-2971.
27. Serra-Pagès, C., et al., *Liprins, a family of LAR transmembrane protein-tyrosine phosphatase-interacting proteins*. The Journal of biological chemistry, 1998. **273**(25): p. 15611-20.
28. Xie, X., et al., *Structural basis of liprin- α -promoted LAR-RPTP clustering for modulation of phosphatase activity*. Nature Communications, 2020. **11**(1): p. 1-12.
29. Kypta, R.M., H. Su, and L.F. Reichardt, *Association between a transmembrane protein tyrosine phosphatase and the cadherin-catenin complex*. The Journal of cell biology, 1996. **134**(6): p. 1519-29.
30. Müller, T., et al., *Phosphorylation and free pool of β -catenin are regulated by tyrosine kinases and tyrosine phosphatases during epithelial cell migration*. Journal of Biological Chemistry, 1999. **274**(15): p. 10173-10183.
31. Haapasalo, A., et al., *Presenilin/ γ -Secretase-mediated Cleavage Regulates Association of Leukocyte-Common Antigen-related (LAR) Receptor Tyrosine Phosphatase with β -Catenin*. The Journal of biological chemistry, 2007. **282**(12): p. 9063-9072.
32. Barlan, K., M. Cetera, and S. Horne-Badovinac, *Fat2 and Lar Define a Basally Localized Planar Signaling System Controlling Collective Cell Migration*. Developmental cell, 2017. **40**(5): p. 467-477.e5.
33. Xin, W., L.P. Weng, and Y.U. Qiang, *Specific inhibition of FGF-induced MAPK activation by the receptor-like protein tyrosine phosphatase LAR*. Oncogene, 2000. **19**(19): p. 2346-2353.
34. Machide, M., et al., *Contact Inhibition of Hepatocyte Growth Regulated by Functional Association of the c-Met/Hepatocyte Growth Factor Receptor and LAR Protein-tyrosine Phosphatase*. The Journal of biological chemistry, 2006. **281**(13): p. 8765-8772.

35. Tian, X., et al., *PTPRF as a novel tumor suppressor through deactivation of ERK1/2 signaling in gastric adenocarcinoma*. *Onco Targets Ther*, 2018. **11**: p. 7795-7803.
36. Kulas, D.T., B.J. Goldstein, and R.A. Mooney, *The Transmembrane Protein-tyrosine Phosphatase LAR Modulates Signaling by Multiple Receptor Tyrosine Kinases (*)*. *The Journal of biological chemistry*, 1996. **271**(2): p. 748-754.
37. Kulas, D.T., et al., *Insulin receptor signaling is augmented by antisense inhibition of the protein tyrosine phosphatase LAR*. *Journal of Biological Chemistry*, 1995. **270**(6): p. 2435-2438.
38. Hashimoto, N., W.R. Zhang, and B.J. Goldstein, *Insulin receptor and epidermal growth factor receptor dephosphorylation by three major rat liver protein-tyrosine phosphatases expressed in a recombinant bacterial system*. *Biochemical Journal*, 1992. **284**(2): p. 569-576.
39. Ahmad, F. and B.J. Goldstein, *Functional association between the insulin receptor and the transmembrane protein-tyrosine phosphatase LAR in intact cells*. *The Journal of biological chemistry*, 1997. **272**(1): p. 448-57.
40. Streuli, M., et al., *Expression of the receptor-linked protein tyrosine phosphatase LAR: proteolytic cleavage and shedding of the CAM-like extracellular region*. *Embo j*, 1992. **11**(3): p. 897-907.
41. Serra-Pages, C., H. Saito, and M. Streuli, *Mutational analysis of proprotein processing, subunit association, and shedding of the LAR transmembrane protein tyrosine phosphatase*. *The Journal of biological chemistry*, 1994. **269**(38): p. 23632-41.
42. Bilwes, A.M., et al., *Structural basis for inhibition of receptor protein-tyrosine phosphatase- α by dimerization*. *Nature*, 1996. **382**(6591): p. 555-559.
43. Aicher, B., et al., *Cellular redistribution of protein tyrosine phosphatases LAR and PTPsigma by inducible proteolytic processing*. *The Journal of cell biology*, 1997. **138**(3): p. 681-96.
44. Wang, Z., et al., *Mutational analysis of the tyrosine phosphatome in colorectal cancers*. *Science*, 2004. **304**(5674): p. 1164-1166.
45. Du, W.W., et al., *MicroRNA miR-24 enhances tumor invasion and metastasis by targeting PTPN9 and PTPRF to promote EGF signaling*. *Journal of cell science*, 2013. **126**(Pt 6): p. 1440-53.
46. DaSilva, J.O., et al., *Neuroendocrine-derived peptides promote prostate cancer cell survival through activation of IGF-1R signaling*. *The Prostate*, 2013. **73**(8): p. 801-812.
47. Konishi, N., et al., *Overexpression of leucocyte common antigen (LAR) P-subunit in thyroid carcinomas*. *British Journal of Cancer*, 2003. **88**(8): p. 1223-1228.
48. LeVea, C. and R. Mooney, *The Leukocyte Common Antigen-Related Protein LAR: Candidate PTP for Inhibitory Targeting*. *Current Topics in Medicinal Chemistry*, 2005. **3**(7): p. 809-819.
49. Yang, T., et al., *Leukocyte common antigen-related tyrosine phosphatase receptor: increased expression and neuronal-type splicing in breast cancer cells and tissue*. *Mol Carcinog*, 1999. **25**(2): p. 139-49.

50. Zhai, Y.F., et al., *Increased expression of specific protein tyrosine phosphatases in human breast epithelial cells neoplastically transformed by the neu oncogene*. *Cancer research*, 1993. **53**(10 Suppl): p. 2272-8.
51. Gan, T., et al., *Inhibition of protein tyrosine phosphatase receptor type F suppresses Wnt signaling in colorectal cancer*. *Oncogene*, 2020. **39**(44): p. 6789-6801.
52. Nunes-Xavier, C.E., et al., *Protein tyrosine phosphatases as novel targets in breast cancer therapy*. *Biochimica et Biophysica Acta (BBA) - Reviews on Cancer*, 2013. **1836**(2): p. 211-226.
53. Bera, R., et al., *Functional genomics identified a novel protein tyrosine phosphatase receptor type f-mediated growth inhibition in hepatocarcinogenesis*. *Hepatology*, 2014. **59**(6): p. 2238-2250.
54. Clevers, H. and R. Nusse, *Wnt/ β -Catenin Signaling and Disease*. *Cell*, 2012. **149**(6): p. 1192-1205.
55. Janda, C.Y., et al., *Structural Basis of Wnt Recognition by Frizzled*. *Science*, 2012. **337**(6090): p. 59-64.
56. Colozza, G. and B.-K. Koo, *Wnt/ β -catenin signaling: Structure, assembly and endocytosis of the signalosome*. *Development, Growth & Differentiation*, 2021. **63**(3): p. 199-218.
57. Bilic, J., et al., *Wnt Induces LRP6 Signalosomes and Promotes Dishevelled-Dependent LRP6 Phosphorylation*. *Science (American Association for the Advancement of Science)*, 2007. **316**(5831): p. 1619-1622.
58. Taelman, V.F., et al., *Wnt Signaling Requires Sequestration of Glycogen Synthase Kinase 3 inside Multivesicular Endosomes*. *Cell*, 2010. **143**(7): p. 1136-1148.
59. Grainger, S., et al., *EGFR is required for Wnt9a–Fzd9b signalling specificity in haematopoietic stem cells*. *Nature Cell Biology*, 2019. **21**(6): p. 721-730.
60. Gerlach, J.P., et al., *TMEM59 potentiates Wnt signaling by promoting signalosome formation*. *Proceedings of the National Academy of Sciences of the United States of America*, 2018. **115**(17): p. E3996-E4005.
61. Jiang, Y., X. He, and P.H. Howe, *Disabled-2 (Dab2) inhibits Wnt/ β -catenin signalling by binding LRP6 and promoting its internalization through clathrin*. *The EMBO journal*, 2012. **31**(10): p. 2336-49.
62. Saito-Diaz, K., et al., *APC Inhibits Ligand-Independent Wnt Signaling by the Clathrin Endocytic Pathway*. *Dev Cell*, 2018. **44**(5): p. 566-581 e8.
63. Yamamoto, H., H. Komekado, and A. Kikuchi, *Caveolin is necessary for Wnt-3a-dependent internalization of LRP6 and accumulation of beta-catenin*. *Dev Cell*, 2006. **11**(2): p. 213-223.
64. Yamamoto, H., et al., *Wnt3a and Dkk1 Regulate Distinct Internalization Pathways of LRP6 to Tune the Activation of β -Catenin Signaling*. *Developmental Cell*, 2008. **15**(1): p. 37-48.
65. Demir, K., et al., *RAB8B Is Required for Activity and Caveolar Endocytosis of LRP6*. *Cell Reports*, 2013. **4**(6): p. 1224-1234.
66. Lajoie, P. and I.R. Nabi, *Lipid Rafts, Caveolae, and Their Endocytosis*. 2010, Elsevier. p. 135-163.
67. Lobos-González, L., et al., *Caveolin-1 in Melanoma Progression*. *Advances in Malignant Melanoma - Clinical and Research Perspectives*, 2011.

68. Parton, R.G., K.A. McMahon, and Y. Wu, *Caveolae: Formation, dynamics, and function*. *Current Opinion in Cell Biology*, 2020. **65**: p. 8-16.
69. Nomura, R. and T. Fujimoto, *Tyrosine-phosphorylated Caveolin-1: Immunolocalization and Molecular Characterization*. <https://doi.org/10.1091/mbc.10.4.975>, 2017. **10**(4): p. 975-986.
70. Zimnicka, A.M., et al., *Src-dependent phosphorylation of caveolin-1 Tyr-14 promotes swelling and release of caveolae*. <https://doi.org/10.1091/mbc.E15-11-0756>, 2016. **27**(13): p. 2090-2106.
71. Parton, R.G., B. Joggerst, and K. Simons, *Regulated internalization of caveolae*. *Journal of Cell Biology*, 1994. **127**(5): p. 1199-1215.
72. Pelkmans, L., D. Püntener, and A. Helenius, *Local Actin Polymerization and Dynamin Recruitment in SV40-Induced Internalization of Caveolae*. *Science (American Association for the Advancement of Science)*, 2002. **296**(5567): p. 535-539.
73. Siegel, R.L., et al., *Cancer Statistics, 2021*. CA: A Cancer Journal for Clinicians, 2021. **71**(1): p. 7-33.
74. Schepers, A. and H. Clevers, *Wnt signaling, stem cells, and cancer of the gastrointestinal tract*. *Cold Spring Harbor perspectives in biology*, 2012. **4**(4): p. a007989-a007989.
75. Clevers, H., *Searching for adult stem cells in the intestine*. *EMBO Molecular Medicine*, 2009. **1**(5): p. 255-259.
76. Tian, H., et al., *Opposing activities of notch and wnt signaling regulate intestinal stem cells and gut homeostasis*. *Cell Reports*, 2015. **11**(1): p. 33-42.
77. Sailaja, B.S., X.C. He, and L. Li, *The regulatory niche of intestinal stem cells*. *The Journal of Physiology*, 2016. **594**(17): p. 4827-4836.
78. Garabedian, E.M., et al., *Examining the role of Paneth cells in the small intestine by lineage ablation in transgenic mice*. *The Journal of biological chemistry*, 1997. **272**(38): p. 23729-40.
79. Sato, T., et al., *Paneth cells constitute the niche for Lgr5 stem cells in intestinal crypts*. *Nature*, 2011. **469**(7330): p. 415-418.
80. Durand, A., et al., *Functional intestinal stem cells after Paneth cell ablation induced by the loss of transcription factor Math1 (Atoh1)*. *Proceedings of the National Academy of Sciences of the United States of America*, 2012. **109**(23): p. 8965-70.
81. Kim, T.-H., S. Escudero, and R.A. Shivdasani, *Intact function of Lgr5 receptor-expressing intestinal stem cells in the absence of Paneth cells*. *Proceedings of the National Academy of Sciences of the United States of America*, 2012. **109**(10): p. 3932-7.
82. Farin, H.F., et al., *Visualization of a short-range Wnt gradient in the intestinal stem-cell niche*. *Nature*, 2016. **530**(7590): p. 340-343.
83. San Roman, A.K., et al., *Wnt secretion from epithelial cells and subepithelial myofibroblasts is not required in the mouse intestinal stem cell niche in vivo*. *Stem Cell Reports*, 2014. **2**(2): p. 127-134.
84. Kabiri, Z., et al., *Stroma provides an intestinal stem cell niche in the absence of epithelial Wnts*. *Development (Cambridge, England)*, 2014. **141**(11): p. 2206-15.

85. Greicius, G., et al., *PDGFR α + pericryptal stromal cells are the critical source of Wnts and RSPO3 for murine intestinal stem cells in vivo*. Proceedings of the National Academy of Sciences of the United States of America, 2018. **115**(14): p. E3173-E3181.
86. Chee, Y.C., et al., *Intrinsic Xenobiotic Resistance of the Intestinal Stem Cell Niche*. Developmental Cell, 2018. **46**(6): p. 681-695.e5.
87. Greicius, G. and D.M. Virshup, *Stromal control of intestinal development and the stem cell niche*. Differentiation, 2019.
88. Aoki, R., et al., *Foxl1-Expressing Mesenchymal Cells Constitute the Intestinal Stem Cell Niche*. Cellular and Molecular Gastroenterology and Hepatology, 2016. **2**(2): p. 175-188.
89. Shoshkes-Carmel, M., et al., *Subepithelial telocytes are an important source of Wnts that supports intestinal crypts*. Nature, 2018. **557**(7704): p. 242-246.
90. Kaestner, K.H., *The Intestinal Stem Cell Niche: A Central Role for Foxl1-Expressing Subepithelial Telocytes*. Cellular and molecular gastroenterology and hepatology, 2019. **8**(1): p. 111-117.
91. Yang, B. and S. Kumar, *Nedd4 and Nedd4-2: closely related ubiquitin-protein ligases with distinct physiological functions*. Cell death and differentiation, 2010. **17**(1): p. 68-77.
92. N Zheng, N.S., *Ubiquitin ligases: structure, function, and regulation*. Annu. Rev. Biochem., 2017. **86**: p. 129-157.
93. Kravtsova-Ivantsiv, Y. and A. Ciechanover, *Non-canonical ubiquitin-based signals for proteasomal degradation*. Journal of cell science, 2012. **125**(3): p. 539-548.
94. Rotin, D. and S. Kumar, *Physiological functions of the HECT family of ubiquitin ligases*. 2009, Nature Publishing Group. p. 398-409.
95. Ding, Y., et al., *HECT domain-containing E3 ubiquitin ligase NEDD4L negatively regulates Wnt signaling by targeting dishevelled for proteasomal degradation*. Journal of Biological Chemistry, 2013. **288**(12): p. 8289-8298.
96. Goel, P., J.A. Manning, and S. Kumar, *NEDD4-2 (NEDD4L): The ubiquitin ligase for multiple membrane proteins*. Gene, 2015. **557**(1): p. 1-10.
97. Staub, O., et al., *WW domains of Nedd4 bind to the proline-rich PY motifs in the epithelial Na⁺ channel deleted in Liddle's syndrome*. The EMBO Journal, 1996. **15**(10): p. 2371-2380.
98. Chen, M., et al., *The Anti-Helminthic Niclosamide Inhibits Wnt/Frizzled1 Signaling*. Biochemistry (Easton), 2009. **48**(43): p. 10267-10274.
99. Wong, T.H., et al., *Tyrosine phosphorylation of tumor cell caveolin-1: impact on cancer progression*. Cancer and Metastasis Reviews 2020 39:2, 2020. **39**(2): p. 455-469.
100. Spit, M., B.-K. Koo, and M.M. Maurice, *Tales from the crypt: intestinal niche signals in tissue renewal, plasticity and cancer*. Open Biology, 2018. **8**(9): p. 180120.
101. Wen, Y.A., et al., *Downregulation of SREBP inhibits tumor growth and initiation by altering cellular metabolism in colon cancer*. Cell Death Dis, 2018. **9**(3): p. 265.

102. Wen, Y.A., et al., *Adipocytes activate mitochondrial fatty acid oxidation and autophagy to promote tumor growth in colon cancer*. *Cell Death Dis*, 2017. **8**(2): p. e2593.
103. Liu, J., et al., *Loss of PHLPP expression in colon cancer: role in proliferation and tumorigenesis*. *Oncogene*, 2009. **28**(7): p. 994-1004.
104. Li, X., et al., *PHLPP is a negative regulator of RAF1, which reduces colorectal cancer cell motility and prevents tumor progression in mice*. *Gastroenterology*, 2014. **146**(5): p. 1301-12 e1-10.
105. Stevens, P.D., et al., *Erbin Suppresses KSR1-Mediated RAS/RAF Signaling and Tumorigenesis in Colorectal Cancer*. *Cancer Res*, 2018. **78**(17): p. 4839-4852.
106. Mao, B., et al., *Kremen proteins are Dickkopf receptors that regulate Wnt/beta-catenin signalling*. *Nature*, 2002. **417**(6889): p. 664-7.
107. Li, X., J. Liu, and T. Gao, *beta-TrCP-mediated ubiquitination and degradation of PHLPP1 are negatively regulated by Akt*. *Mol Cell Biol*, 2009. **29**(23): p. 6192-205.
108. Chen, M., et al., *The anti-helminthic niclosamide inhibits Wnt/Frizzled1 signaling*. *Biochemistry*, 2009. **48**(43): p. 10267-74.
109. Subramanian, A., et al., *Gene set enrichment analysis: a knowledge-based approach for interpreting genome-wide expression profiles*. *Proc Natl Acad Sci U S A*, 2005. **102**(43): p. 15545-50.
110. Gao, S., et al., *Ubiquitin ligase Nedd4L targets activated Smad2/3 to limit TGF-beta signaling*. *Mol Cell*, 2009. **36**(3): p. 457-68.
111. Raikwar, N.S., A. Vandewalle, and C.P. Thomas, *Nedd4-2 interacts with occludin to inhibit tight junction formation and enhance paracellular conductance in collecting duct epithelia*. *Am J Physiol Renal Physiol*, 2010. **299**(2): p. F436-44.
112. Xiong, X., et al., *Upregulation of CPT1A is essential for the tumor-promoting effect of adipocytes in colon cancer*. *Cell Death Dis*, 2020. **11**(9): p. 736.
113. Li, X., et al., *The deubiquitination enzyme USP46 functions as a tumor suppressor by controlling PHLPP-dependent attenuation of Akt signaling in colon cancer*. *Oncogene*, 2012. **32**(4): p. 471-8.
114. Xiong, X., et al., *PHLPP regulates hexokinase 2-dependent glucose metabolism in colon cancer cells*. *Cell Death Discov*, 2017. **3**: p. 16103.
115. Xiong, X., et al., *Pleckstrin Homology (PH) Domain Leucine-rich Repeat Protein Phosphatase Controls Cell Polarity by Negatively Regulating the Activity of Atypical Protein Kinase C*. *J Biol Chem*, 2016. **291**(48): p. 25167-25178.
116. Bilić, J., et al., *The Promise and Perils of Wnt Signaling Through beta -Catenin*. *Science*, 2007. **296**(5573): p. 1644-1646.
117. Rock, S.A., et al., *Neurotensin Regulates Proliferation and Stem Cell Function in the Small Intestine in a Nutrient-Dependent Manner*. *Cellular and Molecular Gastroenterology and Hepatology*, 2022. **13**(2): p. 501-516.
118. Siegel, R.L., K.D. Miller, and A. Jemal, *Cancer Statistics, 2017*. *CA Cancer J Clin*, 2017. **67**(1): p. 7-30.
119. Smith, R.A., et al., *Cancer screening in the United States, 2018: A review of current American Cancer Society guidelines and current issues in cancer screening*. *CA Cancer J Clin*, 2018. **68**(4): p. 297-316.

120. O'Connell, J.B., et al., *Colorectal cancer in the young*. Am J Surg, 2004. **187**(3): p. 343-8.
121. Reya, T. and H. Clevers, *Wnt signalling in stem cells and cancer*. Nature, 2005. **434**(7035): p. 843-50.
122. Schatoff, E.M., B.I. Leach, and L.E. Dow, *Wnt Signaling and Colorectal Cancer*. Curr Colorectal Cancer Rep, 2017. **13**(2): p. 101-110.
123. Niehrs, C., *The complex world of WNT receptor signalling*. Nat Rev Mol Cell Biol, 2012. **13**(12): p. 767-79.
124. Clevers, H., *Wnt/beta-catenin signaling in development and disease*. Cell, 2006. **127**(3): p. 469-80.
125. Nusse, R. and H. Clevers, *Wnt/beta-Catenin Signaling, Disease, and Emerging Therapeutic Modalities*. Cell, 2017. **169**(6): p. 985-999.
126. Komiya, Y. and R. Habas, *Wnt signal transduction pathways*. Organogenesis, 2008. **4**(2): p. 68-75.
127. Stamos, J.L. and W.I. Weis, *The beta-catenin destruction complex*. Cold Spring Harb Perspect Biol, 2013. **5**(1): p. a007898.
128. Julien, S.G., et al., *Inside the human cancer tyrosine phosphatome*. Nat Rev Cancer, 2011. **11**(1): p. 35-49.
129. Virshup, D.M. and S. Shenolikar, *From promiscuity to precision: protein phosphatases get a makeover*. Mol Cell, 2009. **33**(5): p. 537-45.
130. Johnson, K.G. and D. Van Vactor, *Receptor protein tyrosine phosphatases in nervous system development*. Physiol Rev, 2003. **83**(1): p. 1-24.
131. Barlan, K., M. Cetera, and S. Horne-Badovinac, *Fat2 and Lar Define a Basally Localized Planar Signaling System Controlling Collective Cell Migration*. Dev Cell, 2017. **40**(5): p. 467-477 e5.
132. Du, W.W., et al., *MicroRNA miR-24 enhances tumor invasion and metastasis by targeting PTPN9 and PTPRF to promote EGF signaling*. J Cell Sci, 2013. **126**(Pt 6): p. 1440-53.
133. Nunes-Xavier, C.E., et al., *Protein tyrosine phosphatases as novel targets in breast cancer therapy*. Biochim Biophys Acta, 2013. **1836**(2): p. 211-26.
134. Levea, C.M., et al., *PTP LAR expression compared to prognostic indices in metastatic and non-metastatic breast cancer*. Breast Cancer Res Treat, 2000. **64**(2): p. 221-8.
135. Wang, Z., et al., *Mutational analysis of the tyrosine phosphatome in colorectal cancers*. Science, 2004. **304**(5674): p. 1164-6.
136. Bera, R., et al., *Functional genomics identified a novel protein tyrosine phosphatase receptor type F-mediated growth inhibition in hepatocarcinogenesis*. Hepatology, 2014. **59**(6): p. 2238-50.
137. Bujko, M., et al., *Expression changes of cell-cell adhesion-related genes in colorectal tumors*. Oncol Lett, 2015. **9**(6): p. 2463-2470.
138. Barr, A.J., et al., *Large-scale structural analysis of the classical human protein tyrosine phosphatome*. Cell, 2009. **136**(2): p. 352-63.
139. Kreso, A., et al., *Self-renewal as a therapeutic target in human colorectal cancer*. Nat Med, 2014. **20**(1): p. 29-36.
140. Wu, D. and W. Pan, *GSK3: a multifaceted kinase in Wnt signaling*. Trends in biochemical sciences, 2010. **35**(3): p. 161-168.

141. Stewart, K., et al., *Inactivation of LAR family phosphatase genes Ptpns and Ptpnf causes craniofacial malformations resembling Pierre-Robin sequence*. Development, 2013. **140**(16): p. 3413-22.
142. Voloshanenko, O., et al., *Wnt secretion is required to maintain high levels of Wnt activity in colon cancer cells*. Nat Commun, 2013. **4**: p. 2610.
143. Flanagan, D.J., E. Vincan, and T.J. Phesse, *Wnt Signaling in Cancer: Not a Binary ON:OFF Switch*. Cancer Res, 2019. **79**(23): p. 5901-5906.
144. Flanagan, D.J., et al., *Frizzled-7 Is Required for Wnt Signaling in Gastric Tumors with and Without Apc Mutations*. Cancer Res, 2019. **79**(5): p. 970-981.
145. Vermeulen, L., et al., *Defining stem cell dynamics in models of intestinal tumor initiation*. Science, 2013. **342**(6161): p. 995-8.
146. Vermeulen, L., et al., *Wnt activity defines colon cancer stem cells and is regulated by the microenvironment*. Nat Cell Biol, 2010. **12**(5): p. 468-76.
147. Yamamoto, H., H. Komekado, and A. Kikuchi, *Caveolin is necessary for Wnt-3a-dependent internalization of LRP6 and accumulation of beta-catenin*. Dev Cell, 2006. **11**(2): p. 213-23.
148. Kim, I., et al., *Clathrin and AP2 are required for PtdIns(4,5)P2-mediated formation of LRP6 signalosomes*. J Cell Biol, 2013. **200**(4): p. 419-28.
149. Hagemann, A.I., et al., *In vivo analysis of formation and endocytosis of the Wnt/beta-catenin signaling complex in zebrafish embryos*. J Cell Sci, 2014. **127**(Pt 18): p. 3970-82.
150. Mana, G., et al., *PPFIA1 drives active alpha5beta1 integrin recycling and controls fibronectin fibrillogenesis and vascular morphogenesis*. Nat Commun, 2016. **7**: p. 13546.
151. Harder, K.W., et al., *Coexisting amplifications of the chromosome 1p32 genes (PTPRF and MYCL1) encoding protein tyrosine phosphatase LAR and L-myc in a small cell lung cancer line*. Genomics, 1995. **27**(3): p. 552-3.
152. Konishi, N., et al., *Overexpression of leucocyte common antigen (LAR) P-subunit in thyroid carcinomas*. Br J Cancer, 2003. **88**(8): p. 1223-8.
153. Soulieres, D., et al., *PTPRF Expression as a Potential Prognostic/Predictive Marker for Treatment with Erlotinib in Non-Small-Cell Lung Cancer*. J Thorac Oncol, 2015. **10**(9): p. 1364-1369.
154. Östman, A., C. Hellberg, and F.D. Böhmer, *Protein-tyrosine phosphatases and cancer*. Nature Reviews Cancer, 2006. **6**(4): p. 307-320.
155. Nam, H.J., et al., *Crystal structure of the tandem phosphatase domains of RPTP LAR*. Cell, 1999. **97**(4): p. 449-57.
156. Nikolaienko, R.M., B. Agyekum, and S. Bouyain, *Receptor protein tyrosine phosphatases and cancer: new insights from structural biology*. Cell Adh Migr, 2012. **6**(4): p. 356-64.
157. Cornejo, F., et al., *LAR Receptor Tyrosine Phosphatase Family in Healthy and Diseased Brain*. Front Cell Dev Biol, 2021. **9**: p. 659951.
158. Rotin, D. and S. Kumar, *Physiological functions of the HECT family of ubiquitin ligases*. Nat Rev Mol Cell Biol, 2009. **10**(6): p. 398-409.
159. Harvey, K.F., et al., *The Nedd4-like Protein KIAA0439 Is a Potential Regulator of the Epithelial Sodium Channel*. Journal of Biological Chemistry, 2001. **276**(11): p. 8597-8601.

160. Lu, C., et al., *The PY Motif of ENaC, Mutated in Liddle Syndrome, Regulates Channel Internalization, Sorting and Mobilization from Subapical Pool*. *Traffic*, 2007. **8**(9): p. 1246-1264.
161. Ding, Y., et al., *HECT domain-containing E3 ubiquitin ligase NEDD4L negatively regulates Wnt signaling by targeting dishevelled for proteasomal degradation*. *J Biol Chem*, 2013. **288**(12): p. 8289-8298.
162. Novellasedemunt, L., et al., *NEDD4 and NEDD4L regulate Wnt signalling and intestinal stem cell priming by degrading LGR5 receptor*. *The EMBO Journal*, 2019.
163. Gao, P., et al., *E3 ligase Nedd4l promotes antiviral innate immunity by catalyzing K29-linked cysteine ubiquitination of TRAF3*. *Nat Commun*, 2021. **12**(1): p. 1194.
164. Goh, L.K. and A. Sorokin, *Endocytosis of receptor tyrosine kinases*. *Cold Spring Harb Perspect Biol*, 2013. **5**(5): p. a017459.
165. Haglund, K. and I. Dikic, *The role of ubiquitylation in receptor endocytosis and endosomal sorting*. *J Cell Sci*, 2012. **125**(Pt 2): p. 265-75.
166. Bache, K.G., et al., *Hrs regulates multivesicular body formation via ESCRT recruitment to endosomes*. *J Cell Biol*, 2003. **162**(3): p. 435-42.
167. Novellasedemunt, L., et al., *NEDD4 and NEDD4L regulate Wnt signalling and intestinal stem cell priming by degrading LGR5 receptor*. *EMBO J*, 2020. **39**(3): p. e102771.
168. Fei, C., et al., *Smurf1-mediated Lys29-linked nonproteolytic polyubiquitination of axin negatively regulates Wnt/beta-catenin signaling*. *Mol Cell Biol*, 2013. **33**(20): p. 4095-105.
169. Fox, A.N. and K. Zinn, *The heparan sulfate proteoglycan syndecan is an in vivo ligand for the Drosophila LAR receptor tyrosine phosphatase*. *Curr Biol*, 2005. **15**(19): p. 1701-11.
170. Koo, B.-K., et al., *Tumour suppressor RNF43 is a stem-cell E3 ligase that induces endocytosis of Wnt receptors*. *Nature*, 2012. **488**(7413): p. 665-669.
171. Zhang, Y., et al., *RNF146 is a poly(ADP-ribose)-directed E3 ligase that regulates axin degradation and Wnt signalling*. *Nat Cell Biol*, 2011. **13**(5): p. 623-9.
172. Bienz, M., *Signalosome assembly by domains undergoing dynamic head-to-tail polymerization*. *Trends in biochemical sciences (Amsterdam. Regular ed.)*, 2014. **39**(10): p. 487-495.
173. Buwa, N., D. Mazumdar, and N. Balasubramanian, *Caveolin1 Tyrosine-14 Phosphorylation: Role in Cellular Responsiveness to Mechanical Cues*. *The Journal of Membrane Biology* 2020 253:6, 2020. **253**(6): p. 509-534.
174. Clevers, H., *The intestinal crypt, a prototype stem cell compartment*. *Cell*, 2013. **154**(2): p. 274-84.
175. Clevers, H., K.M. Loh, and R. Nusse, *Stem cell signaling. An integral program for tissue renewal and regeneration: Wnt signaling and stem cell control*. *Science*, 2014. **346**(6205): p. 1248012.
176. Feng, Q. and N. Gao, *Keeping Wnt Signalosome in Check by Vesicular Traffic*. *Journal of Cellular Physiology*, 2015. **230**(6): p. 1170-1180.
177. Verheyen, E.M. and C.J. Gottardi, *Regulation of Wnt/ β -catenin signaling by protein kinases*. *Developmental Dynamics*, 2009: p. NA-NA.

178. Li, S., R. Seitz, and M.P. Lisanti, *Phosphorylation of caveolin by src tyrosine kinases. The alpha-isoform of caveolin is selectively phosphorylated by v-Src in vivo.* J Biol Chem, 1996. **271**(7): p. 3863-8.
179. Zimnicka, A.M., et al., *Src-dependent phosphorylation of caveolin-1 Tyr-14 promotes swelling and release of caveolae.* Mol Biol Cell, 2016. **27**(13): p. 2090-106.
180. Sverdlov, M., A.N. Shajahan, and R.D. Minshall, *Tyrosine phosphorylation-dependence of caveolae-mediated endocytosis.* J Cell Mol Med, 2007. **11**(6): p. 1239-50.
181. Labrecque, L., et al., *Src-mediated tyrosine phosphorylation of caveolin-1 induces its association with membrane type 1 matrix metalloproteinase.* J Biol Chem, 2004. **279**(50): p. 52132-40.
182. Joshi, B., et al., *Phosphorylated caveolin-1 regulates Rho/ROCK-dependent focal adhesion dynamics and tumor cell migration and invasion.* Cancer Res, 2008. **68**(20): p. 8210-20.
183. Shajahan, A.N., et al., *Tyrosine-phosphorylated caveolin-1 (Tyr-14) increases sensitivity to paclitaxel by inhibiting BCL2 and BCLxL proteins via c-Jun N-terminal kinase (JNK).* J Biol Chem, 2012. **287**(21): p. 17682-17692.
184. Wehinger, S., et al., *Phosphorylation of caveolin-1 on tyrosine-14 induced by ROS enhances palmitate-induced death of beta-pancreatic cells.* Biochim Biophys Acta, 2015. **1852**(5): p. 693-708.
185. Liu, C.-C., et al., *Tyrosine-based signal mediates LRP6 receptor endocytosis and desensitization of Wnt/ β -catenin pathway signaling.* The Journal of biological chemistry, 2014. **289**(40): p. 27562-70.
186. Liu, C.C., et al., *Tyrosine-based signal mediates LRP6 receptor endocytosis and desensitization of Wnt/beta-catenin pathway signaling.* J Biol Chem, 2014. **289**(40): p. 27562-70.
187. Sclip, A. and T.C. Sudhof, *LAR receptor phospho-tyrosine phosphatases regulate NMDA-receptor responses.* Elife, 2020. **9**.
188. Dajani, R., et al., *Structural basis for recruitment of glycogen synthase kinase 3beta to the axin-APC scaffold complex.* EMBO J, 2003. **22**(3): p. 494-501.
189. Gao, C., et al., *FAK/PYK2 promotes the Wnt/beta-catenin pathway and intestinal tumorigenesis by phosphorylating GSK3beta.* Elife, 2015. **4**.
190. Yokoyama, N. and C.C. Malbon, *Dishevelled-2 docks and activates Src in a Wnt-dependent manner.* J Cell Sci, 2009. **122**(Pt 24): p. 4439-51.
191. Chen, Q., et al., *Tyrosine phosphorylation of LRP6 by Src and Fer inhibits Wnt/ -catenin signalling.* EMBO reports, 2014. **15**(12): p. 1254-1267.
192. Ren, Z., et al., *Syndecan-1 promotes Wnt/ β -catenin signaling in multiple myeloma by presenting Wnts and R-spondins.* Blood, 2018. **131**(9): p. 982-994.
193. Kopan, R. and M.X.G. Ilagan, *The Canonical Notch Signaling Pathway: Unfolding the Activation Mechanism.* Cell, 2009. **137**(2): p. 216-233.
194. Schaapveld, R.Q., et al., *Impaired mammary gland development and function in mice lacking LAR receptor-like tyrosine phosphatase activity.* Dev Biol, 1997. **188**(1): p. 134-46.

195. Yeo, T.T., et al., *Deficient LAR expression decreases basal forebrain cholinergic neuronal size and hippocampal cholinergic innervation*. J Neurosci Res, 1997. **47**(3): p. 348-60.
196. Van Lieshout, E.M., et al., *A decrease in size and number of basal forebrain cholinergic neurons is paralleled by diminished hippocampal cholinergic innervation in mice lacking leukocyte common antigen-related protein tyrosine phosphatase activity*. Neuroscience, 2001. **102**(4): p. 833-41.
197. Jung, Y.-S. and J.-I. Park, *Wnt signaling in cancer: therapeutic targeting of Wnt signaling beyond β -catenin and the destruction complex*. Experimental & Molecular Medicine, 2020. **52**(2): p. 183-191.
198. Köhn, M., *Turn and Face the Strange: A New View on Phosphatases*. ACS Central Science, 2020. **6**(4): p. 467-477.
199. Wesslowski, J., et al., *eGFP-tagged Wnt-3a enables functional analysis of Wnt trafficking and signaling and kinetic assessment of Wnt binding to full-length Frizzled*. Journal of Biological Chemistry, 2020: p. jbc.RA120.012892-jbc.RA120.012892.
200. Haber, A.L., et al., *A single-cell survey of the small intestinal epithelium*. Nature, 2017. **551**(7680): p. 333-339.

VITA

Ashley Taylor Skaggs (Stevens)

Doctoral Candidate
Department of Molecular and Cellular Biochemistry
Markey Cancer Center
University of Kentucky College of Medicine

Educational Institutions

University of Kentucky, Lexington, KY 2013-2017
Bachelor of Science, Agricultural and Medical Biotechnology

University of Kentucky, Lexington, KY 2017-2022
Doctorate in Philosophy, Molecular and Cellular Biochemistry (in progress)

Professional Positions

BGSO Outreach Committee Member 2017-2022
Markey Cancer Center Trainee Advisory Council Member 2018-2022
Appointed Student Representative Markey Cancer Center Education and Mentoring Committee 2019-2022

Scholastic and Professional Honors

Markey Cancer Center Research Day 1st Place Oral Presentation 2021
Markey Cancer Center Mentor Award Nominee 2021
UK College of Medicine Outstanding Graduate Student Biochemistry Finalist 2021
NSF Graduate Research Fellowship Recipient 2019
Markey Cancer Center Education and Mentoring Committee - Student Rep 2019
American Society for Biochemistry and Molecular Biology Travel Award 2019
University of Kentucky Integrated Biomedical Sciences Scholarship 2017

Publications

Xiaopeng Xiong, Sumati Hasani, Lyndsay E. A. Young, Dylan Rivas, **Ashley T. Skaggs**, Rebecca Martinez, Chi Wang, Heidi L. Weiss, Matthew S. Gentry, Ramon C. Sun, and Tianyan Gao. Activation of Drp1 promotes fatty acids-induced metabolic reprogramming to potentiate Wnt signaling in colon cancer. (2022) *Cell Death & Differentiation*. PMID: 35332310

Bianqin Guo, Xiaopeng Xiong, Sumati Hasani, Yang-An Wen, Austin T Li, Rebecca Martinez, **Ashley T Skaggs**, and Tianyan Gao. Downregulation of PHLPP induced by endoplasmic reticulum stress promotes eIF2 α 2 phosphorylation and chemoresistance in colon cancer. (2021) *Cell Death & Disease*, 12(11), 960–960. PMCID: PMC8523518

Gan T*, **Stevens AT***, Xiong X, Wen YA, Farmer TN, Li AT, Stevens PD, Golshani S, Weiss HL, Evers BM, Gao T. Inhibition of protein tyrosine phosphatase receptor type F suppresses Wnt signaling in colorectal cancer. *Oncogene*. 2020 Oct;39(44):6789-6801. PMID: PMC7606795. (*contributed equally)

Stevens PD, Wen YA, Xiong X, Zaytseva YY, Li AT, Wang C, **Stevens AT**, Farmer TN, Gan T, Weiss HL, Inagaki M, Marchetto S, Borg JP, Gao T. Erbin Suppresses KSR1-Mediated RAS/RAF Signaling and Tumorigenesis in Colorectal Cancer. *Cancer Res*. 2018 Sep 1;78(17):4839-4852. PMID: PMC6510240.

Stevens AT, Howe DK, Hunt AG. Characterization of mRNA polyadenylation in the apicomplexa. *PLoS One*. 2018 Aug 30;13(8):e0203317. PMID: PMC6117058.

Ashley T. Skaggs, Dylan Rivas, Tianyan Gao. NEDD4L promotes the ubiquitination and internalization of PTPRF to inhibit Wnt Signaling. (2022) *Journal of Biological Chemistry*. *In revision*.

Ashley Taylor Skaggs